A STUDY OF IONOSPHERIC WIND DRIFTS OVER AHMEDABAD

A thesis submitted

by

M.SETHURAMAN

to the Gujarat University

for the degree of

DOCTOR OF PHILOSOPHY

July, 1959

PHYSICAL RESEARCH LABORATORY

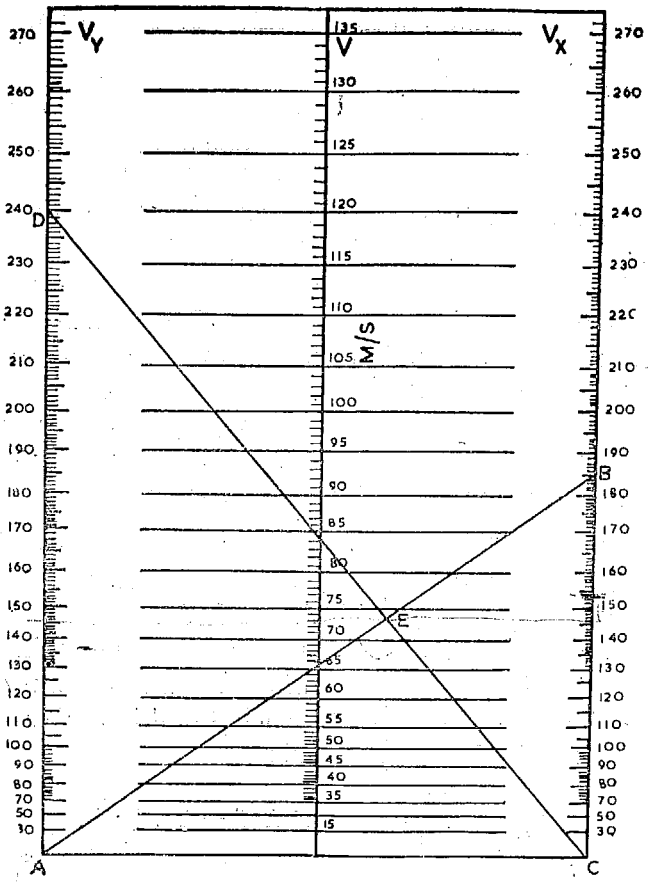

FIG. 2. Nomogram for determining drift speed.

calculation gave a value of 53°. The quadrant in which the drift vector lies has to be decided by the leads or the lags in the fading patterns in the N and the W aerials with reference to the reference aerial. The result of observations carried out over a period of 15 months are summarised below.

RESULTS

(1) *Observations on* 2·6 *Mc./s.*—Hourly observations on this frequency were started in August 1956. Owing to heavy absorption it was difficult, during many months, to get reflections at this frequency between 11 and 14 hours. Night observations were started in October 1956 and are taken on about eight nights a month. The night time reflections refer to the F layer and the day-time reflections to the E layer,

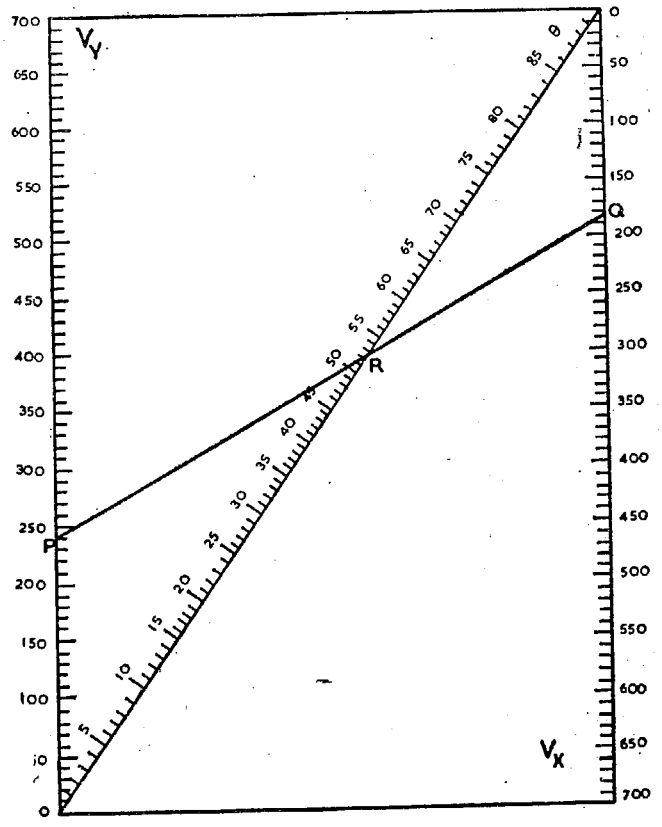

FIG. 3. Nomogram for determining drift direction.

Composite diagrams showing individual observations of drift direction and speed are shown in Figs. 4 and 5. The available data are grouped according to seasons; December–February (winter), March–May (spring), June–August (summer) and September–November (autumn). The diagrams on the left-hand side refer to the direction towards which the drift took place, while those on the right-hand side show the speeds. A continuous curve is drawn in the latter diagram passing through the median values of the speeds at the different hours of the day. The apparent continuity of the data of the day and the night hours should be viewed with caution as they refer to two different regions (E and F).

In winter months, the direction of the drift showed a diurnal variation with a predominant north-westward movement during the day hours (06–18 hours), but with significant south-eastward drift in the night hours. The scatter in the night observations was larger than on the day-time. In

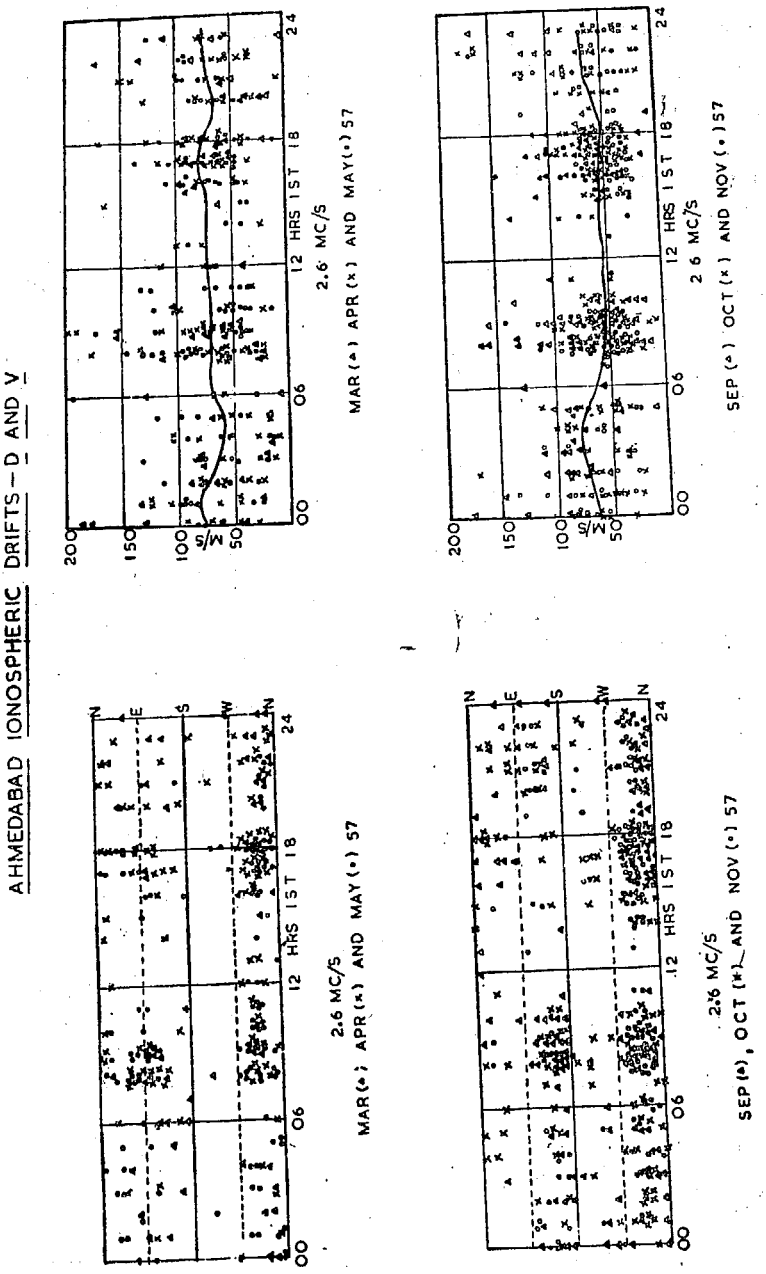

FIG. 5. Diurnal variation of drift direction and speed—Spring and Autumn.

Owing to insufficient day-time observations between 11 and 15 hours, the transition from one direction to the other could not be followed. During night time, there was much scatter in the former part of the night but the

direction, tended towards N-W after midnight. In the equinoctial months, the general flow was towards north-west with significant occurrences of south-eastward or eastward flow particularly in the morning hours. On the whole, the general drift observed on 2·6 Mc./s. at Ahmedabad is towards N-W but this is modified by a pronounced drift towards east in the morning hours of the summer months. The morning eastward drift was also noticced on many days in spring and autumn.

The speeds of drift in winter showed a tendency to a minimum at about sunrise and sunset. In the summer months, the mean speed showed a maximum at about midnight and it did not show any significant change during the day hours of observation. In the transition months, the diurnal variations of speed were intermediate between those in summer and in winter.

The mean N-S and E-W components of the drift in different hours of the day in each of the four seasons are plotted in Fig. 6.

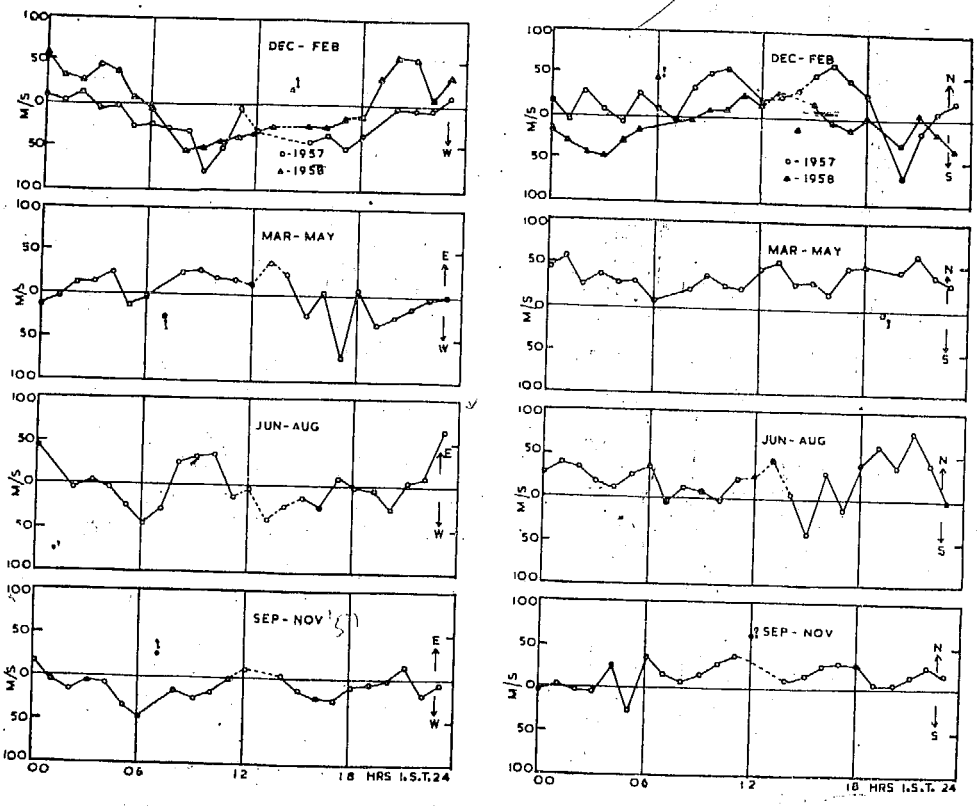

FIG. 6. Diurnal variation of E-W and N-S components of drift in different seasons.

The diurnal variation is very clear in winter and there is evidence of a semi-diurnal variation in summer. It will be noticed that the drift has a northward component through the major part of the year.

The month to month variations in the drift direction can be more clearly seen in the wind roses for the hours 06–18 and 19–05 given in Figs. 7 and 8. It may be noted that the directions shown are the directions *towards* which the drift took place. This is different from the convention adopted in meteorology. In the winter months, the dominant day-time direction was towards N-W with a maximum occurrence (52% of the total observation) along that direction in January and February 1957. The eastward drift will be seen to increase gradually from then onwards and attain a maximum (with 52% of the total observations eastward) in August 1957. In the night time wind roses also, the month to month changes in drift direction are clearly seen (Fig. 7).

The monthly speed distributions for the two periods are shown in Figs. 9 and 10. It will be seen that the speeds are more spread-out in winter than in summer. They are also more scattered in the night hours than in day hours.

The monthly variations of the mean drift speed for the period October 1956 to January 1958 are shown in Fig. 11. In the same diagram, the mean speeds observed on 4·0 Mc./s. during the day hours are also shown. It will be seen that there is no clear difference between the mean speeds of drift observed on 2·6 Mc./s. and 4·0 Mc./s. This suggests that the inhomogeneities whose drifts were responsible for the fading of the waves of both the frequencies were located in the same region of the ionosphere.

During the summer months, especially in July 1957, reflections could be obtained on many nights from E_s. Such observations could not be obtained in the winter months. In July 1957, 31 observations of the E_s drift showed a principal direction of movement towards N-W. The mean speed was 69 m./s. The details of these observations are not included in this paper.

(2) *Observations on* 4·0 *Mc./s.*—Hourly observations on 4 Mc./s. between 06 and 18 hours were started in February 1957. They refer to F layer reflections in the day-time. During the summer months, the critical frequency of the E layer at Ahmedabad went beyond 4·0 Mc./s. in mid-day and early afternoon hours. During such periods, no observations of the F region drift could be made.

The wind roses for the 4·0 Mc./s. observations are given in Fig. 12. Here again, the main direction was towards N-W in winter and spring, and

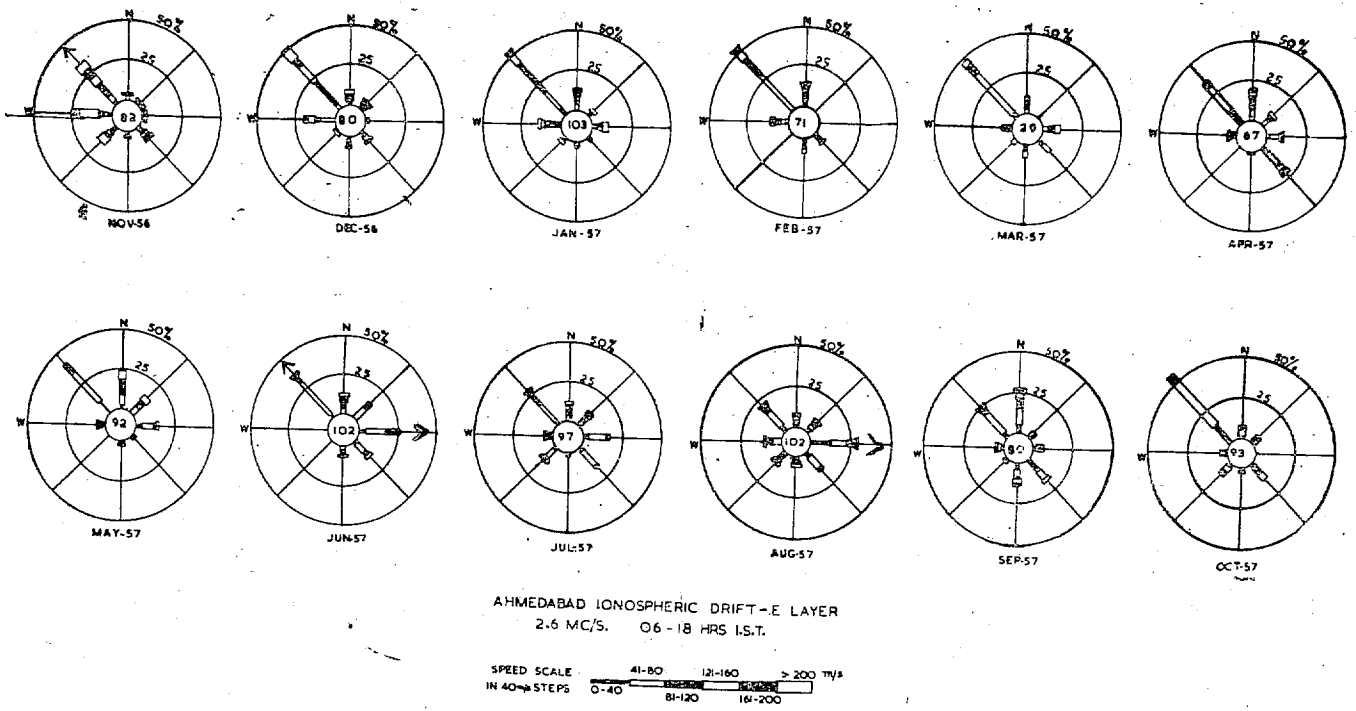

FIG. 7. Wind roses for day-time E region drifts (06–18 hours). The frequencies relate to the direction *towards* which the drift occurs. The figures in the innermost circles represent the total number of observations in each case.

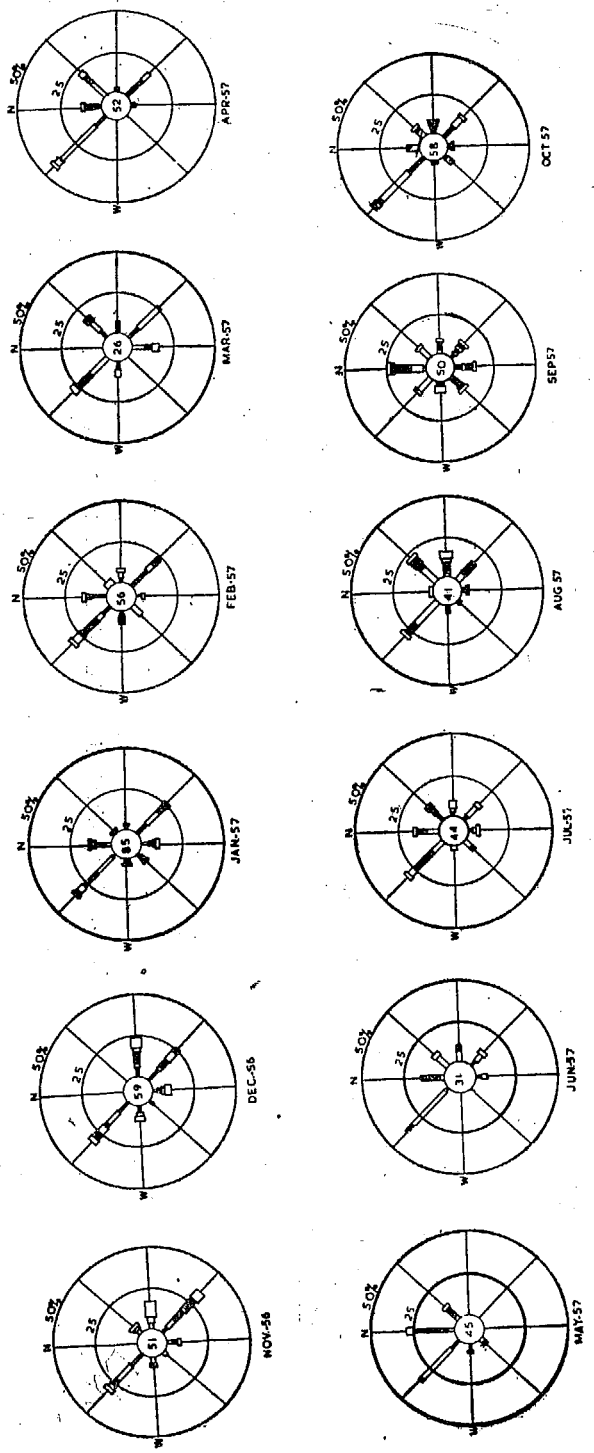

FIG. 8. Wind roses for night time F layer (19–05 hours) drifts on 2·6 Mc./s. The frequencies relate to the directions *towards* which the drift takes place. The figures in the innermost circles represent the total number of observations.

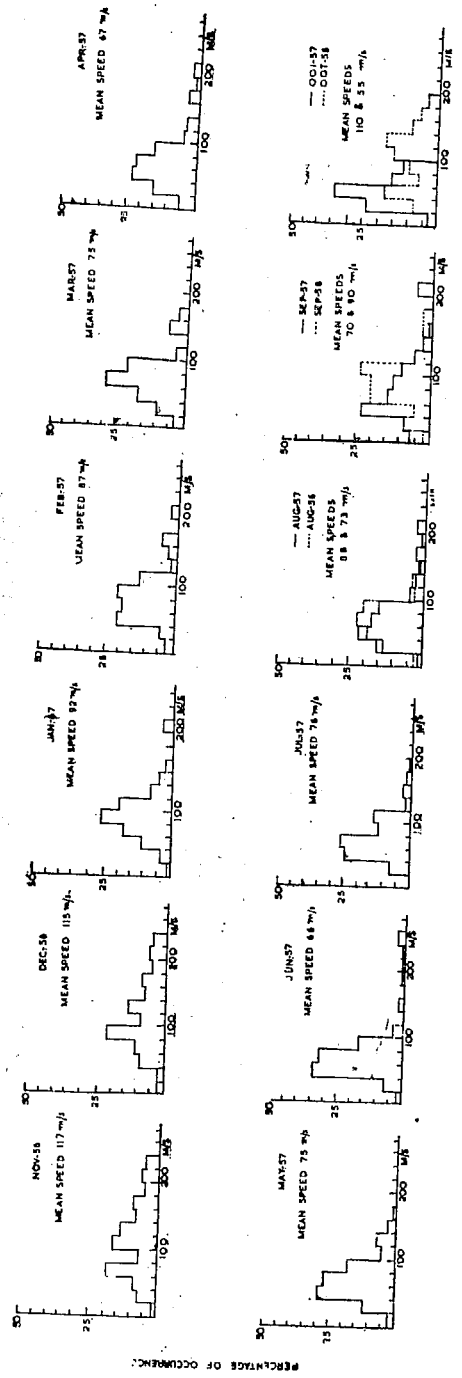

FIG. 9. Speed distribution of day-time E on 2·6 Mc./s.

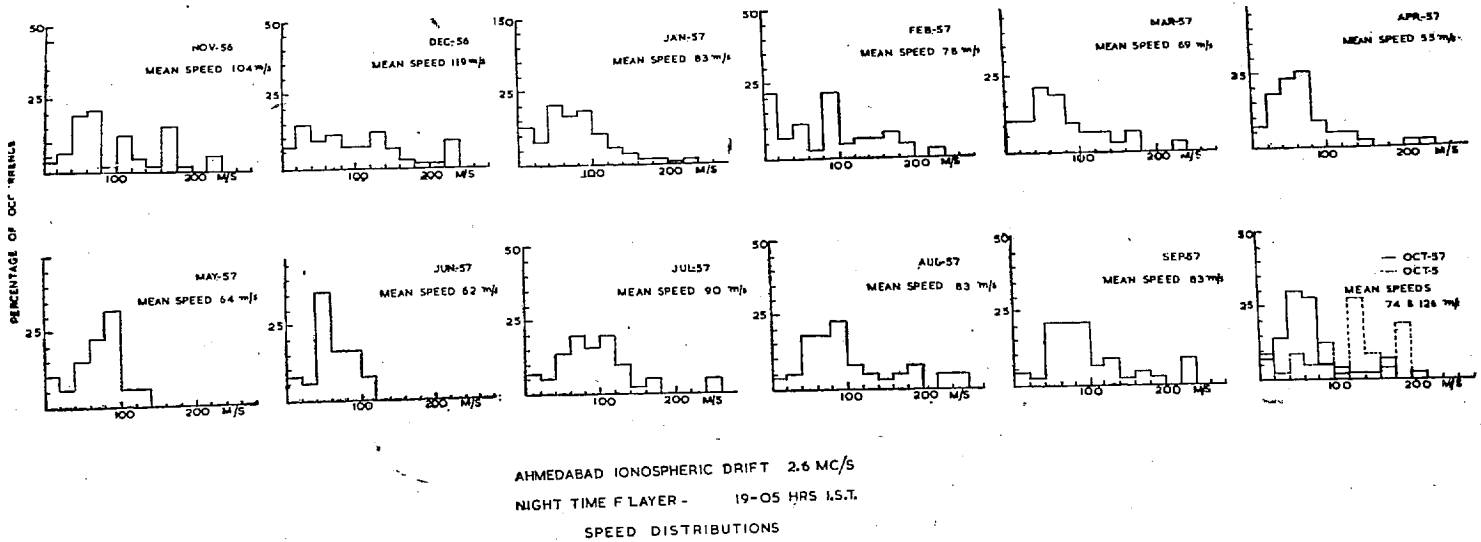

FIG. 10. Speed distribution of night time F on 2·6 Mc./s.

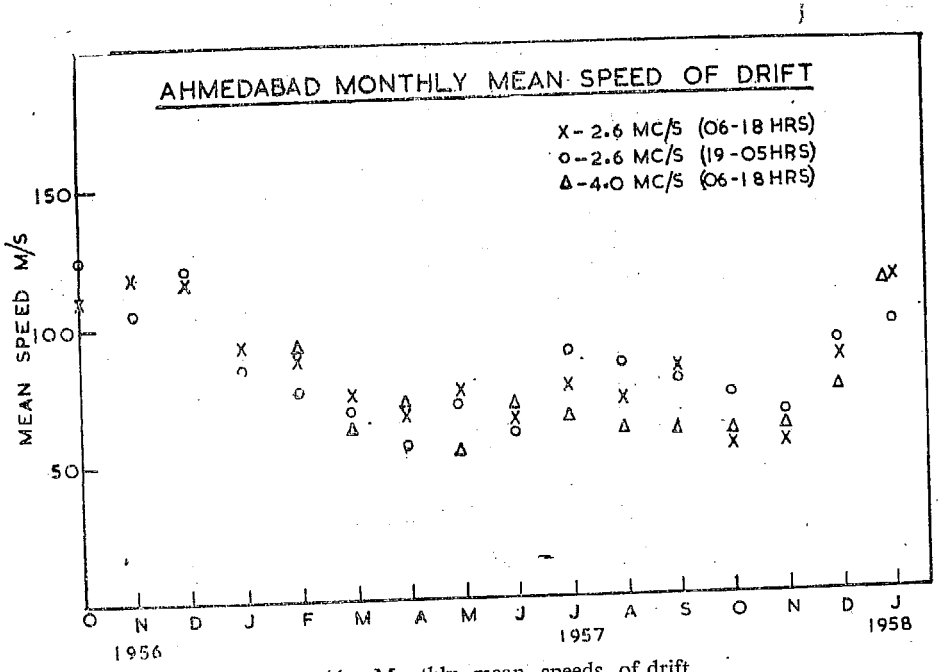

FIG. 11. Monthly mean speeds of drift.

eastward in the morning hours of summer and autumn, the eastward drift being maximum in August 1957. In Fig. 13, the speed distribution for the various months at this frequency are shown. The speeds are more spread-out in winter than in summer. The mean monthly speeds in Fig. 11 show a variation similar to those on 2·6 Mc./s.

Comparison of results with those obtained elsewhere.—Observations of ionospheric drift by the spaced aerial method on a frequency around 2·6 Mc./s. have been made at a number of places, most of them in middle latitudes. Comprehensive reports of the observations have been published for Cambridge (Phillips, 1952; Briggs and Spencer, 1954) and Kjeller (Harang and Pederson, 1956). Reports have also been published of observations made in France (Harnischmacher and Rawer, 1956), Washington (Salzberg and Greenstone, 1951), Montreal and Ottawa (Chapman, 1953), and Brisbane (Burke and Jenkinson, 1957). Limited low latitude observations are also available from Puerto Rico (Yerg, 1953) and Waltair (Rao *et al.*, 1956). Very few stations have published the results of the drift observations at higher frequencies and hence a comparison of the observations on 4·0 Mc./s. has not been undertaken.

In general, all observers in middle latitudes report an eastward drift in summer and a south-westward drift in winter. This is accompanied by a

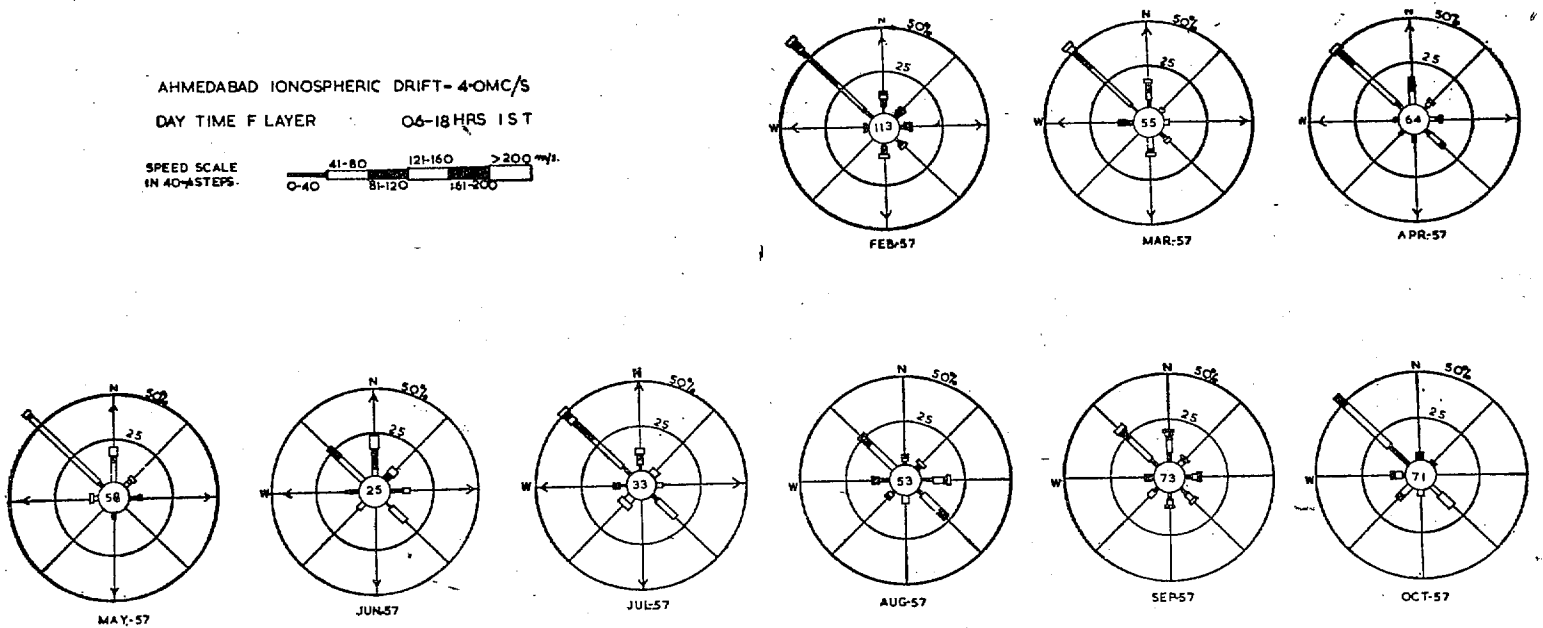

FIG. 12. Wind roses for day-time F region drifts on 4 Mc./s. (06–18 hours). The directions indicate the directions *towards* which the drift takes place. The figures in the innermost circles represent the total number of observations in the period.

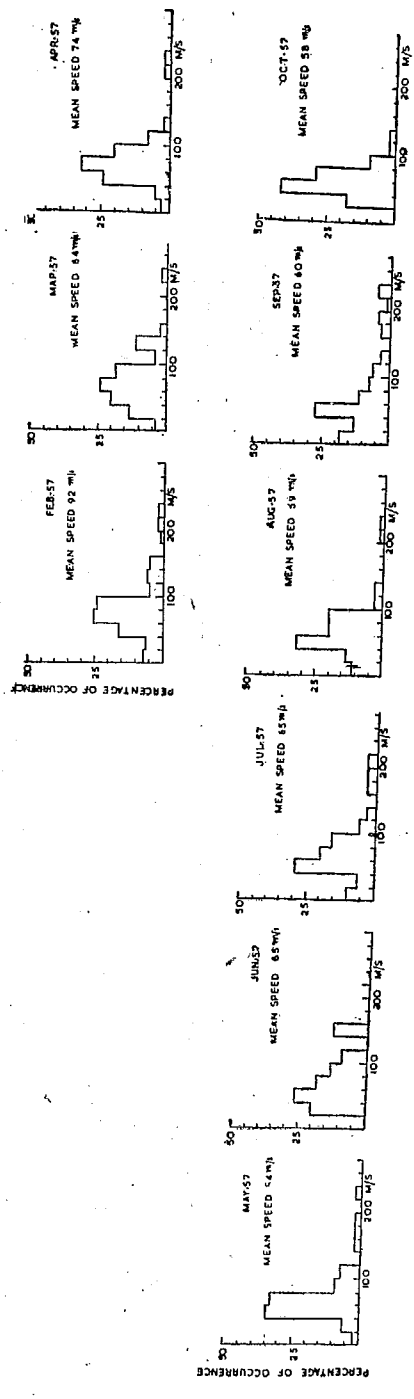

FIG. 13. Speed distribution of day-time F drifts on 4 Mc./s.

semi-diurnal variation of the direction of drift in a clockwise direction in the course of the day on many months, notably in winter. For the tropical stations, we do not possess sufficient data to evaluate the diurnal variation. The day-time drift at Waltair showed a seasonal variation, being towards south-west in winter and towards south-east in summer. The Ahmedabad observations showed that in summer mornings, the directions were towards east or south-east, and in summer evenings towards north-west; in winter, they remained north-west throughout the day. At night, the direction of drift was variable, the most common directions being towards north-west or south-east. No clear semi-diurnal variation of drift could be established, although there was a suggestion of it in some periods.

At most of the above places, the speeds of drift generally lay in the range 40–80 m./s. Only at Puerto Rico, where the correlation method of analysis was used in the claculations (Yerg, 1956), low values of speed, between 0–30 m./s. were obtained for reflections on 2·6 Mc./s. Most stations have recorded a wider distribution of speed in winter than in summer.

Summary

Results of observations of ionospheric drift carried out over a period of 15 months at Ahmedabad on 2·6 Mc./s. and 4·0 Mc./s. by the spaced aerial method are presented in this paper. The prevailing day-time drift was towards north-west in autumn and winter. In summer, and to a less marked degree in spring and autumn, the morning direction of drift was towards east or south-east. The evening direction was always towards north-west. During the night hours, the direction of drift were more spread-out, but the most frequent directions were still towards north-west and south-east. The speeds lay mostly in the range 40–100 m./s. and the mean speed was larger in winter than in summer. The Ahmedabad results are compared with those at other places.

Acknowledgements

The author is deeply grateful to Prof. K. R. Ramanathan for suggesting the problem and guiding the work. He is thankful to Mr. S. K. Alurkar and Mr. Girish D. Desai for help in taking the observations and to Dr. U. D. Desai for his keen interest and advice on technical questions. The scheme is receiving financial support from the Indian Council of Scientific and Industrial Research.

REFERENCES

Briggs, B. H. and Spencer, M. .. *Rep. Progr. Phys.*, 1954, **27,** 245.

Burke, M. J. and Jenkinson, I. S. .. *Aus. Jour. Phys.*, 1957, **10,** 378.

Chapman, J. H. .. *Canad. Jour. Phys.*, 1953, **31,** 120.

Harang, L. and Pederson, K. .. *Geofys. Publikasjner*, 1956, **19,** (10).

Harnischmacher, E. and Rawer, K. *Compt. Rend. Acad. Sci.*, 1956, **243,** 783.

Nanda, N. G. .. Thesis for the M.Sc. degree of the Gujarat University, 1955.

Phillips, G. J. .. *Jour. Atmos. Terr. Phys.*, 1952, **2,** 141.

Rao, B. R., Rao, M. S. and Murthy, D. S. *Jour. Sci. and Ind. Res.*, (India), 1956, **15 A,** 75.

Salzberg, C. D. and Greenstone, R. *Jour. Geophys. Res.*, 1951, **56,** 521.

Yerg, D. G. .. *Jour. Atmos. Terr. Phys.*, 1956, **2,** 247.

APPENDIX I

Summary of Observations of Ionospheric Drift made on 5 Mc./s. at Ahmedabad during 1954

By N. G. Nanda*

Mr. Nanda's measurements on ionospheric drift were made on a frequency of 5 Mc./s. at 0800, 1100, 1400 and 1700 hours I.S.T. in the months July to October 1954. Reflections were either from the F region (97 observations) or from E_s (30 observations). The results are summarised in Figs. 14 and 15.

In the F region reflections, the drift in the summer months at 0800 hours was mainly towards the east. At 1100 and 1400 hours, their directions were

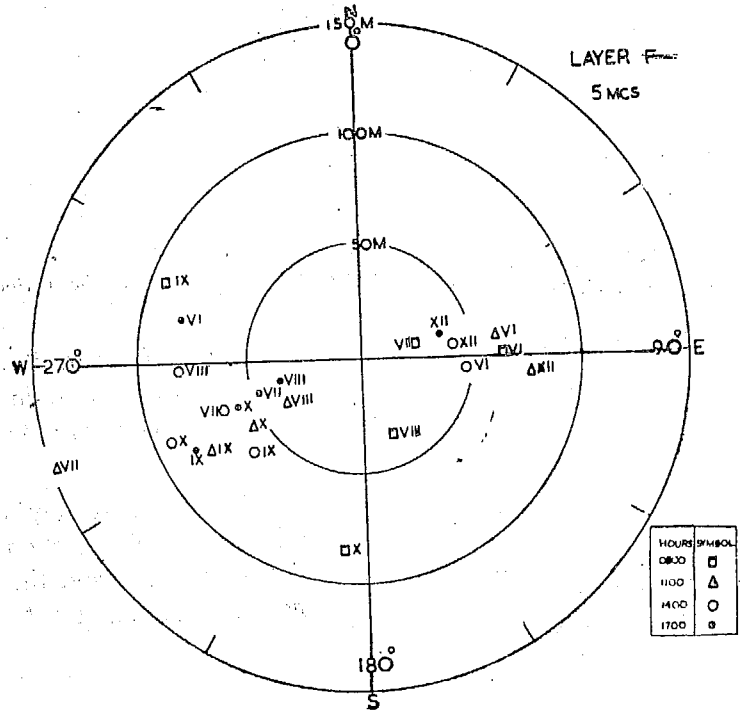

FIG. 14. Polar diagrams of drifts in the F region on 5 Mc./s. during the period June-December 1954 (Mr. N. G. Nanda).

* Extracted from Mr. N. G. Nanda's Thesis for the M.Sc. Degree of the Gujarat University.—K.R.R.

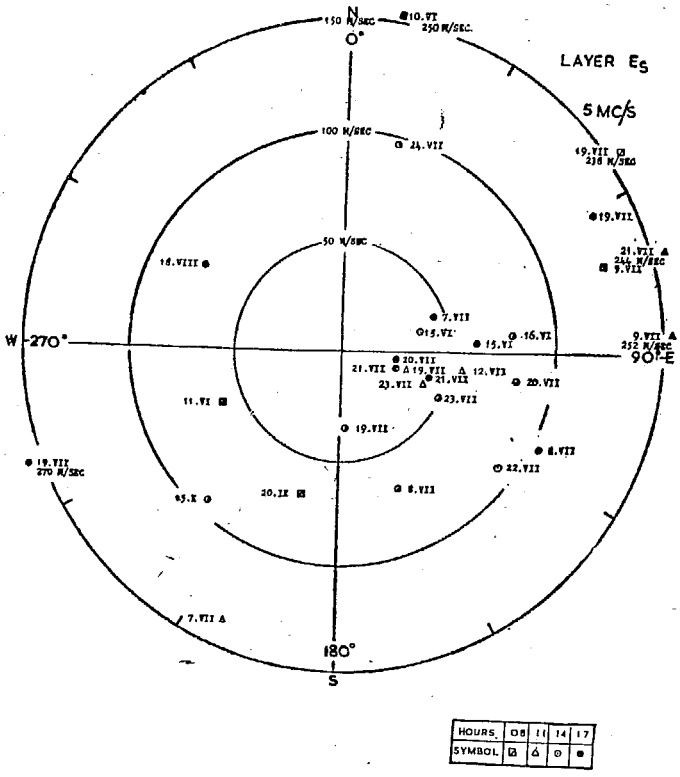

FIG. 15. Polar diagram of drifts in E_s on 5 Mc./s. during the period July–December 1954 (Mr. N. G. Nanda).

equally distributed between E and WSW and at 1700 hours it was mainly towards west. The most frequently occurring speeds were in the range 60–80 m./s. and the maximum and minimum speeds were 120 m/s. and 20 m/s. respectively.

The E_s observations were taken mainly in June and July 1954. The prevailing direction was towards east with individual directions between ENE and ESE. The usual speeds were around 50 m./s. and the scatter in speed distribution was greater for E_s reflections, speeds up to 250 m./s. being sometimes recorded.

APPENDIX II

Monthly Mean Vectors of Drift and Their Standard Deviations

By R. Sethuraman and S. K. Alurkar

The mean vectors V_R of the drift on 2·6 Mc./s. and their standard deviations (σ) were calculated for the various seasons. Since the number of observations was largest in the period 08 hours to 10 hours and in 17 and 18 hours representing morning and evening conditions, the calculations were confined to these hours.

The mean vector V_R.—The N-S and E-W components of the individual drift vectors were tabulated and their mean values for the two periods in each season computed. The mean vector was determined by vertical addition of the components. In the months April to August, more than one prevailing direction of drift was noticed and the data were therefore divided into two groups, and the mean vectors corresponding to each of the principal directions was found. In computing the mean vector, a small number of exceptionally large velocities was discarded.

The standard vector deviation σ is a measure of the dispersion of the vector round the mean value. A circle drawn with the centre at the end point of the mean vector, with radius σ, will include 63% of the observations. It is defined as the square-root of the mean square of the modulus of the vector deviations from the mean vector. If V_R is the mean vector, V the individual vector and

$$\vec{v} = \vec{V} - \vec{V}_R,$$

$$\text{then, } \sigma = \sqrt{\frac{\Sigma v^2}{N}}$$

It can be easily shown (H.M.S.O., 1953*) that

$$\sum \frac{v^2}{N} = \frac{\Sigma V^2}{N} + V_R{}^2.$$

Thus by calculating the square of the modulus of the velocities and V_R, σ can be calculated.

---

* *A Handbook of Statistical Methods in Meteorology*, H.M.S.O., London, 1953.

TABLE I

n, V_R, D, σ and q of ionospheric drifts over Ahmedabad on 2·6 Mc./s. Morning and Evening

Months	08–10 hours					17–18 hours				
	n	V_R m./s.	Mean D-degrees from N	σ	*q* Per cent.	*n*	V_R m./s.	Mean D-degrees from N	σ	*q* Per cent.
December 1956 to February 1957	96	84	317	45	68	59	62	304	27	65
March 1957 to May 1957	39 25	54 50	322 118	55 36	41	39	65	325	35	55
June 1957 to August 1957	46 42	60 63	51 307	51 44	34	32	62	311	55	45
September 1957 to November 1957	74 34	66 55	320 143	19 41	40	49	50	316	17	65

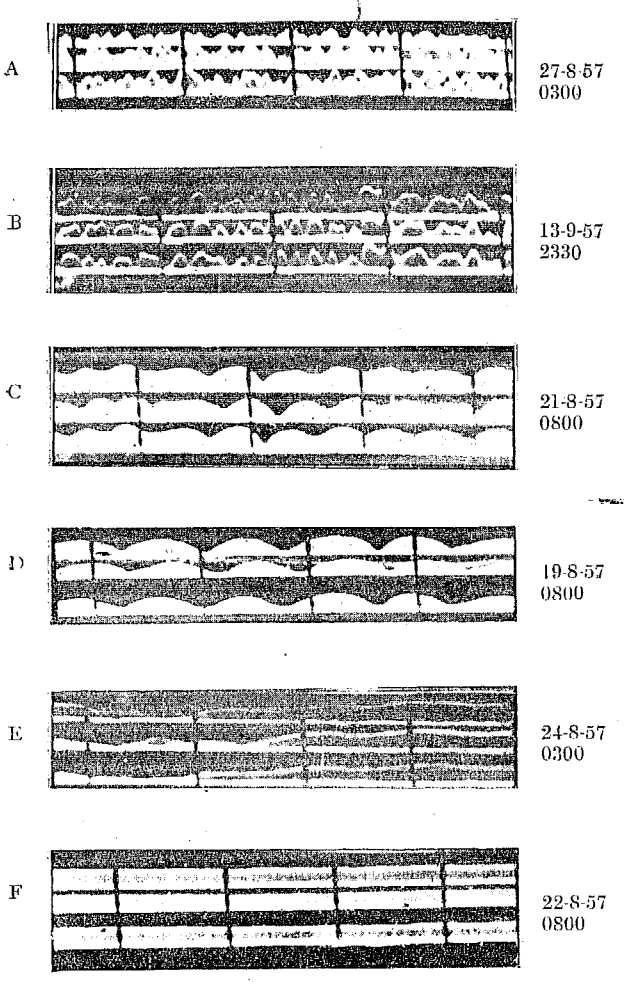

FIG. 1. Some fading patterns of drift at Ahmedabad on 2·6 Mc./s.

The constancy 'q' of the vector is defined by the equation $q = 100\ V_R/V_s$, where V_s is the scalar mean of the drift velocity for the period under consideration. When the drift takes place in the same direction throughout, V_R will be equal to V_s and the constancy is 100. When it is qually distributed in all directions with the same average speed, V_R is equal to zero and q is zero. Thus q is a measure of the variability of the drift.

The computed values of these quantities along with the number of observations in each case (n) are given in Table I. The value of σ is largest in summer and least in winter. It is also larger in the morning than in the evening hours in all seasons except summer.


BANGALORE
PRESS
BANGALORE
CITY

CHAPTER IV

1. Measurement of Ionospheric drift at Ahmedabad from fading patterns of Reflections on 2.6 Mc/s and 4.0 Mc/s ($23^{\circ}02'N$, $72^{\circ}38'E$) - Paper published in the Proceedings of the Indian Academy of Sciences, Vol. 47, 84-105 (1958).

2. Further measurements of Ionospheric drift at Ahmedabad and discussion of some features found from the observations.

Further measurements of Ionospheric drift at Ahmedabad and discussion of some features found from the observations.

Ionospheric drift observations made by the spaced aerial method over a period of 15 months in 1956-57 at Ahmedabad have been already described. (Sethuraman, 1958a). The observations were continued during the years 1957-1958 and the results found to be in general agreement with those obtained in the previous years. Observations on 2.6 Mc/s refer to the E layer during day time and to F layer during night time and those on 4.0 Mc/s refer to the day time F region. Reflections from sporadic E layer obtained during night hours are not included in those reports. In this note, the general features of the drift at Ahmedabad are presented together with some other special features observed.

General features of drift at Ahmedabad (Figs. 1-4) :

Ionospheric drifts at Ahmedabad exhibit seasonal as well as diurnal changes in velocity. In winter, the prevailing direction during the day time is towards NW, but in summer, the day time direction shows a change, the east-ward drift in the morning hours changing to a north-westward drift in the after noon hours. This change is also shown in the equinoctial months, but on fewer occasions. At night, the prevailing direction is either towards SW or NE. It will

Direction

Velocity

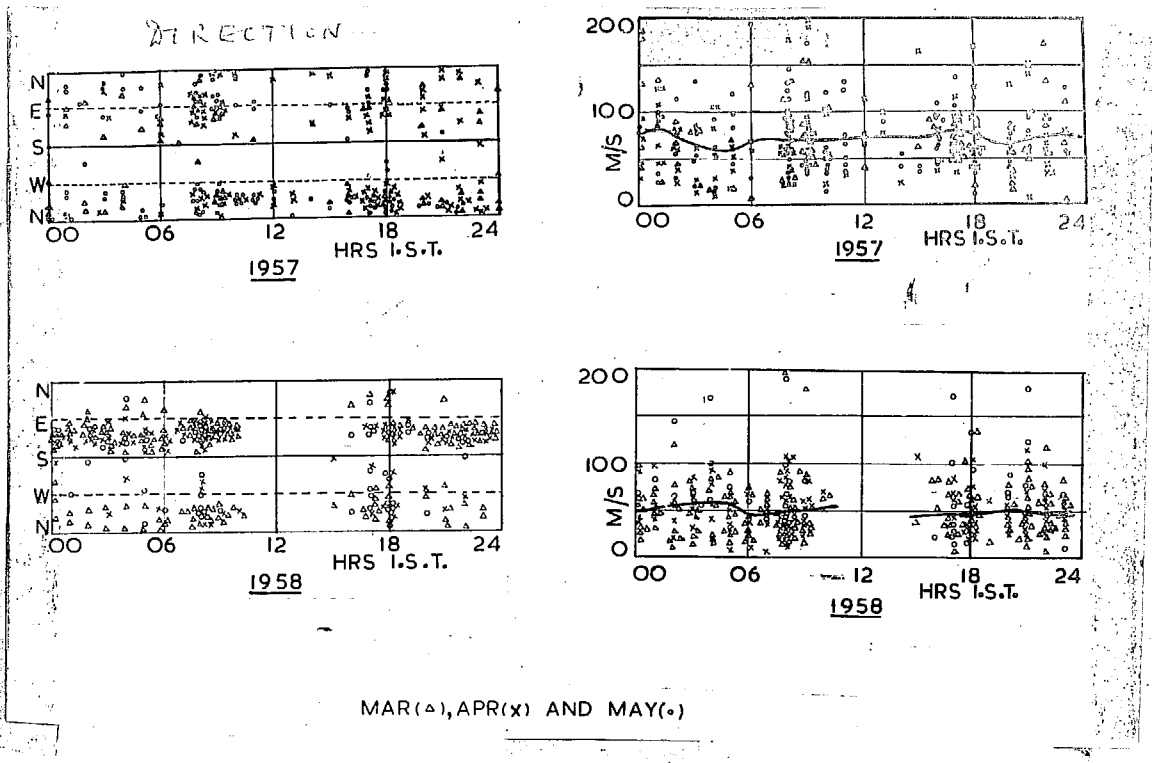

Fig. 1 - Ionospheric drifts at Ahmedabad in 1956-57 and 1957-58 2.6 Mc/s - Winter

be seen that consistent change were observed in both years of study. It is unfortunate that the day time change in the direction of the drift could not be followed on many days during the years 1956 - 1958, owing to heavy absorption in the middle of the day. Only in the winter of 1958-1959, observations could be obtained throughout the day on a few days, when fifteen minutes observations were made in order to follow the changes of the drift direction and speed. On some of these days a quick change in the direction of the

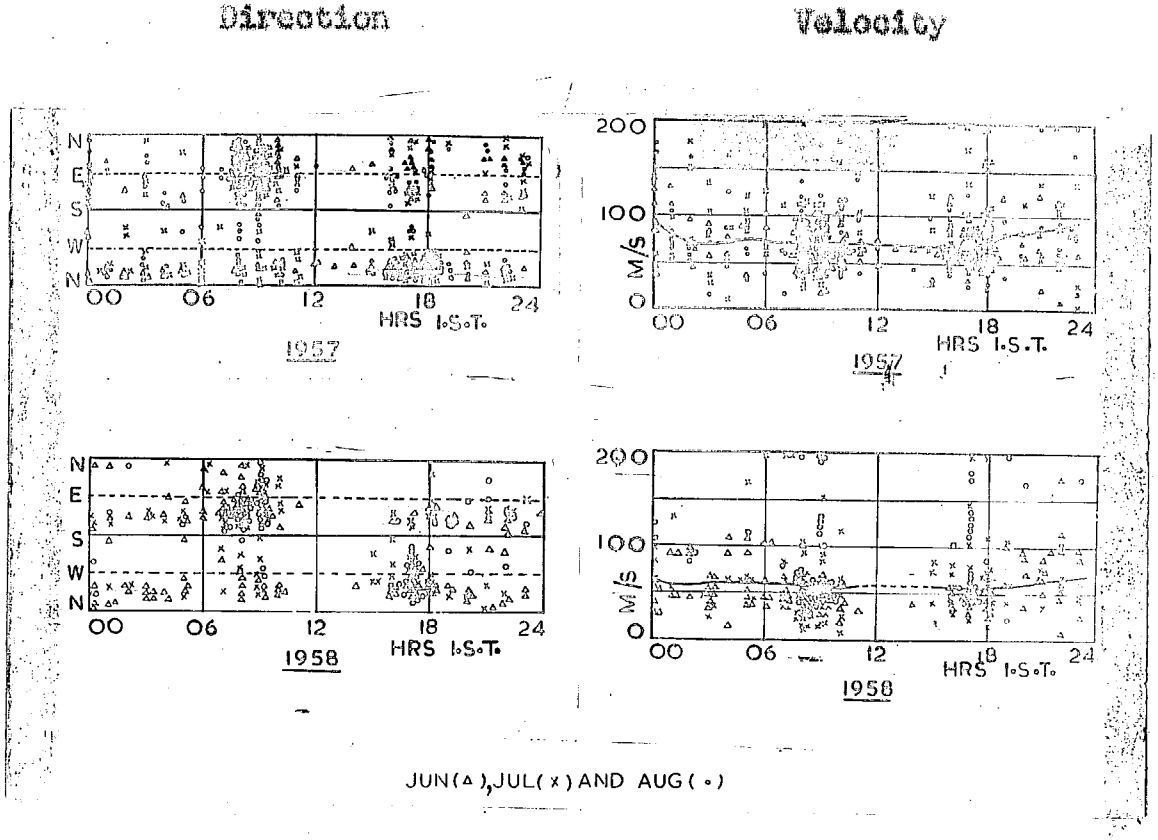

Fig. 2 - Ionospheric drifts at Ahmedabad in 1956-57 and 1957-58. 2.6 Mc/s - Summer

drift was noted during the day time (Fig.3) but on other days the direction remained towards NW throughout the day. The abrupt change was found to occur in the fore-noon of those days, the actual hour of occurrence differing from day-to-day.

The speeds were generally larger in winter than in summer. The dispersion in the values of the speeds were also larger in winter. This is in conformity with the observations of other workers. No large diurnal changes in the drift speeds were noticed, but in winter significant

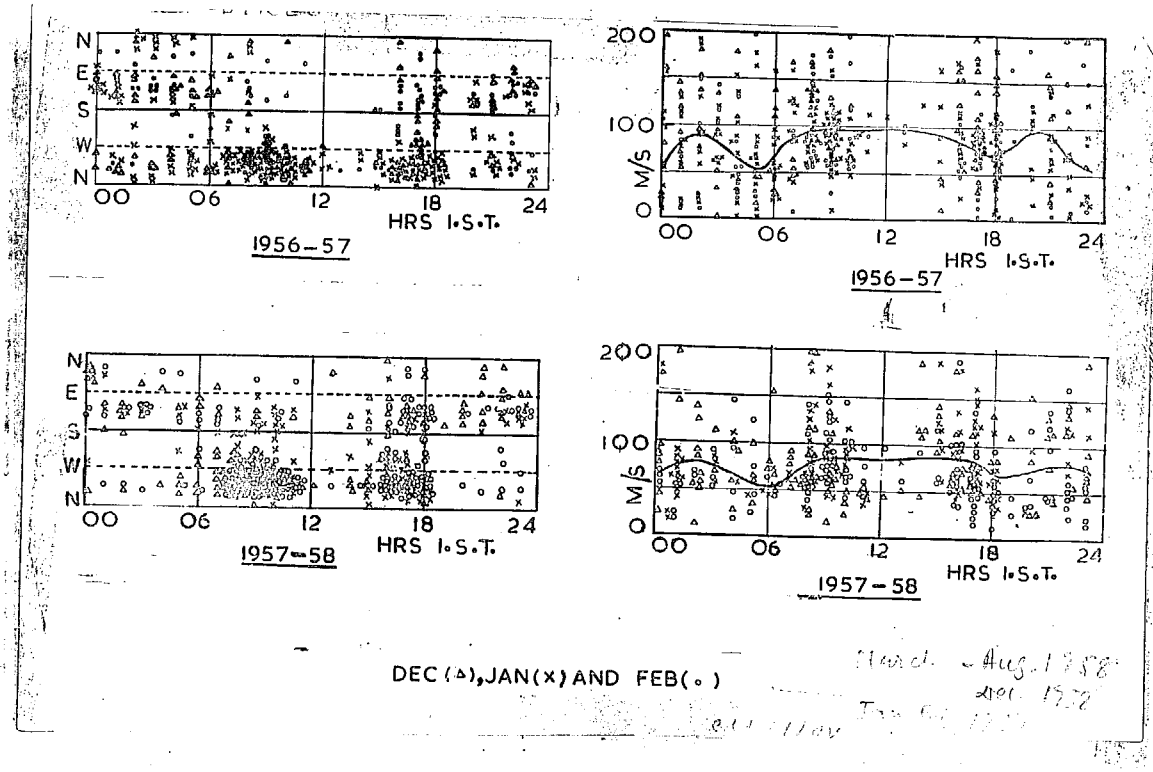

Fig. 3 - Ionospheric drifts at Ahmedabad in 1956-57 and 1957-58 2.6 Mc/s - Spring

decreases were observed near sun-rise and sun-set. These decreases were found in both the years.

Drift observations on two frequencies near each other :- On a few days, in the winter of 1958-59, observations were taken on 2.4 Mc/s and 2.6 Mc/s within three minutes of each other. Waves of these two neighbouring frequencies would be reflected from the ionosphere at two slightly different levels. It was found (Fig. 5) that the two velocities differ slightly both in magnitude and in direction. In general, the speeds on 2.6 Mc/s were found

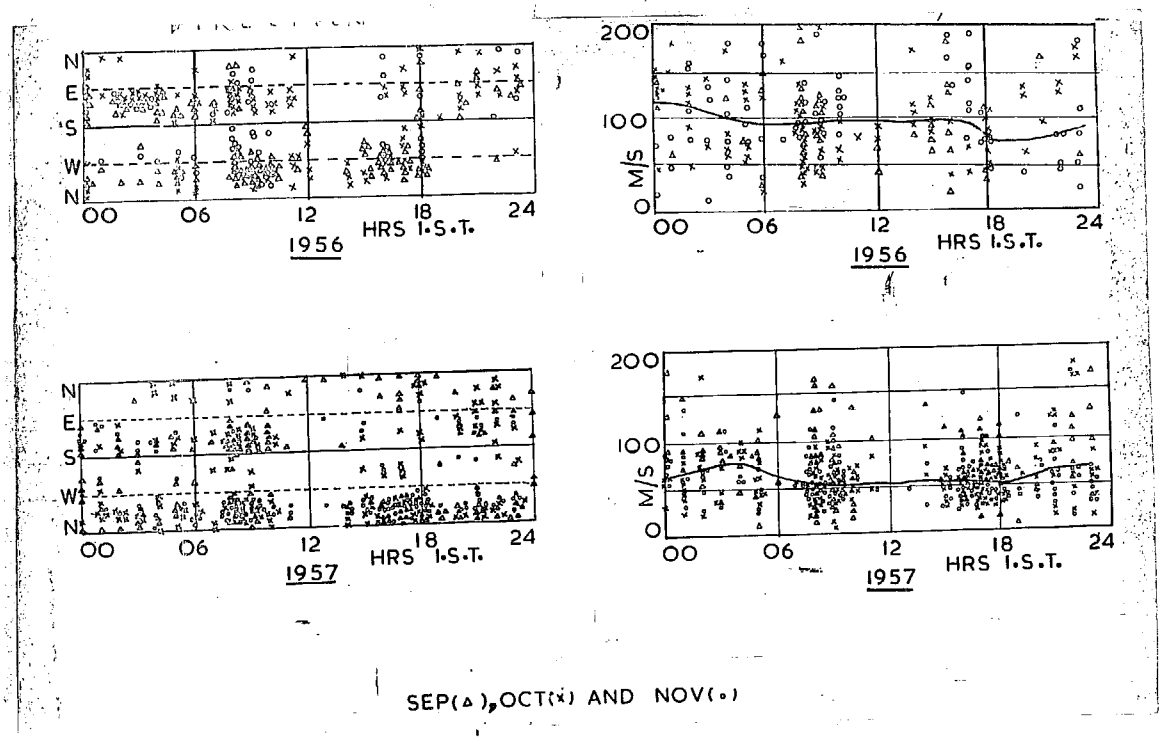

Fig. 4 - Ionospheric drifts at Ahmedabad in 1956-57 and 1957-58. 2.6 Mc/s - Autumn

to be a little larger than those on 2.4 Mc/s. The changes in the directions were similar, but took place at slightly different times. These observations are being continued.

Correlation of the wind vector obtained on 2.6 Mc/s and on 4.0 Mc/s :- Observations of drift during day time were made on these two frequencies within three minutes of each other during the years 1957-58. It was found that they showed similar trends in seasonal and diurnal variations. On many occasions, the speeds and the directions observed were found to be the same. The individual observations at

Direction Velocity

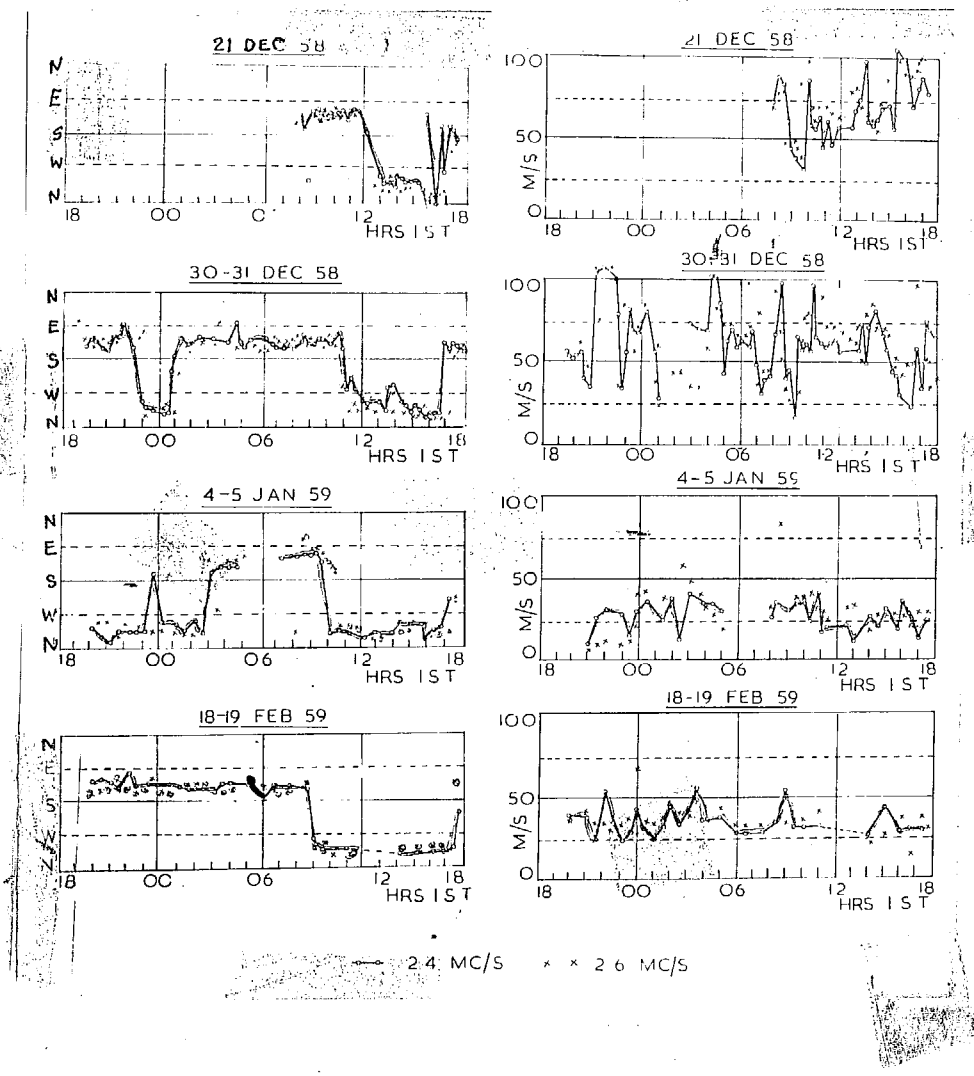

Fig. 5 - Daily variations of drift direction and speed on individual days in December 1958 to February 1959.

those frequencies are plotted in Fig. 6 (Directions) and in Fig. 7 (Speeds). It will be noticed that there is a tendency for the points to lie along the diagonal, indicatin that the directions found for the drift observations at the

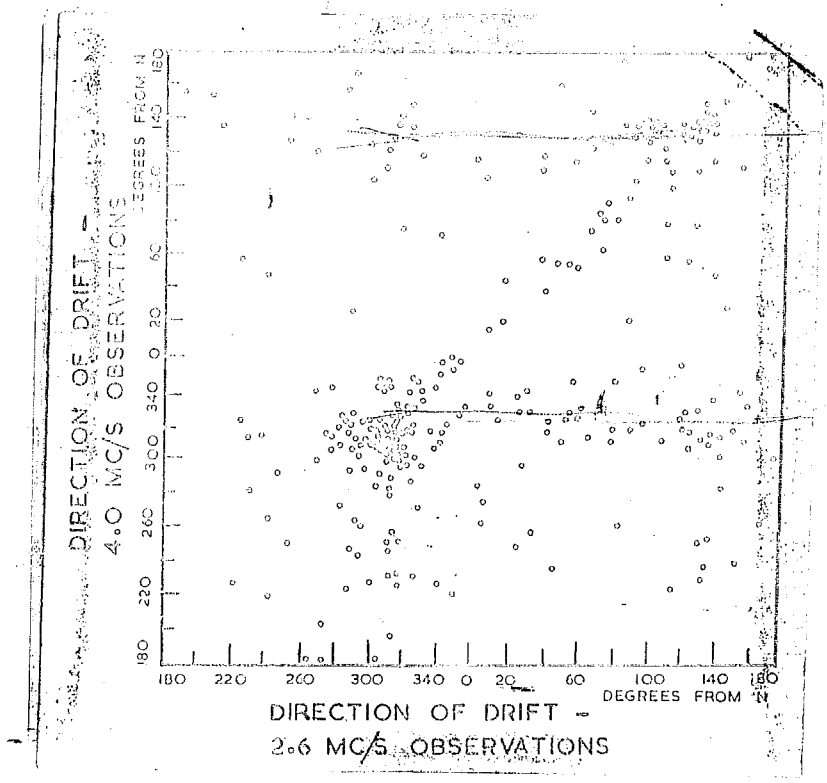

Fig. 6 - Correlation of speed directions on 2.6 Mc/s and 4.0 Mc/s.

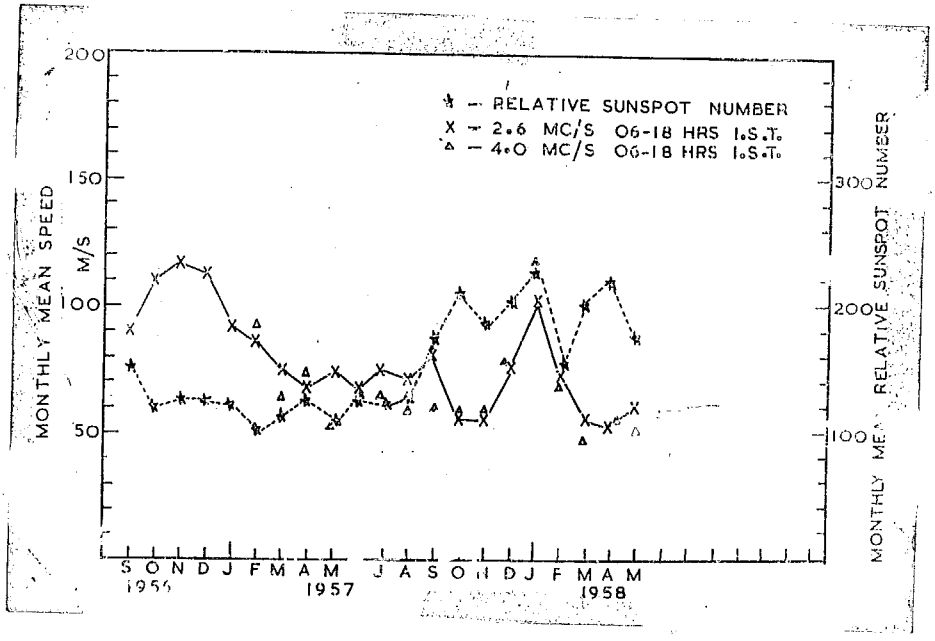

Fig. 7 - Speed of drift on 2.6 Mc/s vs. speed of drift on 4.0 Mc/s.

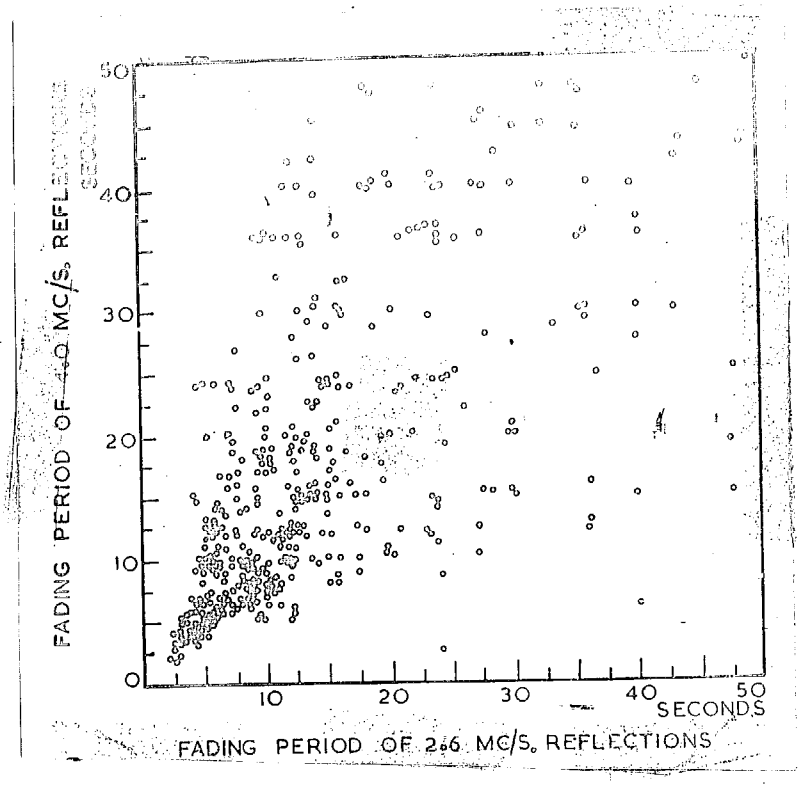

Fig. 8 - Fading period of 2.6 Mc/s reflections vs. fading period of 4.0 Mc/s reflections.

two frequencies were, on a number of occasions, the same. There was also a significant number of occasions when the drift on 2.6 Mc/s was south-eastward, while the drift on 4.0 Mc/s was in the opposite direction. Such days occurred mainly during spring and autumn, as reported earlier (Sethuraman, 1956a). Fig. 7 shows that there are no clear differences between the two frequencies as regards speeds.

It was also noticed that on many occasions the fading period of the 2.6 Mc/s reflections was about the same as that of 4.0 Mc/s but there was a tendency for the 4.0 Mc/s period to be larger. The average fading period was found by averaging the times between successive maxima

in the record. A wide range of fading periods from 5 to 15 Mc/s was found for the reflections of both frequencies. This will be seen from Fig. 8, in which the fading periods on the two frequencies obtained from records taken within three minutes of each other are plotted. It will be seen that while the dispersion of the points is large for large fading periods, there is a clear correlation between the periods at times of quick fading. It is also interesting to note that short period fading is more common during magnetically quiet conditions (Sethuraman, 1950b).

Effect of sunspot number on the drift speed :- The monthly mean speed of drift on 2.6 Mc/s and 4.0 Mc/s are plotted in Fig. 9 together with the mean sunspot number for the same months. It is found that there is a rough inverse relationship between the monthly mean sunspot number and the

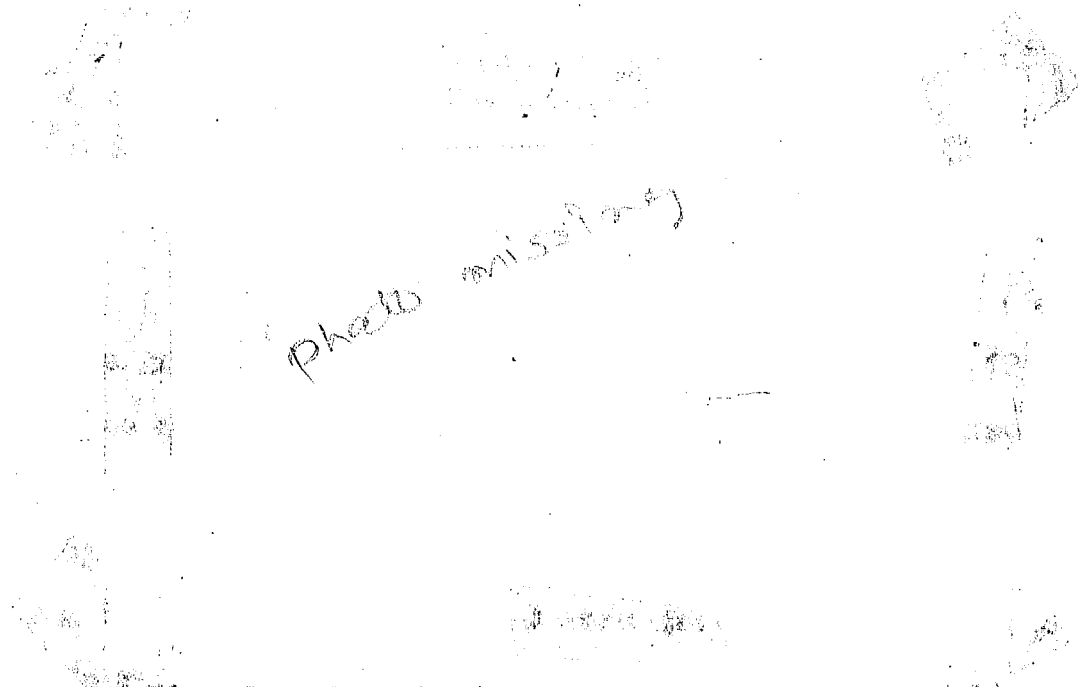

Fig. 9 - Monthly mean speed and monthly mean relative sunspot number.

mean speed of drift. The annual variation of the daily mean speed seen in Figs. 1-4 can also be attributed to the variation in the sunspot activity during the years. The dependence of the mean speeds on individual days on the days sunspot number was examined by plotting the mean speed from the day hourd observations on 2.6 Mc/s against the value of the daily relative sunspot number supplied

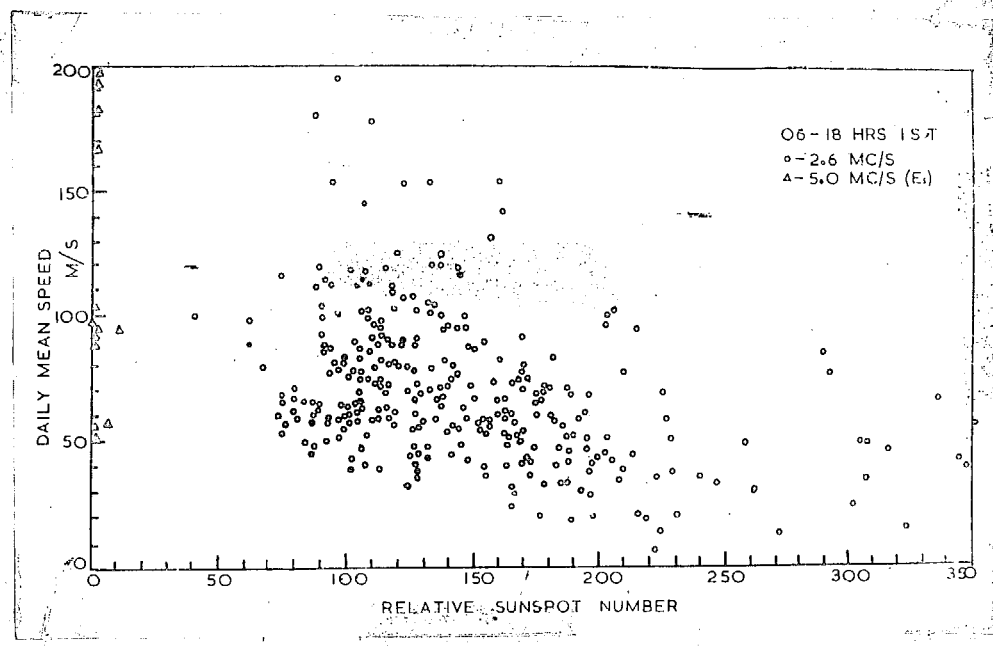

Fig. 10 - Daily mean speed vs relative sunspot number.

by the Astrophysical Observatory, Kodaikanal (Fig. 10). It will be seen that drift speed decreases with increase in the relative sunspot number. Such a trend is absent altogether in the night-time observations, and is present to a small extent in the 4.0 Mc/s day-time observations. These refer to a period of high sunspot activity (Sept. '56 - Mar. 58). To study the behaviour in low sunspot years, the

observations of Mr.M.C.Nanda on 5.0 Mc/s reflections in 1954 (no reflections) are also plotted in Fig. 10. They are on the extreme left of the figure and are represented by triangles. It will be seen that there is no clear continuity in the relationship. Moreover, the number of observations during 1954 was very small. Further observations are needed to study the behaviour in low sunspot years.

An attempt was made to correlate the drift speeds with magnetic activity, as defined by the value of C_p. Various workers in middle and high latitudes have found that speeds in the E region are independent of the magnetic activity, provided, the activity is not too high and that drift speeds in the F layer increase rapidly with magnetic activity (Chapman, 1952; Millman, 1952; Briggs and Spence, 1954; and others). At Ahmedabad, with 4.0 Mc/s, no such dependence could be found.

Summary

The general features of ionospheric drift measured at Ahmedabad by the spaced receiver method during the years 1956-58 are summarised. The direction of the drift is found to show seasonal as well as diurnal changes. The speeds are larger in winter than in summer, but do not show any significant diurnal changes except in winter when decreases in speed are observed at times of sunset and sunrise. Nearly simultaneous observations on two neighbouring frequencies

indicate the presence of an increase of drift velocity with the increase in the height of reflection in the E layer. The correlation of the drifts measured with 2.6 Mc/s and with 4.0 Mc/s is examined. It is found that the directions observed on both the frequencies are nearly the same on many occasions. The speeds, however, show no clear relationship. An examination of the fading periods at these frequencies indicates a good correlation when the fading is quick. The speeds of drift during the daytime showed an inverse relationship with sunspot number during the period September 1956 to March 1958. Such a relationship could not be found in the night time observations. No dependence of drift speed on magnetic activity was found when observed with waves of 2.6 Mc/s and 4.0 Mc/s.

References

Briggs, B.H. & Spencer, M	1954	Rep. Progr. Phys. 27, 245.
Chapman, J.H.	1952	Canad. Jour. Phys. 31, 120.
Hillman, G.M.	1952	Sc. Rep. Ionos. Res. Lab. Penn. State University.
Sethuraman, R.	1958a	Proc. Ind. Acad. Sc. 47, 84.
Sethuraman, R.	1958b	Jour. Sc. Ind. Res. 17A, Supplement, 50.

CHAPTER V

Rates of Fading of Reflected pulses of vertically incident electromagnetic waves at Ahmedabad on 2.6 Mc/s and 4.0 Mc/s - Paper published in the Journal of Scientific & Industrial Research, Vol.17A, Supplement pages 50 - 59 (1958).

Reprinted from the
Journal of Scientific & Industrial Research, 1958, Vol. 17A, No. 12, Supplement, pp. 50-53

Rates of Fading of Reflected Pulses of Vertically Incident Electromagnetic Waves at Ahmedabad on 2·6 & 4·0 Mc/s.

R. SETHURAMAN
Physical Research Laboratory, Ahmedabad

IONOSPHERIC drift measurements have been made at the Physical Research Laboratory, Ahmedabad, since 1954 from fading records obtained with spaced aerials[1]. The present note summarizes the results of a study of the variations of the fading periods of signals due to various factors during the period October 1956 to March 1958.

The quantity studied is the average fading period in definite intervals. This is found by counting the number of peaks in the pattern over a given time and finding the average interval between two peaks. A wide range of fading periods, from one second to over a minute, has been found. In some instances, the peaks are so flat that no accurate estimate of the period could be obtained. Steady signals were treated as signals with infinite fading period.

Diurnal variation of the fading period

The daily observations during the entire period were grouped into four quarters of the day, 00-06 hrs representing the pre-dawn second half of the night, 06-12 hrs representing the first half of the day, 13-18 hrs representing the second half of the day and 19-23 hrs representing the first half of the night. The fading periods were grouped in the ranges 0-5 sec., 6-10 sec., 11-15 sec., etc. As it was difficult to determine periods greater than 30 sec. with any accuracy, they were broadly grouped as 31-90 sec., 90-200 sec., >200 sec., and steady signals. It was noticed that the normal fading periods for vertically incident signals were 5-15 sec. Fig. 1 gives the percentage occurrence of the various fading periods in the different quarters of the day. The fading periods were, in general, greater in the afternoon than in the morning hours. Very slow fading was sometimes observed in the nighttime. Quick fading (less than 5 sec.) was least frequent between 14 and 18 hrs and most frequent during night. The occurrence of steady signals was found to be a maximum around sunset and a minimum in the morning hours after sunrise.

Seasonal variations in the fading period

The year was divided into four quarters, corresponding roughly to the four seasons, and the fading periods were arranged as for

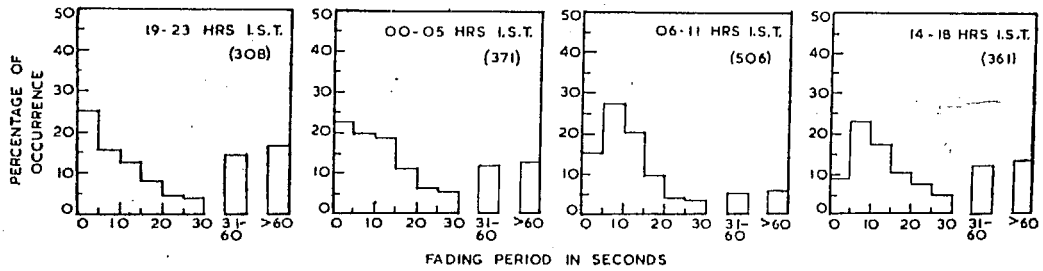

FIG. 1 — DIURNAL VARIATION OF THE FADING PERIODS OF 2·6 MC/S. REFLECTIONS
[Figures in parentheses indicate the total number of observations]

the study of the diurnal variations. No significant seasonal trends were observed in the fading periods.

Fading periods and geomagnetic activity

Many workers have reported a dependence of the fading period of F_2 reflections on geomagnetic activity. It was desired to find whether any relationship existed for reflections on 2·6 and 4·0 Mc/s. at Ahmedabad. In Fig. 2, the mean fading periods for day and night are plotted against the value of the index for geomagnetic activity, C_p, for the corresponding day. It will be seen that, in general, there is an increase of the fading period with geomagnetic activity. The sensitivity of the E and F layers to geomagnetic activity, as determined by the slope of the line joining the medians of fading periods for various values of C_p, shown by thick lines in Fig. 2, is not the same. The maximum effect is seen in the reflection of 2·6 Mc/s. signals during 19-05 hrs (nighttime F_2 layer), while reflections from the daytime E layer are least affected. The scatter of points is also larger for the F layer reflections than for the E layer reflections. Various workers[2,3] in the middle latitudes have reported a dependence of the fluctuation amplitude of scintillations of radio-star with geomagnetic activity. Millman[4], working on 75 kc/s., got fading periods up to 8 min. and found that rapid fading was associated with large values of C_p.

No clear relationship has been found between the fading period and the sunspot number.

Fading period and spread F — A very close relationship is found to exist between the fading period and the amount of spread F present in the p'-f records at about the same time. p'-f records are normally taken hourly at Ahmedabad with an automatic ionospheric recorder. These records, however, are timed at full hours corresponding to 75° EMT, while the drift observations are timed at full hours corresponding to Indian Standard Time. There is a difference of half an hour between the two records. Records corresponding to the same nominal hours were compared.

The ionospheric p'-f records are grouped into four classes, depending on the amount of spread present. Table 1 gives the classification adopted for the purpose.

This classification is similar to the one adopted by Wright *et al.*[5] and Briggs[6] and

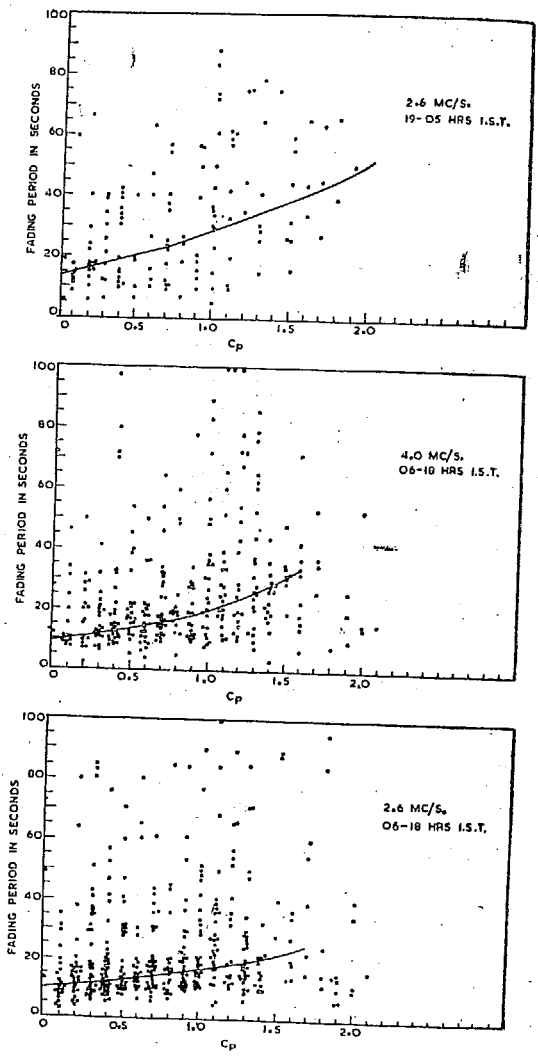

FIG. 2 — FADING PERIOD OF PULSE REFLECTIONS AND GEOMAGNETIC ACTIVITY

TABLE 1 — CLASSIFICATION OF p'-f RECORDS

F-SCATTER INDEX	NATURE OF F-SCATTER
0	No spread observed
I	A slight amount of spread is present, and the ordinary and extraordinary critical frequencies can be distinguished
II	The spread is so much that the ordinary and the extraordinary critical frequencies cannot be accurately estimated
III	Complete spread F_2

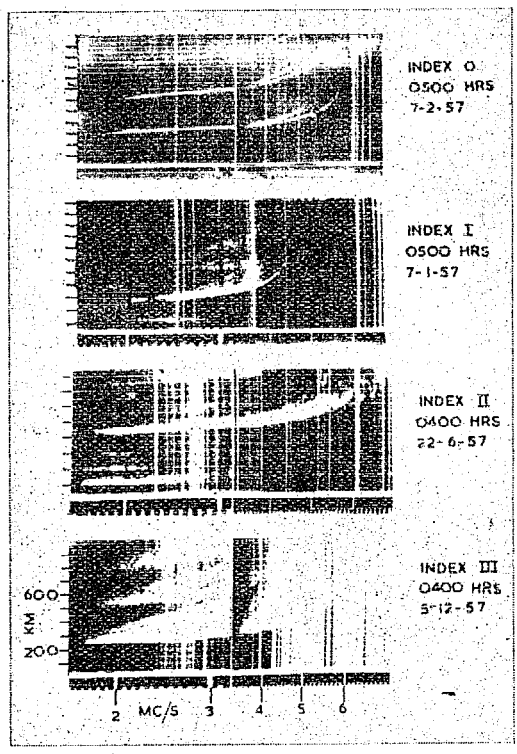

FIG. 3 — INDEX NUMBERS OF F_2-SCATTER WITH SAMPLE IONOGRAMS

others. Typical p'-f records to illustrate the classification are shown in Fig. 3. No doubt the amount of spread F present depends on the sensitivity of the receiver also, but the latter was maintained reasonably constant throughout the period.

The fading periods of pulse reflections, when each of these kinds of spread were present, were analysed. Fig. 4 gives the histograms of fading periods for the various indices of spread F_2. The mean values of the fading periods for each of these indices are also given in the diagrams. It will be seen that during periods of large spread (index III), the fading was most rapid (0-5 sec.). During periods of complete spread, the rapidity of fading was as much as 1 per sec. Under such conditions, it was difficult to select any particular echo for study with the finite resolution of the gate of the equipment. The records from the three spaced aerials under such conditions show no correlation among themselves and are useless for drift analysis. These indicate that under conditions represented by large spread F, intense short period turbulence is present in the ionosphere. In general, fading period decreases with the amount of spread present in the records.

An attempt was made to study the relationship between the speed of drift and the fading

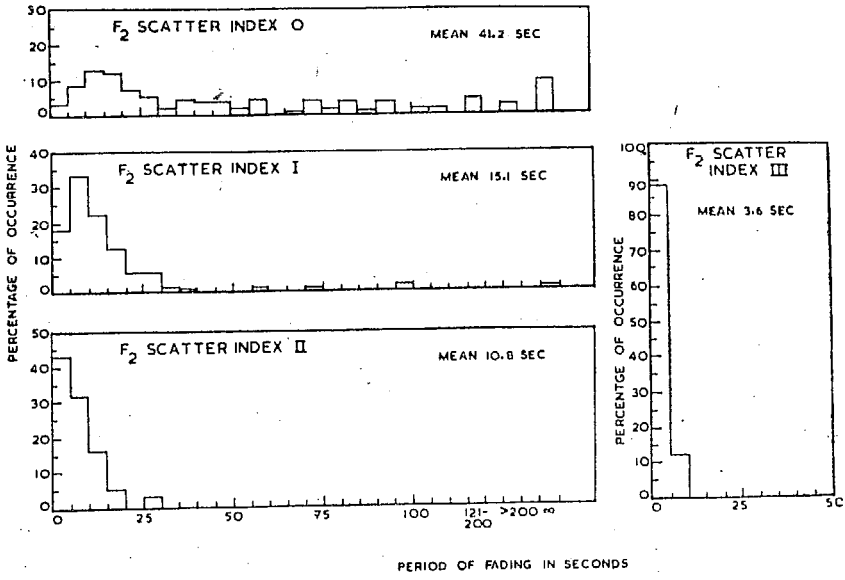

FIG. 4 — FREQUENCY OF OCCURRENCE OF FADING PERIOD VS F_2-SCATTER INDEX

1. Harang and Pederson[7] and others reported decreased fading periods with ısing speeds. No such clear relation- ould be found from the observations at dabad. There was also no relationship en the fading period and the height of ion.

ıary

ıe of the characteristics of the fading l of vertically incident pulse signals 5 and 4·0 Mc/s. are reported. It is that rapid fading, with periods below occurs mostly during the night hours. lear seasonal changes are evident. ıding periods are found to show some dence on magnetic activity, low values ɔeing generally associated with quicker . The nighttime F_2 layer is found sensitive to changes in magnetic acti- the daytime E layer does not show ıarked effect. *The fading periods of F_2 reflections have a marked correlation ıe amount of spread F present in the p'-f records, large amounts of spread being associated with quicker fading.*[1] No relationship between fading period and the speed of drift or the height of reflection was noticed.

Acknowledgement

The author is deeply grateful to Prof. K. R. Ramanathan for suggesting the analysis and guiding the work. He is thankful to Dr U. D. Desai for his interest in the work. The scheme is in receipt of financial assistance from the Council of Scientific & Industrial Research, New Delhi.

References

1. Sethuraman R., *Proc. Indian Acad. Sci.*, **48** (1958), 86.
2. Dagg, M., *J. atmos. terr. Phys.*, **10** (1957), 194.
3. Hewish, A., *Proc. roy. Soc.*, **214A** (1952), 494.
4. Millman, G. H., *Sci. Rep. ionos. Res. Lab. Pennsyl. St. Univ.*, No. 37, 1953.
5. Wright, R. W., Koster, J. R. & Skinner, N. J., *J. atmos. terr. Phys.*, **8** (1956), 340.
6. Briggs, B. H., *J. atmos. terr. Phys.*, **12** (1957), 34.
7. Harang & Pederson.

CHAPTER VI

A comparison of Ahmedabad results with those obtained at other places.

CHAPTER VI

A COMPARISON OF AHMEDABAD RESULTS WITH THOSE OBTAINED AT OTHER PLACES

1. Observations of ionospheric drift have been made at a number of places by the spaced receiver method. The region directly below the E region of the ionosphere has also been studied by meteor methods. The object of this chapter is to compare the results obtained at Ahmedabad with similar results obtained at other places and study some of the general features.

2. There are a few important considerations which should be borne in mind when attempting a comparison of the results obtained at the different places. So far as the E region is concerned, most of the stations have employed the spaced aerial method with closely spaced receivers. These operate on a frequency of 2 - 2.6 Mc/s. During the day time between 0700 and 1700 hours when the E layer is present, the reflections take place at 100-110 km. The Ahmedabad results during the day time can be directly compared with similar day-time results elsewhere. Observations taken on 2 to 2.6 Mc/s. during the night-time are generally reflected from the F layer or from Es patches. The range of variation of the level of Es is greater than

that of E but its level is rarely more than 130 km. The height of the F layer is however very different from that of the E layer. For example, at Ahmedabad the height of the E layer varied from 100 to 120 km during the day, while h'F at night varied from 210 km to 390 km in 1957 depending on the hour of the night and the month. There is little significance in finding a diurnal or semidiurnal wave by combining the 2.6 Mc/s drifts during the day and night in one group. Most of the night-time observations in Ahmedabad were made on the F layer and it is better to treat the day-time and night-time drifts separately.

3. It is known from the meteor observations (Greenhow, 1955; Elford, 1959) that between 80 and 100 km the wind velocity varies with height. Simultaneous observations on two frequencies near each other, which were made by Jones (1957) at Cambridge and by the author at Ahmedabad on a few days during the winter of 1958-59 have shown only a small difference in speed between the drifts obtained with the two frequencies when they are well below the critical frequency of the layer. However, as the exploring frequency approaches the critical frequency of the layer and reflections take place from a higher layer, it would be difficult to say which of these two layers is responsible for the fading pattern, since the wave would be presumably affected by both of them. This question was examined by Booker (1955) who concluded

that the fading is superimposed at the level at which local wave length is six or seven times the free space wave length. This would mean that the irregularities whose motions are studied are situated in a region within a few percent of the level of critical reflections.

Reflections obtained with 4 Mc/s during day-time would be affected by the E layer. Although the actual reflections may be from the F layer, the double passage through the E layer would seriously affect the intensity of the reflected wave. The author (chapter IV of this thesis) took near-simultaneous observations (within three minutes of each other) on 2.6 Mc/s and 4.0 Mc/s during day-time on many days in 1957-58. Reflections were obtained from E on 2.6 Mc/s and from F on 4.0 Mc/s. It was found that on many occasions, the directions of drifts obtained with these two frequencies were the same, though the speeds showed considerable differences. This might have been due to the fact that 4.0 Mc/s being nearer the critical frequency of the E layer, the waves that passed through it suffered deviative absorption. The drifts observed on 2.6 Mc/s would refer to the lower E layer, while those on 4.0 Mc/s would be affected by both the movements of the F layer above and by the main part of the E layer.

4. Observations made at Ahmedabad during the winter of 1958-59 (chapter IV of this thesis) also showed that on many days a rapid change of drift took place in the

forenoon and that the hours of this change varied from day to day. L. Harang and K. Pederson (1956), refering to observations on E and Es echoes at Kjeller, say "There is a sudden change in the direction of the E-E component in the morning and in the afternoon at about the time when the critical frequency of the normal E layer crosses the test frequency, 2.0 Mc/s". The study of individual day's winds is of great importance before trying to study them by harmonic analysis.

5. At a tropical station like Ahmedabad, and in the high sunspot years 1957 and 1958 we have found difficulty of heavy day-time absorption round noon hours. It has not been possible with the transmitter power that was available to obtain observations more or less uniformly distributed round the clock.

6. Methods like those of Findlay (1953) employing changes in phase path, back scatter echoes (Clerk and Peterson, 1956) or the study of movements of Es patches over widely separated stations (Gerson, 1949) which have also been used for estimating drifts in the E region do not provide us with data which can be compared directly with those obtained at Ahmedabad and have not been considered in the following sections.

7. These difficulties and also the paucity of data over wide regions of earth are handicaps in forming a coherent picture of the drift circulation in the

ionosphere even in a limited height range.

7. Observations of ionospheric drifts by the closely spaced receiver method over sufficiently long periods of time to enable a proper comparison are available for a few stations at the present time. In particular, data are available for Cambridge (1949-52) (Briggs & Spencer, 1954), Kjeller (1953-55) (Harang and Pedersen, 1956), Neuf-Brisach in W.Germany (Harnischmacher and Rawer, 1957) and Washington (Salzberg and Greenstone, 1951) in the middle latitudes of the northern hemisphere and Brisbane (1952-54) (Burke and Jenkinson, 1957) in the southern hemisphere. The Ahmedabad work (1956-58) has provided some useful data for the tropics. Limited amount of data also exists for Waltair (Rao et al, 1955) and Puerto Rico (Yerg, 1955). Data from meteor observations exist for Manchester (Greenhow, 1955), Adelaide (Hurley, 1956 and Elford, 1959) and Stanford (Manning et al, 1951). They refer to heights lower than 105 km and are particularly valuable for forming an idea of the changes of wind with height in the D region and the semidiurnal variations.

9. The following are some of the main features of wind drifts in the ionosphere.

(a) All the stations report mean speeds of 40-100 m/s and the speeds are larger in winter than in summer. Larger amounts of spread in the values of speed are observed in winter at most of the stations.

(b) The mean values of the zonal component of the drift shows some definite trends at all stations. The monthly mean values of the zonal components of the drift at noon in various months for Cambridge, Kjeller, Washington, Ahmedabad and Lower Hutt (New Zealand) are given in Fig. 1. Since the monthly mean values are not

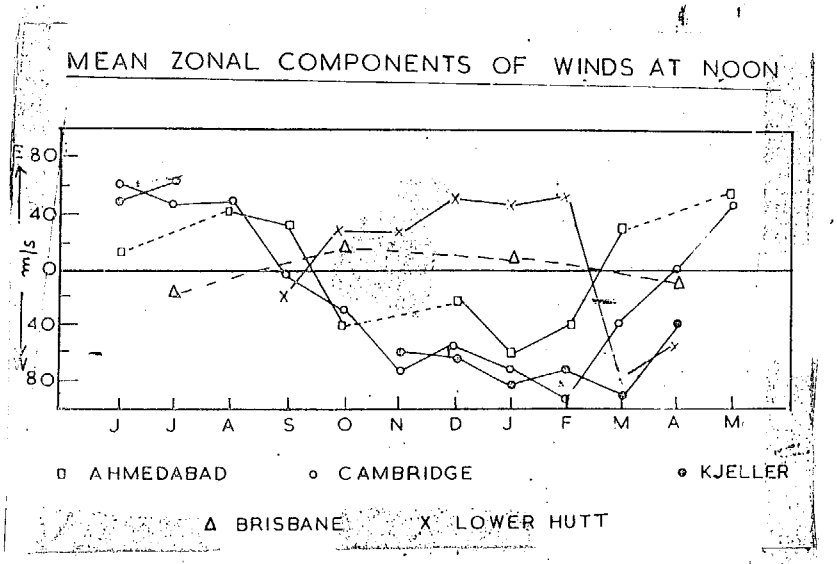

Fig. 1 - Mean zonal components of wind at noon.

available for Brisbane, the seasonal value, obtained from published curves of E-W component of drift are plotted in the same diagram. It will be noticed that in any given month, the noon zonal component behaves in opposite ways in the two hemisphere. In the summer hemisphere, it is eastward and in the winter hemisphere, westward. This behaviour is more pronounced in mid-winter and mid-summer.

(c) The values of the day-time ionospheric drift velocities (speed and direction) in the mornings and evenings are plotted for the different stations for winter

and summer in Fig. 2. Many stations, particularly in middle latitudes, exhibit gradual changes in direction of drift

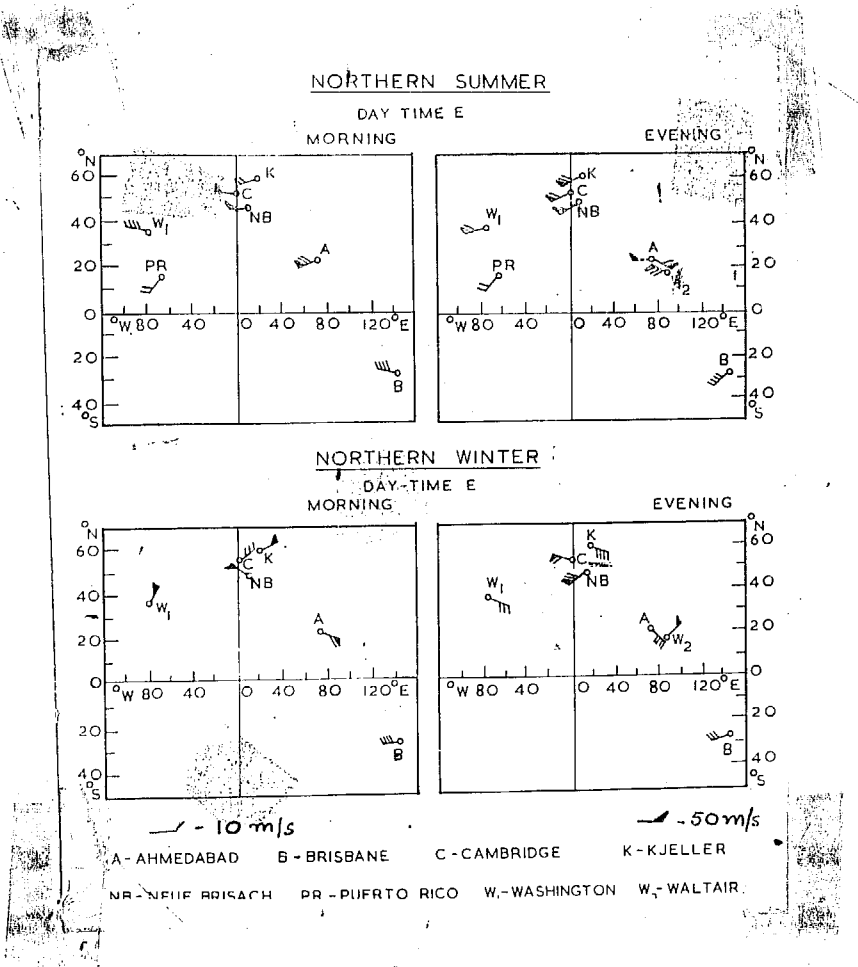

Fig. 2 - Drifts in the F layer of ionosphere in summer and winter.

during the day-time and the data are therefore divided into morning and evening hours. Due to the insufficiency of material, the Waltair data could not be so separated and are therefore plotted along with the evening data only. The Puerto Rico data were analysed by the correlation method and show small values of speed. The arrows in the diagram show the direction towards which the drift moves.

(d) While the day-time changes of drift directions take place gradually in middle latitude stations, they are abrupt at Ahmedabad.

(e) In summer, the wind drifts are generally towards the east throughout the day in middle latitudes, and in the mornings only in the low latitudes. In the evenings north-westward winds are more common at Ahmedabad. In winter, the drifts are westward, with a strong southward component in the mornings and northward component in the afternoons. In low latitudes, the prevailing movement is toward the west or north-west throughout the day.

10. Drifts in the F layer during night :- It has already been mentioned that the night-time measurements at Ahmedabad refer to the F layer and should therefore be compared with F layer data elsewhere. h'F undergoes much larger daily and seasonal variations than h'E. Variation with latitude is also greater.

The rapid change in the direction of drift which is observed to take place at Ahmedabad within an hour or two after sunrise and before sunset are undoubtedly due to change in the height of reflection. It is interesting to note that there is no very large change in the mean speeds of drift between day and night, although the scatter of values is larger with the higher level echoes.

The data obtained at Cambridge show that the

F layer drift during night is mainly westward with an added southward component during most of the year and a northward component in summer. In contrast to this, the a night-time drift at Ahmedabad in the F layer is primarily towards E to SE and secondarily towards NE in all the seasons except summer. In summer, the north-westward flow is as common as the eastward flow. In the southern hemisphere the measurements of Burke and Jenkinson show that the mean seasonal F layer night-time drifts over Brisbane are to the north in all seasons and to the west in all seasons except summer. That is, the general night-time drift is towards NW. In summer only, the drift in the first half of the night changes to north-eastward instead of north-westward.

At a lower latitude over Sydney (Munro, 1950) the drifts were found to be mainly towards the east with a strong northward component in southern winter and autumn, and southward component in southern spring and summer.

In both hemispheres, it thus appears that the prevailing drift is towards the west in middle latitudes, while it is towards the east in tropical latitudes. More data are required for an adequate discussion.

CHAPTER VI

REFERENCES

Booker, H.G.	1955	Jour. Atmos. Terr. Phys., 7, 343.
Briggs, B.H. and Spencer, M.	1954	Rep. Progr. Phys., 17, 245.
Burke, M.J. and Jenkinson, I.S.	1957	Austr. Jour. Phys., 10, 378.
Clerk, C. and Peterson, A.N.	1956	Nature, 178, 486.
Elford, W.G.	1959	Planet Space Science, 1, 94.
Findlay, J.W.	1953	Jour. Atmos. Terr. Phys., 3, 73.
Gerson, N.C.	1955	Jour. Met., 12, 74.
Greenhow, J.S.	1959	Phil. Mag., (Ser. 8), 1, 1157.
Harang, L. and Pedersen, K.	1956	Geophys. Publi. XII, No. 10.
Harnischmacher, E. and Rawer, K.	1956	C. R. Acad. Sc., 243, 782.
Huxley, L.G.H.	1957	Annals of I.G.Y. Vol. III, 250.
Jones, I.L.	1958	Jour. Atmos. Terr. Phys., 12, 68.
Manning, L.A. Villard, O.G. and Peterson, A.N.	1950	Proc. I.R.E., 38, 877.
Munro, G.H.	1950	Proc. Roy. Soc., A202, 208.
Rao, B.R., Rao, R.S. and Murthy, S.D.	1956	Jour. Sc. Ind. Res., 15A, 75.
Salzberg, C.D. and Greenstone, R.	1951	Jour. Geophys. Res., 56, 521.
Yeh, K.C.	1956	Jour. Atmos. Terr. Phys., 8, 247.

An isotropic ground pattern which changes as it moves has four velocities (Briggs et al, 1950). (1) The fading velocity :- This is the ratio of the space drift to the time drift necessary to produce equal changes in the amplitude of the pattern i.e. $Ve' = x_o/t_o$, where x_o and t_o satisfy the condition $\rho(x_o, 0) = \rho(0, t_o)$. (2) The drift velocity :- This is the velocity with which the observer must travel in order that he observes the slowest possible fading rate, due only to the internal random velocities of the cloud itself. This means that if he compares his signals at times t_1 apart and covers the distance ξ_o with such a velocity V that $\rho(\xi_o, t_1)$ is a maximum, $V = \xi_o/t_1$. (3) The characteristic velocity Vc :- This is the velocity which will be found by an observer moving with the velocity V defined above. This measures the random movements in the configuration. To this observer, the ratio of the ~~phase~~ space shift to the time shift needed to produce a similar change in amplitude is $Vc = x_o/\tau_1$. (4) The apparent drift velocity V' :- If we examine the fading records of receivers separated by ξ_o, we find that the maximum correlation is found for a certain time shift τ_o. The apparent velocity V' is defined as ξ_o/τ_o. If τ_{ox} and τ_{oy} are the time shifts for maximum correlation for the two sets of aerials, and a and b, the two separations, we obtain, $V_x' = a/\tau_{ox}$ and $V_y' = b/\tau_{oy}$, from which the apparent drift speed and direction could be found.

From the correlation coefficients determined by

formulae (12) and (13) we can determine the time τ' to obtain the same cross-correlation coefficients between any two aerials as is obtained for the auto correlation coefficient with a time lag τ. Briggs et al show that

$$\tau'^2 - \tau^2 = (\xi_0^2 - 2V_x \xi_0 \tau) / V'c^2 \qquad (14)$$

Thus, by plotting $\tau'^2 - \tau^2$ against τ and drawing the best straight line passing through the points, the values of V_x and Vc' can be obtained from the intercepts on the two axes. From a similar curve for the other two sets, V_y and Vc' can be determined. Thus, V and Vc' can be calculated. We also have

$$Vc'^2 = Vc^2 + V^2 \qquad (15)$$

from which Vc can be obtained.

The authors assume that the contours of constant correlation are ellipsoids. While this is possibly so for small values of separation and time shifts, it may not be so for larger values of these quantities.

Yeh's method (1955) :- This method, called by its author the six-point correlation method is a simplification of the previous method. In the original method of Briggs et al, a large number of correlation coefficients have to be determined thereby making the calculations laborious. This method, on the other hand, requires the evaluation of only six correlation coefficients and thus shortens the analysis considerably. Equation (13), defining the cross-correlation coefficient

can be expanded by Taylor's theorem as follows

$$\rho(\xi_0, \tau) = A\xi^2 + B\tau^2 + 2H\xi\tau .$$

Since the other terms can be neglected when the quantities involved are small. In the complete two dimensional case, we obtain similarly

$$(\xi_0, \eta_0, t) = 1 + A\xi_0^2 + B\eta_i^2 + C\eta_0^2 + 2H\xi_0\tau + 2M\eta\tau + 2N\xi_0\eta_0 \qquad (16)$$

We have to evaluate the values of A, B, C, H, M and N from experimental data for a complete analysis. If one receiver is at the origin (0,0) and another at $(0, \xi_0)$, the value of $\rho(\xi_0, 0, 0)$ can be easily calculated by comparing two records with zero time delay. We also get on substitution in (16)

$$\rho(\xi_0, 0, 0) = 1 + A\xi^2$$

$$\text{or} \quad A = \frac{\rho(\xi_0, 0, 0) - 1}{\xi_0^2} \qquad (17)$$

similarly we obtain

$$B = \frac{\rho(0, 0, \tau_i) - 1}{\tau_i^2} \qquad (18)$$

and

$$C = \frac{\rho(0, \eta_0, 0) - 1}{\eta_0^2} \qquad (19)$$

Also it can be seen that

$$H = \frac{1 + \rho(\xi_0, 0, \tau_i) - \rho(\xi_0, 0, 0) - \rho(0, 0, \tau_i)}{2\xi_0\tau_i} \qquad (20)$$

$$M = \frac{1 + P(0,\eta_0,\tau_i) - P(0,\eta_0,0) - P(0,0,\tau_i)}{2\eta_0\tau_i} \qquad (21)$$

$$\text{and } N = \frac{1 - P(\xi_0,\eta_0,0) - P(\xi_0,0,0) - P(0,\eta_0,0)}{2\xi_0\eta_0} \qquad (22)$$

We have thus to evaluate only

$$P(\xi_0, 0, 0),\ P(0, \eta_0, 0),\ P(0, 0, \tau_i)$$
$$P(\xi_0, 0, \tau_i),\ P(0, \eta_0, \tau_i) \text{ and } P(\xi_0, \eta_0, 0)$$

for the determination of all the constants. Yerg, by assuming the general ellipsoid equation, does away with the assumption regarding isotropy and shows that

$$V_x = \frac{H/A + HN/AC}{1 - N^2/AC} \qquad (23)$$

$$V_y = \frac{-H/C + HN/AC}{1 - N^2/AC} \qquad (24)$$

$$\text{and} \qquad V_c' = \frac{B(1 - \tan^2\theta)}{A + C^2\tan^2\theta + 2N\tan\theta} \qquad (25)$$

The value of τ_i is chosen arbitrarily in the above analysis and no criterion exists for the selection of its value. The values of V_x and V_y and Vc in general depend upon the value of τ_i chosen. In order that the results may agree with those obtained by Briggs et al, τ_i should, however, be chosen so that the assumption of anisotropy in their treatment is justified. This is possible only if γ

is such that it is within the linear portion of the curve of τ vs $(\tau'^2 - \tau^2)$.

In the following sections, two records are chosen and analysed by all the above methods as examples. The records chosen for the analysis are also reproduced.

11-5-1958, 0830, 2.6 Mc/s (E layer)

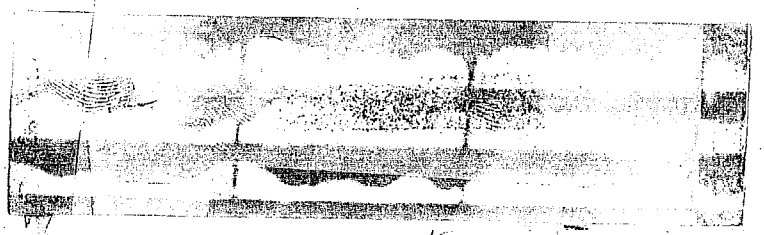

(1) Ratcliffe's method :- The mean values of the time displacements were determined and these were used to calculate the values of the apparent component velocities. The magnitude and direction of the drift were determined by using formulae (4) and (5) with the help of the nomograms given in Sethuraman (1958). The values obtained are 20 m/s and 115°.

(2) Pütter's method :- The velocities corresponding to each set of time shifts are calculated with the help of formulae (4) and (5). These velocities are plotted on polar coordinates. (Fig. 5a) A circle is drawn passing through them and the origin. The diameter to this circle through the origin is drawn and its value gives the magnitude and direction of the drift. The values obtained are V = 17 m/s and θ = 120°.

The individual time shifts are also plotted in

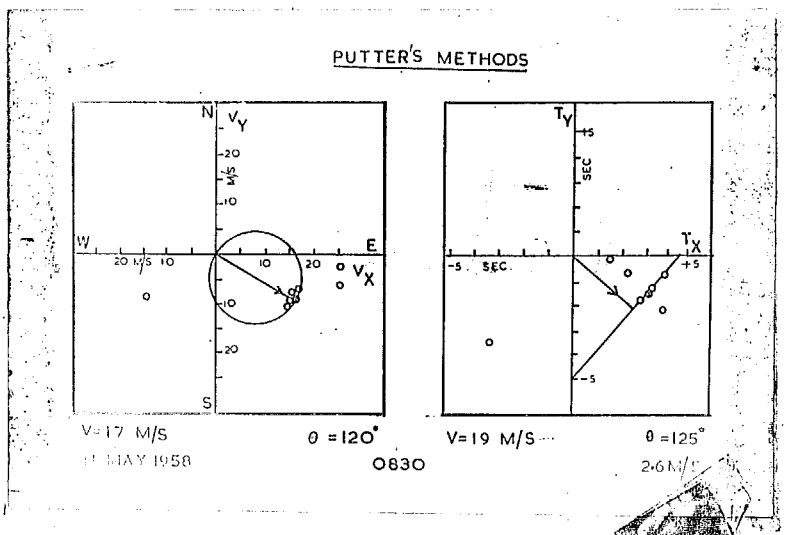

Fig. 5 - Putter's circle and straight line diagrams for determining drift speed and direction.

11th May, 1958, 0830, 2.6 Mo/s.

Fig. 5b. A straight line is drawn through these points and a perpendicular is drawn from the origin to this line. Its direction ($\theta = 125^0$) gives the direction of the drift and the lenght of the hypotenuse gives the value of t. The magnitude of the drift is obtained by dividing the seperation between the aerials by t. The magnitude of the drift obtained by this method is 19 m/s.

The method of Briggs, Phillips and Shinn :- The auto-correlation curves for the three patterns from the central, west and north aerials are plotted in Fig. 6-A. The cross-correlation curves between the central and west and the central and north aerials for various values of time differences, both positive and negative, are given in Fig. 6-B. From these two sets of curves, the value of the time difference on the auto-correlation curve τ' to give a correlation equal to that for a time difference of τ on the cross-correlation curve is determined for both sets of aerials, for various values of τ. Plots of $\tau'^2 - \tau^2$ vs τ are given in Fig. 6-C. Equation (14) viz.

$$\tau'^2 - \tau^2 = \frac{\xi_0^2 - 2 V_x \xi_0 \tau}{V_c'^2} \qquad (14)$$

can be reagranged as

$$\frac{\frac{\xi_0^2}{\tau'^2 - \tau^2}}{V_c'^2} + \frac{\frac{\xi_0}{\tau}}{2 V_x} = 1, \qquad (26)$$

which indicates that the plot would be a straight line. If x' and y' be the intercepts of this line in the X and Y

axes respectively, it can be easily seen that

$$V_x = \xi_o^2/2x' \qquad (27)$$

and $$V_c'^2 = \xi_o^2/y' \qquad (28)$$

The values of V_c' and V_x can thus be calculated. Similarly from the other curve V_y and V_c' can be calculated. The actual value of the drift speed and direction and the mean value of V_c' can be calculated.

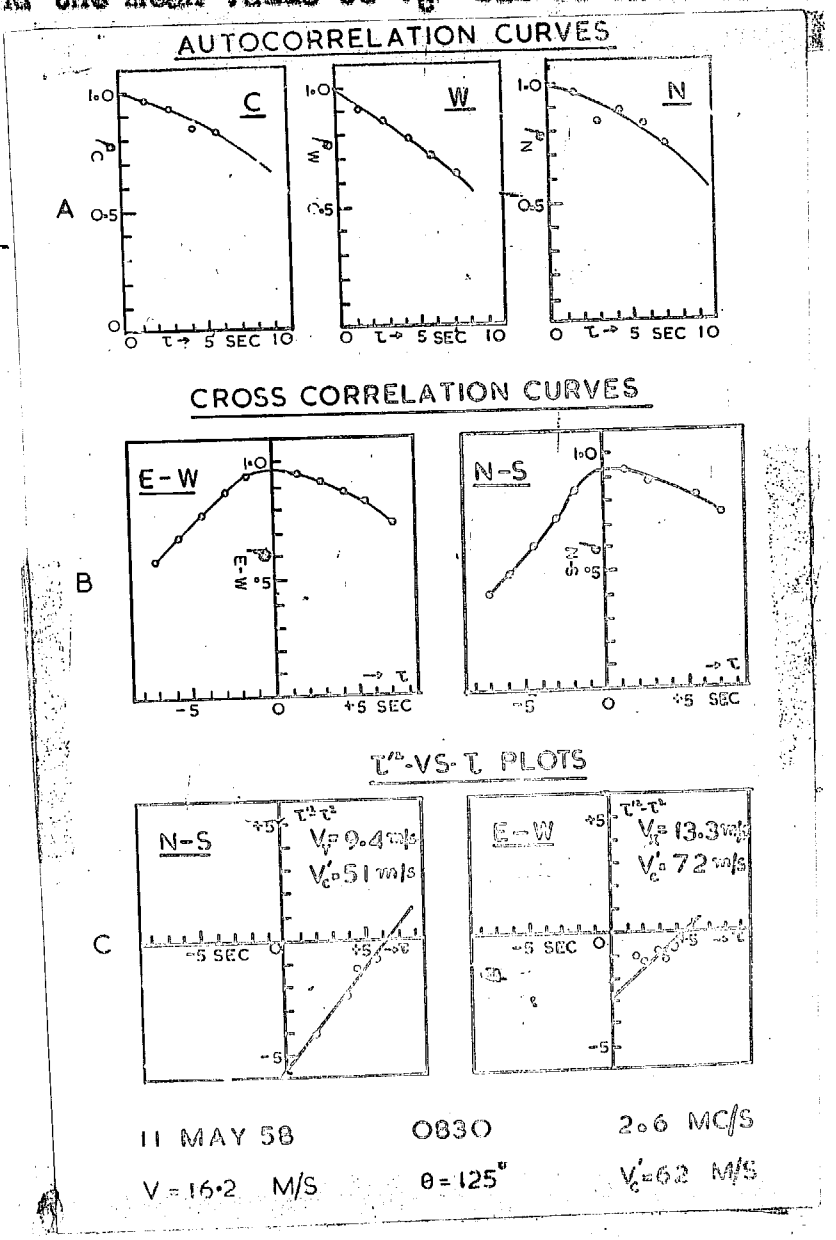

Fig. 6 - Briggs, Phillips and Shinn curves, for

The actual random velocity V_c is given by $V_c^2 = V_c'^2 + V^2$. The values of these quantities obtained by this method are given in Table 1.

Yerg's method :- As mentioned previously, Yerg's method requires the computation of only six correlation coefficients. Three of them are fixed, viz. $\rho(\xi_0,0,0)$, $\rho(0,\eta_0,0)$ and $\rho(\xi_0,\eta_0,0)$ and three involve the choice of an arbitrary time lag τ_i viz. $\rho(0,0,\tau_i)$, $\rho(\xi_0,0,\tau_i)$ and $\rho(0,\eta_0,\tau_i)$. If too large a value of τ_i is chosen, the effects of anisotropy of the pattern would be large and the results would not agree with those obtained by the other methods. In order that such effects may not be large, the time lag chosen should be sufficiently small so that the point corresponding to it on the $\tau'^2 - \tau^2$ vs τ plot lies in the linear portion. In the computation shown below a time lag of three seconds is chosen. The values of the correlation coefficients are

$$\rho(\xi_0,0,0) = 0.97; \quad \rho(0,\eta_0,0) = 0.93$$
$$\rho(\xi_0,\eta_0,0) = 0.94; \quad \rho(0,0,\tau_i) = 0.93$$
$$\rho(\xi_0,0,\tau_i) = 0.88; \quad \rho(0,\eta_0,\tau_i) = 0.91$$

The values of A, B, C, H, M and N are calculated with the help of formulae (17-22) and they are as follows .

$$A = -.03/(120)^2; \quad B = -.07/9; \quad C = -.07/(120)^2$$
$$H = .4/(120)^2; \quad M = +1/120^2 \text{ \& } N = -.02/(120)^2$$

Substituting these values in equations (23-25), we obtain,

V_x = 15.5 m/s, V_y = 8.2 m/s, V = 17.6 m/s, $\theta = 118^0 9'$ and V_0 = 44 m/s. The values of these various parameters obtained by the methods described above are given in table 1.

Table 1

Comparison of the results of drift parameters calculated by different methods (11-5-58, 0830 2.6 Mc/s.)

Method	V or V' m/s	θ Degrees	V_0' m/s	V_0 m/s
Ratcliffe's	20	115	-	-
Putter's circle	17	120	-	-
Putter's St.line	19	125	-	-
B.P.S. method	16	125	62	64
Yerg's method	18	118	40	44

13-9-1959, 2330, 2.6 Mc/s

Ratcliffe's method gives a value of 130 m/s and 25° for the velocity of drift. ~~The~~ Putter's straight line and circle diagrams are drawn in Fig. 7. It will be noticed that the dispersion is greater in this case than in the previous one. This is due to the turbulent nature of the fading pattern. The values of the drift parameters are

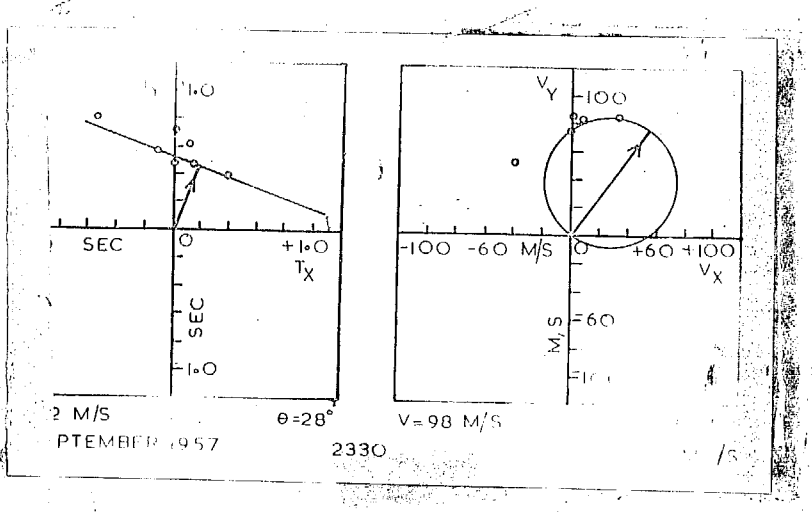

Fig. 7 - Putter's diagrams.

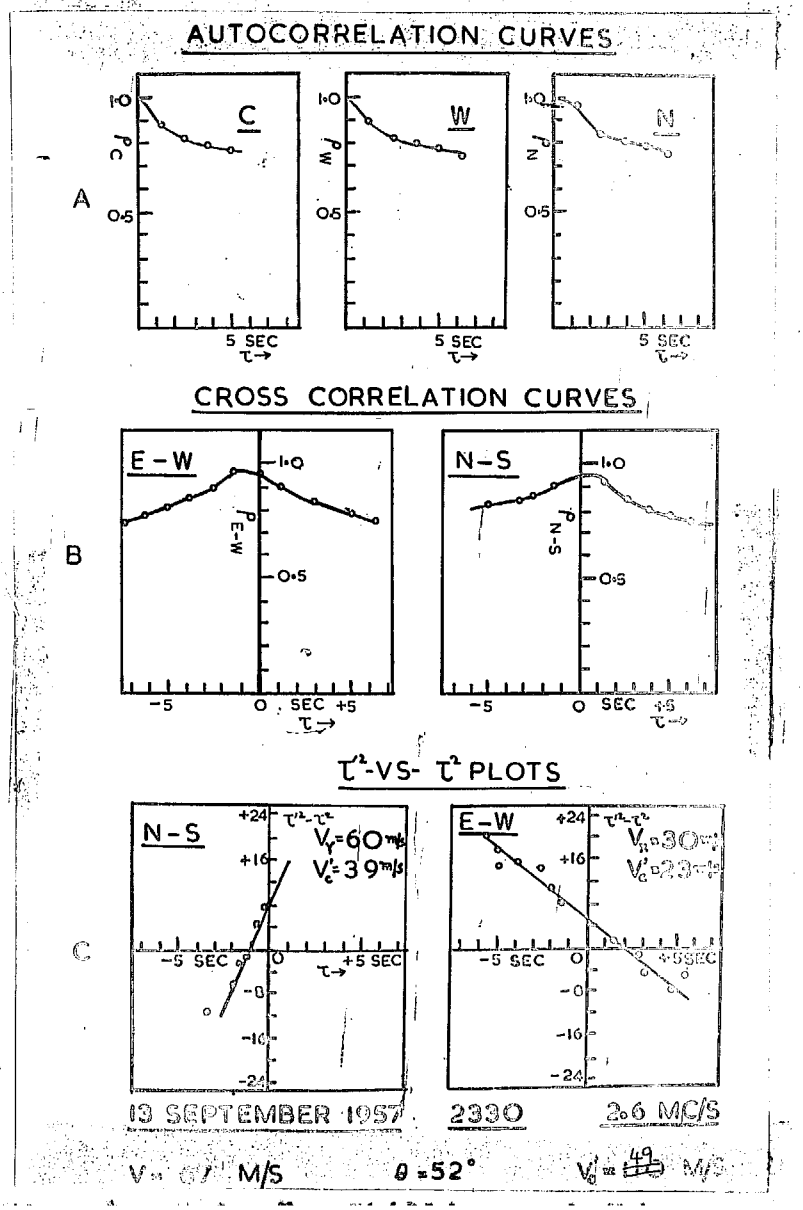

indicated on the diagram itself.

The Briggs, Phillips, Shinn curves are shown in Fig. 8. The values of the drift parameters obtained by this method are given in Table 2.

Yerg's method :- The value of the six correlation coefficients for a time lag of three seconds are as follows.

$$\rho(\xi_o, 0, 0) = 0.96; \quad \rho(0, \eta_o, 0) = 0.97$$
$$\rho(\xi_o, \eta_o, 0) = 0.94; \quad \rho(0, \xi_o, \tau_i) = 0.81$$
$$\rho(\xi_o, 0, \tau_i) = 0.80; \quad \rho(0, \eta_o, \tau_i) = 0.82$$

The values of A, B, C, H, M and N are as given below.

$$A = -0.04/(120)^2; \quad B = -0.19/9 \quad C = -0.03/(120)^2$$
$$H = 0.6/(120)^2; \quad M = 0.8/(120)^2 \text{ \& } N = 0.005/(120)^2$$

The values of V_x and V_y are 19 m/s and 54 m/s giving a value of V of 57.3 m/s and $\theta = 20^\circ$. The value of V_c is 120 m/s. The values are given in Table 2.

Table 2

Comparison of the results of drift parameters calculated by different methods (13-9-1957, 2330, 2.6 Mc/s.)

Method	V or V' m/s	θ degrees	V_c' m/s	V_c m/s
Ratcliffe's	130	25	-	-
Putter's circle	98	35	-	-
Putter's st.line	132	28	-	-
B.P.S. method	67	25 52°	49	83
Yerg's method	57	20	105	120

Thus with records having a large value of the turbulence component, Ratcliffe's method and its variants do not give the true value of the drift. Correlation methods have to be employed in those cases. However, for the analysis of a large number of records obtained at Ahmedabad showing points of clear similarity, the method of similar fades can be used, and this has been done.

References

Banerjee, K.N.	1958	Jour. Atmos. Terr. Phys., 12, 248.
Barber, N.	1957	Jour. Atmos. Terr. Phys. 11, 298.
Briggs, B.H. Phillips, G.J. and Shinn, D.H.	1950	Proc. Phys. Soc., B 63, 106.
Court, C.W.G.	1955	Jour. Atmos. Terr. Phys., 7, 333.
Krautkrämer, J.	1943	Deutsche Luft. S.B.Nr. 1761.
Phillips, G.J. and Spencer, M.	1955	Proc. Phys. Soc., 68B, 481.
Putter, P.C.	1955	Physics of the Ionosphere, Physical Society, London.
Rao, M.S. and Rao, B.R.	1957	Jour. Atmos. Terr. Phys., 10, 307.
Ratcliffe, J.A. and Gawsey,	1933	Proc. Camb. Phil. Soc., 29, 301.
Ratcliffe, J.A.	1954	Jour. Atmos. Terr. Phys., 5, 173.
Ratcliffe, J.A.	1956	Rep. Progr. Phys., 12, 188.
Ramsay, W.J.	1957	Jour. Atmos. Terr. Phys., 11, 255.
Sethuraman, R.	1958	Proc. Ind. Acad. Sc., 48, 84.
Yerg, D.G.	1955	Jour. Geophys. Res., 60, 173.

* * * * * *

CHAPTER II

THE METHOD OF CLOSELY SPACED RECEIVERS

CONTENTS

CHAPTER III

EXPERIMENTAL TECHNIQUE

Contents

CHAPTER III

EXPERIMENTAL TECHNIQUE

The method used ~~in this laboratory~~ at Ahmedabad for drift measurements in the ionosphere is the spaced aerial method originally used by Krauskrämer (1943) and modified by Mitra (1949). The first equipment was designed by Nanda (1955); it could be operated only at a single frequency (5 Mc/s) and its power output was low. The equipment was redesigned by the author for ~~the~~ larger power output and for operation at other desired frequencies. The present chapter gives a brief description of the equipment.

1. General design of the equipment

The whole assembly of the transmitter and receiver is contained in two racks. The aerial system consisting of two dipoles for transmitter and three for receivers were erected in the open space around the laboratory. Separate aerials were used for different frequencies. The transmitter sends out pulses of 100-300 μs duration at the recurrence frequency of the mains supply, which is 50 c/s. Provision is made to go over from one frequency to another by means of switches which connect the appropriate coils in the oscillator and the R.F. amplifier stages of the transmitter. The peak power outputed from the transmitter

is about 1.5 km. The reflected pulses are received at three aerials placed at the corners of an isosceles right angled triangle whose equal sides are 120 meters each. The signals from the three spaced aerials are brought to the receiver unit.

The signals from the three aerials are fed successively into the main receiver by means of an electronic switch. The output from the receiver is applied to one of the Y deflecting plates of the monitor cathode ray tube and to the horizontal plates of the recording cathode ray tube. A gate circuit generates a positive pulse for selecting the set of echoes in the monitor and at the same time it is also applied to the control grid of the recording oscilloscope which is given the cut-off bias. Thus in the recording oscilloscope the spot appears on the screen only when reflections are applied to its deflecting plates. The pulse outputs from the electronic switch are added to give a step wave. This step wave is applied to the other deflecting plate of the recording scope and, in the absence of time base in that scope, appears as three dots one by the side of the other on the screen. The signal from any given aerial and the spot corresponding to that aerial or both synchronised by the common pulse generator which switches the aerial and generates the step. The echoes from the three aerials appear as three bright lines one by the side of the other and are recorded on a movie 35mm film. The detailed description of the component units of the system are given

Transmitting unit

This unit contains the pulse generator, the pulse modulated transmitter and the associated power supply units.

Characteristics of the pulse

The following three characteristics of the pulse are of importance in ionospheric work. (1) Peak power (2) width of the pulse and (3) repetition rate. In addition, the pulse should have short rise and fall times. The design consideration to ensure a satisfactory pulse have been discussed in the literature (Chance et al, 1949) and are summarised below.

The peak power of the transmitter determines the amplitude of the reflected pulse. In the tropics, especially during high sunspot years, the absorption of medium frequency radio waves in the ionosphere is very high and a large power output is therefore required for satisfactory operation. With large powers, however, the design becomes complicated and also the receiver when placed near the transmitter gets paralysed.

The recieved power 'S' of a reflected pulse depends upon the transmitter power, the types of antenna used for transmission and reception, the distribution and nature of the reflecting medium and the absorption in the ionospheric regions. The power density of the transmitted wave is $PG_T/4\pi R^2$, where P is the transmitted power, G_T is the gain of the

antenna and R the distance of the target from the transmitter. When this is radiated without any loss from the target of area σ and reaches the receiver situated close to the transmitter, the received power density is $[P_T/4\pi R^2]\,\sigma/4\pi R^2$ and the power fed into the receiver is obtained by multiplying this quantity by the cross section of the receiving antenna given by $G_R \lambda^2/4\pi$. Thus $S = P.\, G_T G_R \lambda^2 \sigma/(4\pi)^3 R^4$. In ionospheric work, if we define the frequency, we do not have control over any factor except P. It will be seen that the received power is directly proportional to the transmitter power. To be detectable, the reflected signal should have a certain minimum power. This minimum detectable power (S min) is governed principally by the receiver noise and the minimum signal-to-noise ratio which could give a detectable pulse at the recorder.

The transmitter power P depends upon the peak power of the transmitter and the pulse width. The pulse width must be sufficiently small so that at the minimum range at which reflection is to be obtained, usually the E layer in our experiments, the transmitter is quiescent by the time the echo pulse from the layer is returned to the receiver. It is also limited by the resolution required to separate the ordinary and the extraordinary components of the reflected echoes which arrive with a short delay from each other. On the other hand, the minimum pulse width is limited by the band pass restrictions on the R.F. and I.F. amplifiers.

This cannot be very large because of the limitations caused by the interference, the fidelity of reproduction of the pulse, the necessity to restrict the frequency spread of the transmitted side band energy to prevent interference with other services and by the requisite resolution of the critical frequency phenomenon which becomes indistinct when the radiation embraces a very wide band of frequencies. A pulse duration of 100 to 250 μs is used as a compromise. The pulse repetition rate should also be chosen properly. With too high repetition rates, the echo from a given pulse may not return to the receiver until the next pulse is transmitted. This causes an ambiguity since the return echo from any particular pulse cannot be easily identified. At the same time, the repetition rate should be kept high enough to provide an advantageous integrating effect of the received signals from successive pulses.

Although the transmitted peak power is very large (1.5 kW in our case) ordinary tubes can be used in pulse transmitter circuits because of the fact that such large powers are generated only for a short time. Provided the pulse power and the pulse duration are not too large, the average power transmitted can remain well within the rated values for such tubes. In effect, the large period during which the tube is quiescent enables the heat produced to be dissipated safely.

The block diagram of the transmitter unit is given

in Fig. 1.

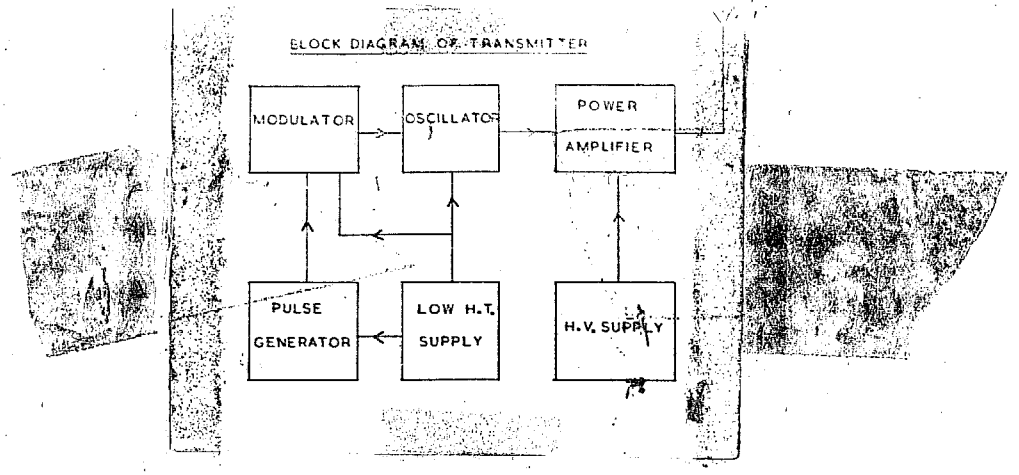

Fig. 1 - Block diagram of transmitter

We shall consider briefly the features of the five sections of the transmitter unit viz. (1) triggered pulse generator (2) modulator (3) power amplifier and (4) power supplies.

Triggered pulse generator :- The circuit diagram of this unit is given in Fig. 2.

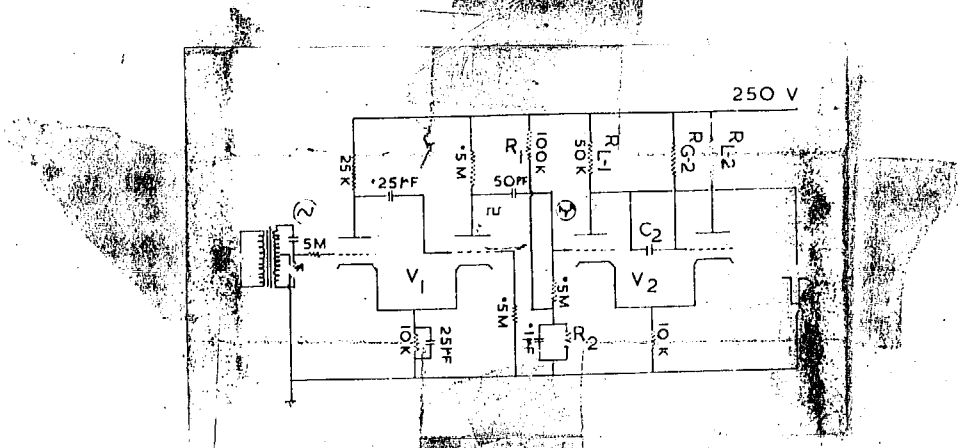

Fig. 2 - Triggered pulse generator

V1 is a square wave generator and is an over-driven amplifier.

An A.C. voltage of about 70V RMS is fed into the grid by the transformer T1. The C-R combination connected across its secondary is used to shift the phase of the input which is fed to the grid of the square wave generator with respect to the mains supply wave. The square wave form obtained at the second anode of the tube is differentiated by the C-R combination at the grid of V2. V2 is operated as a cathode coupled monostable multivibrator, in which the stable state is the one in which the right hand side V1A is nonconducting. During the positive portion of the pipe, indicated at the grid of the first section of V2, the tube starts conducting. This results in the condenser C2 charging upto the value of the D.C. supply voltage. Its charge stops the right hand side of V2 from conducting and leaks through R_{g2} at a rate determined by the $C2R_{g2}$ combination. After a certain interval of time, the tube begins to conduct and the stable state is reached once again. This results in a pulse to be produced which has a negative polarity at the first tube and a positive polarity at the other. This pulse is fed into a differentiating circuit in the transmitter (Fig. 3), in which the resistance part can be adjusted in steps. The output is fed into the pulse-width control tube V3. At the anode of this tube, pulses of variable width are obtained. The modulator tube V5 and V6 are 6L6 tubes. They are amplifiers which invert the polarity of the pulse, thereby making it suitable for modulation and also give it sufficient power to drive the oscillator circuit which they feed. A push-pull oscillator circuit consisting of

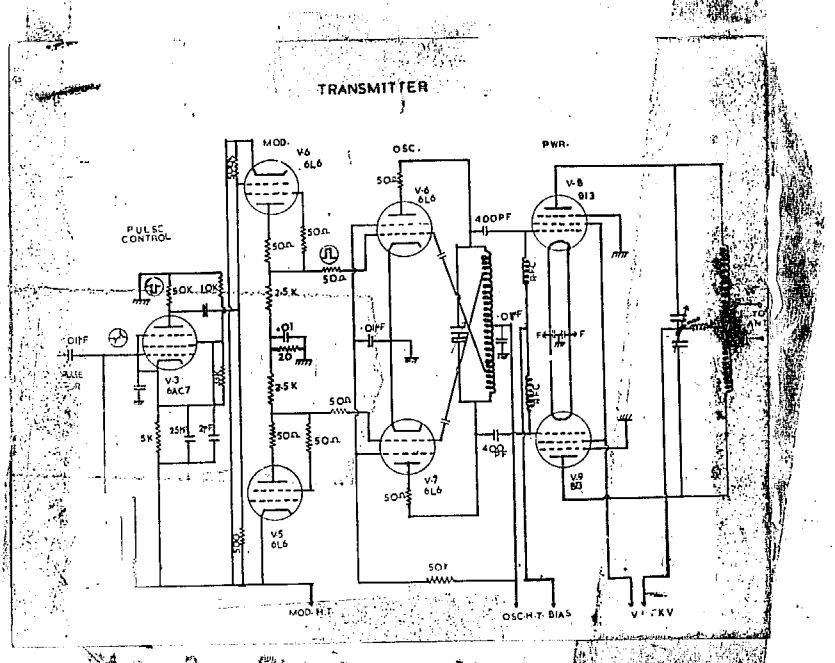

Fig. 3 - The transmitter

V6 and V7 is biassed to cut-off and the pulse from the modulator excites it. The output from the pulsed oscillator is fed into the power tubes V8 and V9 (813's) connected in push-pull and operating under class B conditions. The anode circuit of this stage is tuned and coupled to the antenna. The H.T. applied to the anode of the 813 tubes is 1500 V and it is obtained with the help of a high voltage transformer and a metal rectifier. The bias and the low H.T. supplies are regulated while the H.T. supply for the 813 anode are not.

Dipole antennas are used for both transmission and reception. Two transmitting antennas are used for the transmitter, one for each set of frequencies used in the work. The antennas are brought to the transmitter through an 80 ohm

coaxial cable and coupled to the anode through suitable transformers. The receiving antennas are also dipoles. Only one set of dipole, designed for operation on 2.6 Mc/s, and are used for reception at all frequencies. This arrangement results in a loss of gain at the antenna at all the other frequencies but it was found to be satisfactory. The receiving aerials are connected to an electronic switch through coaxial cables and suitable transformers.

The distance between the receiving aerials is determined by two factors ; with too large separation the correlation between the wave forms at the two aerials decreases while with too small spacing the time shift between corresponding point in the three patterns becomes very small, thereby making it difficult to measure them accurately. Various spacings were tried and it was found that a separation of one wave length at 2.6 Mc/s (120 metere) gave satisfactory results.

Receiving and recording system

The block diagram of this system is given in Fig. 4 . It contains the following elements. (1) An electronic switch to switch-in the three aerials in succession to a common receiver. (2) A receiver suitably modified for pulse reception. (3) A master pulse generator providing a synchronising pulse. (4) Gate generator for selecting the pulse under study and for synchronising the electronic switch. (5) A time base circuit

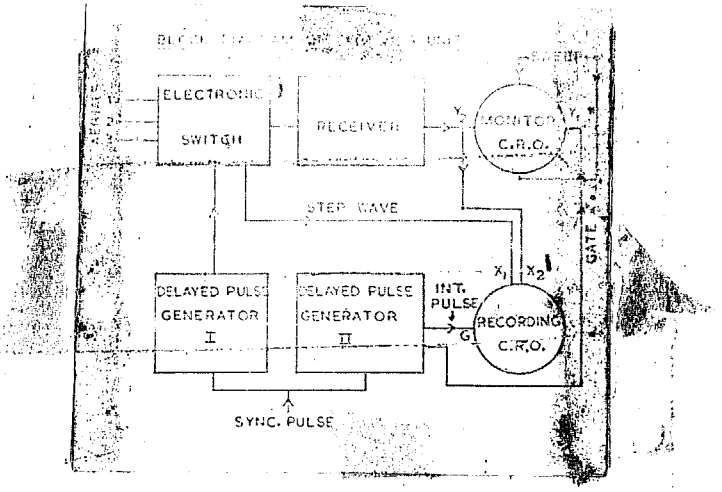

Fig. 4 - Block diagram of receiving unit.

for the monitor cathode ray tube. (6) The monitor and recording cathode ray tubes. (7) Camera unit and time marker for photographing record. (8) Power supply unit for operating all these elements. The various sections are described below.

The electronic switch :- The basic element of the electronic switch used by the author are (1) a three stage ring multivibrator, giving three pulses in succession, (2) three amplifier tubes to which the three aerials are connected and switched in succession by the pulses from the ring multivibrator and (3) an adding circuit which adds up the three pulse wave forms from the ring multivibrator, thereby generating a step-wave form which is applied to the recording oscilloscope. The circuit diagram of the electronic switch is given in Fig. 5 and the various elements are described below.

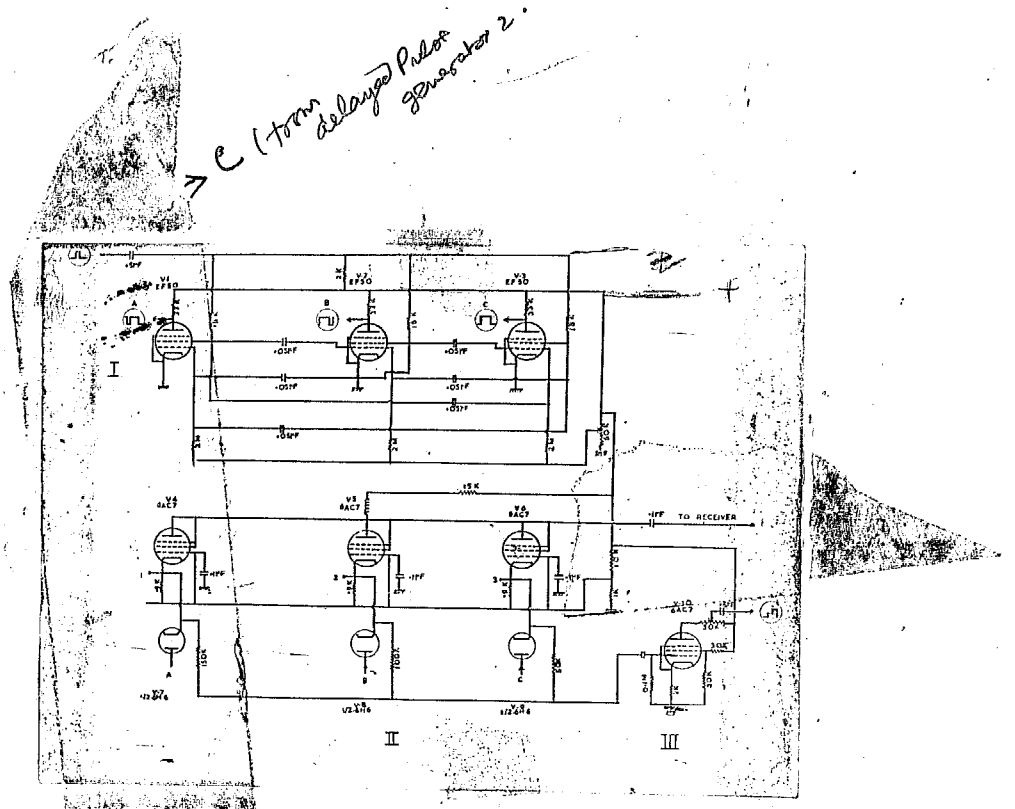

Fig. 5 - The electronic switch.

(1) The ring multivibrator (section I of Fig. 5):- This consists of three tubes V1, V2 and V3 connected as a ring multivibrator. Each of these tubes is triggered by means of synchronising pulse, generated from a delayed pulse generator described later. At any instance, one of the tubes is non-conducting and the other two tubes are conducting. The non-conducting tube charges the C-R combination at its screen to the B+ value and this combination afterwards discharges at a rate determined by its time constant. The next tube then conducts and the cycle is repeated. The whole process is synchronised by the external pulse. The output pulse waveforms are electron-coupled to the anode to prevent interaction of the external circuits on the multivibrator.

(2) The switched R.F. amplifiers (Section II of Fig. 5) :- Three grounded grid amplifiers V4, V5 and V6 are switched by means of the wave-forms A, B and C from the ring multivibrator and these are injected to the cathodes through three diodes. The cathodes of these diodes are returned to a point at a voltage of+27 volts with respect to ground and thus during the positive portions of the pulses it conducts. The cathodes of the 6AC7 tubes (V4, V5 and V6) are kept at a large positive potential with respect to the grid, thereby preventing it from conducting. During the negative portions of the pulses, however, the diodes stop conducting and the grid voltage in the R.F. amplifier tubes is only that due to the 0.9 k ohm the resistance connected in the cathode circuits. The tubes therefore conducts and the R.F. voltage applied to the cathode circuit appears in the output circuit. The anodes of the three tubes are connected to a common load consisting of an R.F. choke and a 15 k ohm resistance. The output from each of the amrials thus appears across the load in succession. This output is taken to the common pulse-receiver through a 0.1 uf condenser.

(3) The step-wave generating circuit (Section III of Fig. 5) :- The switching wave-forms from the ring multivibrator are added through potential divider arrangements having a common resistance of 100 k at the grid of V10 and individual resistor of 50 k, 100 k and 190 k to which the three wave-forms are applied in succession. The resulting step wave-form at the

III

grid of V10 is amplified by the tube and a desired amplitude of the step wave, which determines the spacing between the traces in the recording oscilloscope, is obtained with the help of a potentiometer load at the anode of the amplifier.

The receiver :- Among the desirable characteristics for pulse receiver are (1) a high sensitivity, i.e. the ability to detect weak signals, (2) faithfulness of reproduction, (3) rapid recovery from the effects of large transient input voltages and (4) reasonable linearity between the output and input signal levels.

The useful sensitivity of a pulse receiver for weak signals is influenced by many factors such as the gain of the R.F. stages and the I.F. stages of the receiver, the noise figure of the receiver, the ability to reproduce pulses with as little distortion as possible. The minimum detectable signal by the receiver depends in addition, on the repetition rate of the transmitted pulse. Some of these factors are discussed below.

The noise figure of the receiver :- A signal, no matter how it arrives, has associated with it a certain minimum amount of noise due to the fact that the antenna generates the Johnson noise associated with its radiation resistance at temperature T. It is useful to specify this temperature (noise temperature) of the antenna at which its radiation resistance should be in equilibrium in order to account

for all the noise fed into the receiver. The available noise power is thus equal to kTB, where k is the Boltzman's constant, B the band-width accepted and T the noise temperature. Therefore, at a signal level S, the maximum signal-to-noise ratio at the input terminals is S/kTB. If So and No are the signal and noise outputs from the receivor, the signal-to-noise ratio at the output terminals is So/No. The ratio of these two signal-to-noise ratios is known as the noise figure of the receivor and represents, qualitatively the additional noise introduce by the receiver. In an ideal receivor, this ratio is equal to unity. When the value of S becomes small, as in ionospheric work, where the signal power of the reflected pulse is a few micro-micro-watts, this factor assumes great importance in the design of the receiver. Since the additional noise is confined generally to the first one or two stages and the mixer stage, great care has to be taken in the design of these stages. In radar receivers R.F. stages are omitted for this reason but since a large R.F. gain is essential for ionospheric work, two carefully designed R.F. stages are generally used in the receiver. In fact, the removal or reduction of the noise sources in and around the receiver is one of the major problems of the design of the receiver for ionospheric work.

Band width requirements :- The band width requirements of a receiver for pulse reception are very different from those of a conventional broadcast receivor

and are determined by considering various conflicting factors. Faithful reproduction of the pulse shape requires a large band-width but too large a band-width results in a greater amount of noise to be introduced into the receiver. From the point of view of the best signal-to-noise ratio, the optimum value of the product of the band width B and the duration of the pulse τ is given by $B\tau \simeq 1$. This can be easily seen from the following considerations. Consider an I.F. amplifier whose band-width can be continuously increased from a value zero. At first, the signal level will increase linearly and the noise level will increase as the square root of the band width (since $E_N = \sqrt{4kBTR}$). Thus, there will be an overall increase of the signal-to-noise ratio. When the band-width is sufficiently large to reproduce the flat top of the pulse faithfully, any increase in the band-width will not cause an increase in the signal, but the noise will increase and the S/N ratio will begin to decrease. The optimum value of the band width is obtained when $B\tau = 1$. This value is not critical at all and the band-width twice the value increases the minimum detectable signal by only about 1db. This however, results in a better reproduction of the pulse and therefore in practice this band width is used. Since our minimum pulse width is 100 μs , the band width of the receiver should be 20 kc/s.

There are four methods which have been extensively used to improve the band-width of the receiver. They are,

(1) damping the tuned circuits, thereby reducing the Q and increasing the band-width. Since Q = R/X = fo/B, where the symbols have their usual meanings, knowing X, fo and the B required, the value of R can be calculated.(2) By means of over-coupled circuits. The design of such circuits have been extensively studied (Sturley, 1954). By employing mixed (both capacitive and inductive) couplings of different types double-hump characteristics can be produced in the response curve of the tuned amplifiers giving rise, in effect to flat topped response curves, (3) by means of staggered tuned circuits (Sturley, 1954, Zepler, 1942) and (4) by negative feed back amplifiers where a fraction of the output of a single tuned synchronous amplifier is fed in the inverse phase to the input circuit. More voltage is fed back at resonance than off resonance and hence the response curve becomes flat. Perhaps the simplest of all the methods from the point of view of design is the first method viz. damping of the tuned circuit although this results in a loss of gain of the amplifier. This method is used by the author to get the required band width of 20 kc/s.

A factor of great importance in the design of wide band amplifiers in the figure of merit of the stage. This refers to the ability of the amplifier to give a large gain over a wide band of frequencies. It can be easily shown that in the case of a single tuned amplifier the band width for a 3 db fall in the maximum gain of the amplifier is given by $B = 1/2\pi R_{\parallel} C_{\parallel}$, where $R_{\parallel}$ is the total parallel

impedance across the output circuit and $C_{\parallel}$, the total parallel capacity of the output circuit, including those contributed by the next stage. The gain of the stage is given by $g_m.R_{\parallel}$. The gain band width product is thus $g_m/2\pi C_{\parallel}$. In order to have a large gain over a wide band of frequencies the total parallel capacity across the circuit is kept small by wiring the circuit carefully to reduce the stray capacity and by choosing a tube having a large value of transconductance. Special tubes like 6AC7, 6AK5 with large transconductances have been designed for use in such wide band circuits. In the receiver used in the laboratory, all the amplifiers use 6AC7 tubes.

Rapid recovery from the effects of a strong signal:- A very important further requirement of a pulse receiver situated very near the transmitter, as in the equipment used by the author, is that it should recover rapidly from the effects of the strong ground pulse from the transmitter. The transmitter causes an enormous overloading of the receiver resulting in the paralysis or blocking of the receiver making it insensitive to signals below a certain level for a short while after the ground pulse. This is the result of transient shifts in the electrode voltages of the amplifier tubes produced by charges on the bypass or coupling condensers. The recovery time depends on the time constants of the coupling circuit and may be only a few micro-seconds or several milli-seconds depending on the point

at which the blocking occurs. In extreme cases, as in high power radar, such overloading might burn out the coils and damage the tube. In such cases, a transmit-receive switch is used in conjuction with line transformers to short circuit the receiver terminals while the transmitter is operating (Pink, 1949). Such a procedure is not practicable in ionospheric work because of the low frequency and low power involved. Two methods have been used by the author to eliminate the effect; (1) the use of coupling circuits with short time-constant, consistent with the efficiency of coupling and the fidelity of reproduction and (2) the application of a negative square pulse of suitable width and phase to the supressor grids of the two R.F. stages of the receiver. This cuts out the R.F. stages and thereby the input to the receiver for the duration of the pulse. This pulse is synchronised with the transmitted pulse and thus the receiver is made insensitive when the transmitter is operated.

In addition to the considerations given above, it is also necessary that the receiver has good stability and that no drift occurs in the frequency to which the receiver is tuned. This is achieved by a proper ventilation of the receiver as a whole so that the temperature changes in the oscillator circuits which are mainly responsible for such drifts are minimised and by stabilising the voltages applied to the various circuits

A 52 - 312 receiver, obtained from the Army

surplus disposals equipment, was modified to achieve all the characteristics described above. The following are some of the limitations of the receiver which had to be rectified before it could be used as a pulse receiver. (1) The overall gain of the receiver was small especially when the I.F. stages were damped to get the required band width. This was partly remedied by using 6AC7 tubes which have a large transconductance. (2) The band width of the receiver was 10 kc/s. This band width is sufficient for the purpose for which the receiver was originally intended viz. CW and broadcast reception. As pointed out earlier, the band width expected from the receiver is about 20 kc/s. This is obtained by connecting damping resistors across the I.F. transformers (Fig. 6). This gave an overall band width of

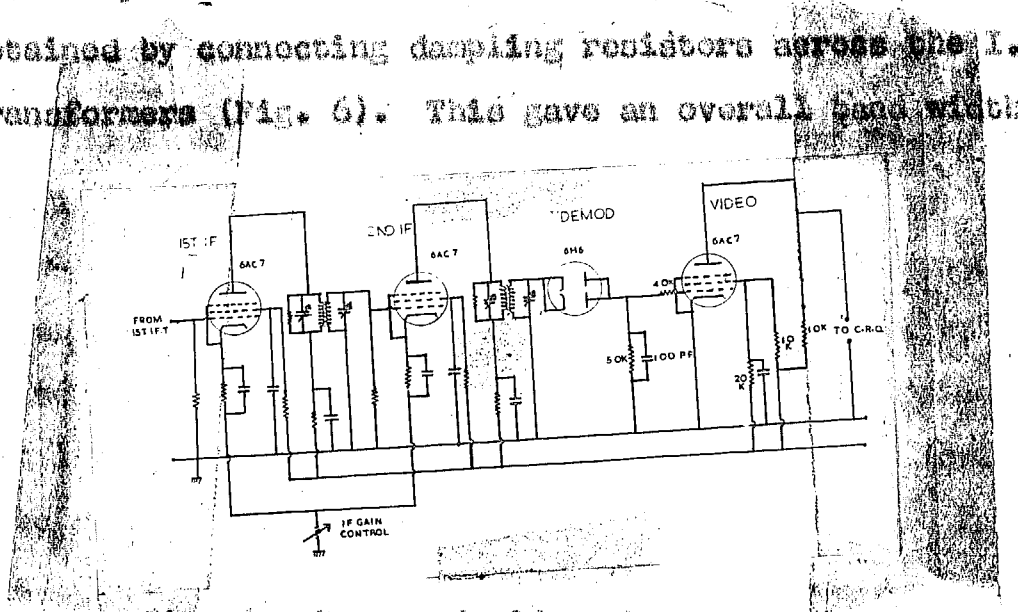

Fig. 6 - I.F. and video stages.

30 kc/s for the I.F. stages for 3 db fall in the signal output from the maximum. The band width of the receiver as a whole however was smaller than this figure because of the tuned circuits in the R.F. stages and was found to be dependent, to some extent, on the frequency to which it

that of E but its level is rarely more than 130 km. The height of the F layer is however very different from that of the E layer. For example, at Ahmedabad the height of the E layer varied from 100 to 120 km during the day, while h'F at night varied from 210 km to 390 km in 1957 depending on the hour of the night and the month. There is little significance in finding a diurnal or semidiurnal wave by combining the 2.6 Mc/s drifts during the day and night in one group. Most of the night-time observations in Ahmedabad were made on the F layer and it is better to treat the day-time and night-time drifts separately.

3. It is known from the meteor observations (Greenhow, 1955; Elford, 1959) that between 80 and 100 km the wind velocity varies with height. Simultaneous observations on two frequencies near each other, which were made by Jones (1957) at Cambridge and by the author at Ahmedabad on a few days during the winter of 1958-59 have shown only a small difference in speed between the drifts obtained with the two frequencies when they are well below the critical frequency of the layer. However, as the exploring frequency approaches the critical frequency of the layer and reflections take place from a higher layer, it would be difficult to say which of these two layers is responsible for the fading pattern, since the wave would be presumably affected by both of them. This question was examined by Booker (1955) who concluded

that the fading is superimposed at the level at which local wave length is six or seven times the free space wave length. This would mean that the irregularities whose motions are studied are situated in a region within a few percent of the level of critical reflections.

Reflections obtained with 4 Mc/s during day-time would be affected by the E layer. Although the actual reflections may be from the F layer, the double passage through the E layer would seriously affect the intensity of the reflected wave. The author (chapter IV of this thesis) took near-simultaneous observations (within three minutes of each other) on 2.6 Mc/s and 4.0 Mc/s during day-time on many days in 1957-58. Reflections were obtained from E on 2.6 Mc/s and from F on 4.0 Mc/s. It was found that on many occasions, the directions of drifts obtained with these two frequencies were the same, though the speeds showed considerable differences. This might have been due to the fact that 4.0 Mc/s being nearer the critical frequency of the E layer, the waves that passed through it suffered deviative absorption. The drifts observed on 2.6 Mc/s would refer to the lower E layer, while those on 4.0 Mc/s would be affected by both the movements of the F layer above and by the main part of the E layer.

4. Observations made at Ahmedabad during the winter of 1958-59 (chapter IV of this thesis) also showed that on many days a rapid change of drift took place in the

forenoon and that the hours of this change varied from day to day. L. Harang and K. Pederson (1956), refering to observations on E and Es echoes at Kjeller, say "There is a sudden change in the direction of the E-E component in the morning and in the afternoon at about the time when the critical frequency of the normal E layer crosses the test frequency, 2.0 Mc/s". The study of individual day's winds is of great importance before trying to study them by harmonic analysis.

5. At a tropical station like Ahmedabad, and in the high sunspot years 1957 and 1958 we have found difficulty of heavy day-time absorption round noon hours. It has not been possible with the transmitter power that was available to obtain observations more or less uniformly distributed round the clock.

6. Methods like those of Findlay (1953) employing changes in phase path, back scatter echoes (Clerk and Peterson, 1956) or the study of movements of Es patches over widely separated stations (Gerson, 1949) which have also been used for estimating drifts in the E region do not provide us with data which can be compared directly with those obtained at Ahmedabad and have not been considered in the following sections.

7. These difficulties and also the paucity of data over wide regions of earth are handicaps in forming a coherent picture of the drift circulation in the

ionosphere even in a limited height range.

7. Observations of ionospheric drifts by the closely spaced receiver method over sufficiently long periods of time to enable a proper comparison are available for a few stations at the present time. In particular, data are available for Cambridge (1949-52) (Briggs & Spencer, 1954), Kjeller (1953-55) (Harang and Pedersen, 1956), Neuf-Brisach in W.Germany (Harnischmacher and Rawer, 1957) and Washington (Salzberg and Greenstone, 1951) in the middle latitudes of the northern hemisphere and Brisbane (1952-54) (Burke and Jenkinson, 1957) in the southern hemisphere. The Ahmedabad work (1956-58) has provided some useful data for the tropics. Limited amount of data also exists for Waltair (Rao et al, 1955) and Puerto Rico (Yerg, 1955). Data from meteor observations exist for Manchester (Greenhow, 1955), Adelaide (Hurley, 1956 and Elford, 1959) and Stanford (Manning et al, 1951). They refer to heights lower than 105 km and are particularly valuable for forming an idea of the changes of wind with height in the D region and the semidiurnal variations.

9. The following are some of the main features of wind drifts in the ionosphere.

(a) All the stations report mean speeds of 40-100 m/s and the speeds are larger in winter than in summer. Larger amounts of spread in the values of speed are observed in winter at most of the stations.

(b) The mean values of the zonal component of the drift shows some definite trends at all stations. The monthly mean values of the zonal components of the drift at noon in various months for Cambridge, Kjeller, Washington, Ahmedabad and Lower Hutt (New Zealand) are given in Fig. 1. Since the monthly mean values are not

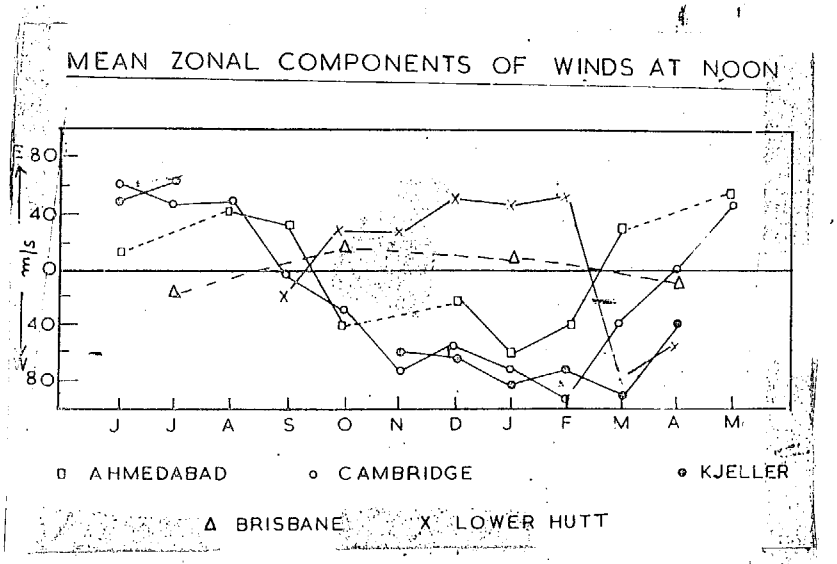

Fig. 1 - Mean zonal components of wind at noon.

available for Brisbane, the seasonal value, obtained from published curves of E-W component of drift are plotted in the same diagram. It will be noticed that in any given month, the noon zonal component behaves in opposite ways in the two hemisphere. In the summer hemisphere, it is eastward and in the winter hemisphere, westward. This behaviour is more pronounced in mid-winter and mid-summer.

(c) The values of the day-time ionospheric drift velocities (speed and direction) in the mornings and evenings are plotted for the different stations for winter

and summer in Fig. 2. Many stations, particularly in middle latitudes, exhibit gradual changes in direction of drift

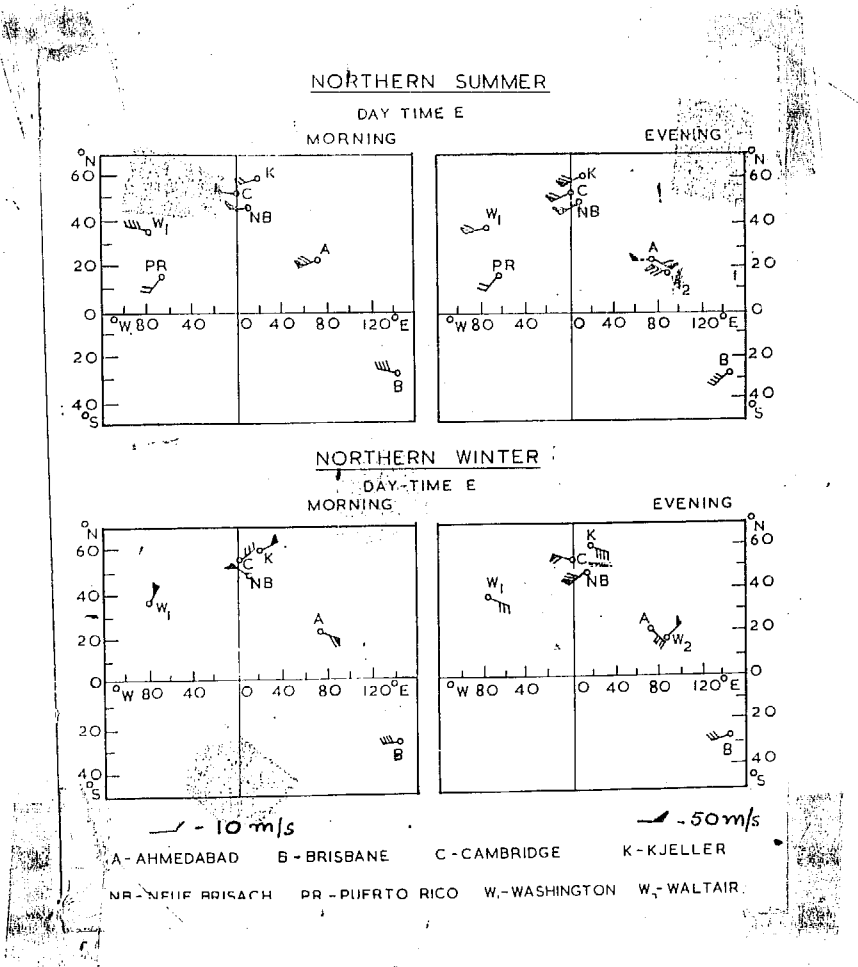

Fig. 2 - Drifts in the F layer of ionosphere in summer and winter.

during the day-time and the data are therefore divided into morning and evening hours. Due to the insufficiency of material, the Waltair data could not be so separated and are therefore plotted along with the evening data only. The Puerto Rico data were analysed by the correlation method and show small values of speed. The arrows in the diagram show the direction towards which the drift moves.

(d) While the day-time changes of drift directions take place gradually in middle latitude stations, they are abrupt at Ahmedabad.

(e) In summer, the wind drifts are generally towards the east throughout the day in middle latitudes, and in the mornings only in the low latitudes. In the evenings north-westward winds are more common at Ahmedabad. In winter, the drifts are westward, with a strong southward component in the mornings and northward component in the afternoons. In low latitudes, the prevailing movement is toward the west or north-west throughout the day.

10. Drifts in the F layer during night :- It has already been mentioned that the night-time measurements at Ahmedabad refer to the F layer and should therefore be compared with F layer data elsewhere. h'F undergoes much larger daily and seasonal variations than h'E. Variation with latitude is also greater.

The rapid change in the direction of drift which is observed to take place at Ahmedabad within an hour or two after sunrise and before sunset are undoubtedly due to change in the height of reflection. It is interesting to note that there is no very large change in the mean speeds of drift between day and night, although the scatter of values is larger with the higher level echoes.

The data obtained at Cambridge show that the

F layer drift during night is mainly westward with an added southward component during most of the year and a northward component in summer. In contrast to this, the a night-time drift at Ahmedabad in the F layer is primarily towards E to SE and secondarily towards NE in all the seasons except summer. In summer, the north-westward flow is as common as the eastward flow. In the southern hemisphere the measurements of Burke and Jenkinson show that the mean seasonal F layer night-time drifts over Brisbane are to the north in all seasons and to the west in all seasons except summer. That is, the general night-time drift is towards NW. In summer only, the drift in the first half of the night changes to north-eastward instead of north-westward.

At a lower latitude over Sydney (Munro, 1950) the drifts were found to be mainly towards the east with a strong northward component in southern winter and autumn, and southward component in southern spring and summer.

In both hemispheres, it thus appears that the prevailing drift is towards the west in middle latitudes, while it is towards the east in tropical latitudes. More data are required for an adequate discussion.

CHAPTER VI

REFERENCES

Booker, H.G.	1955	Jour. Atmos. Terr. Phys., 7, 343.
Briggs, B.H. and Spencer, M.	1954	Rep. Progr. Phys., 17, 245.
Burke, M.J. and Jenkinson, I.S.	1957	Austr. Jour. Phys., 10, 378.
Clerk, C. and Peterson, A.N.	1956	Nature, 178, 486.
Elford, W.G.	1959	Planet Space Science, 1, 94.
Findlay, J.W.	1953	Jour. Atmos. Terr. Phys., 3, 73.
Gerson, N.C.	1955	Jour. Met., 12, 74.
Greenhow, J.S.	1959	Phil. Mag., (Ser. 8), 1, 1157.
Harang, L. and Pedersen, K.	1956	Geophys. Publi. XII, No. 10.
Harnischmacher, E. and Rawer, K.	1956	C. R. Acad. Sc., 243, 782.
Huxley, L.G.H.	1957	Annals of I.G.Y. Vol. III, 250.
Jones, I.L.	1958	Jour. Atmos. Terr. Phys., 12, 68.
Manning, L.A. Villard, O.G. and Peterson, A.N.	1950	Proc. I.R.E., 38, 877.
Munro, G.H.	1950	Proc. Roy. Soc., A202, 208.
Rao, B.R., Rao, R.S. and Murthy, S.D.	1956	Jour. Sc. Ind. Res., 15A, 75.
Salzberg, C.D. and Greenstone, R.	1951	Jour. Geophys. Res., 56, 521.
Yeh, K.C.	1956	Jour. Atmos. Terr. Phys., 8, 247.

An isotropic ground pattern which changes as it moves has four velocities (Briggs et al, 1950). (1) The fading velocity :- This is the ratio of the space drift to the time drift necessary to produce equal changes in the amplitude of the pattern i.e. $Ve' = x_o/t_o$, where x_o and t_o satisfy the condition $\rho(x_o, 0) = \rho(0, t_o)$. (2) The drift velocity :- This is the velocity with which the observer must travel in order that he observes the slowest possible fading rate, due only to the internal random velocities of the cloud itself. This means that if he compares his signals at times t_1 apart and covers the distance ξ_o with such a velocity V that $\rho(\xi_o, t_1)$ is a maximum, $V = \xi_o/t_1$. (3) The characteristic velocity Vc :- This is the velocity which will be found by an observer moving with the velocity V defined above. This measures the random movements in the configuration. To this observer, the ratio of the ~~phase~~ space shift to the time shift needed to produce a similar change in amplitude is $Vc = x_o/\tau_1$. (4) The apparent drift velocity V' :- If we examine the fading records of receivers separated by ξ_o, we find that the maximum correlation is found for a certain time shift τ_o. The apparent velocity V' is defined as ξ_o/τ_o. If τ_{ox} and τ_{oy} are the time shifts for maximum correlation for the two sets of aerials, and a and b, the two separations, we obtain, $V_x' = a/\tau_{ox}$ and $V_y' = b/\tau_{oy}$, from which the apparent drift speed and direction could be found.

From the correlation coefficients determined by

formulae (12) and (13) we can determine the time τ' to obtain the same cross-correlation coefficients between any two aerials as is obtained for the auto correlation coefficient with a time lag τ. Briggs et al show that

$$\tau'^2 - \tau^2 = (\xi_0^2 - 2V_x \xi_0 \tau) / V'c^2 \qquad (14)$$

Thus, by plotting $\tau'^2 - \tau^2$ against τ and drawing the best straight line passing through the points, the values of V_x and Vc' can be obtained from the intercepts on the two axes. From a similar curve for the other two sets, V_y and Vc' can be determined. Thus, V and Vc' can be calculated. We also have

$$Vc'^2 = Vc^2 + V^2 \qquad (15)$$

from which Vc can be obtained.

The authors assume that the contours of constant correlation are ellipsoids. While this is possibly so for small values of separation and time shifts, it may not be so for larger values of these quantities.

Yeh's method (1955) :- This method, called by its author the six-point correlation method is a simplification of the previous method. In the original method of Briggs et al, a large number of correlation coefficients have to be determined thereby making the calculations laborious. This method, on the other hand, requires the evaluation of only six correlation coefficients and thus shortens the analysis considerably. Equation (13), defining the cross-correlation coefficient

can be expanded by Taylor's theorem as follows

$$\rho(\xi_0, \tau) = A\xi^2 + B\tau^2 + 2H\xi\tau .$$

Since the other terms can be neglected when the quantities involved are small. In the complete two dimensional case, we obtain similarly

$$(\xi_0, \eta_0, t) = 1 + A\xi_0^2 + B\eta_i^2 + C\eta_0^2 + 2H\xi_0\tau + 2M\eta\tau + 2N\xi_0\eta_0 \qquad (16)$$

We have to evaluate the values of A, B, C, H, M and N from experimental data for a complete analysis. If one receiver is at the origin (0,0) and another at $(0, \xi_0)$, the value of $\rho(\xi_0, 0, 0)$ can be easily calculated by comparing two records with zero time delay. We also get on substitution in (16)

$$\rho(\xi_0, 0, 0) = 1 + A\xi^2$$

$$\text{or} \quad A = \frac{\rho(\xi_0, 0, 0) - 1}{\xi_0^2} \qquad (17)$$

similarly we obtain

$$B = \frac{\rho(0, 0, \tau_i) - 1}{\tau_i^2} \qquad (18)$$

and

$$C = \frac{\rho(0, \eta_0, 0) - 1}{\eta_0^2} \qquad (19)$$

Also it can be seen that

$$H = \frac{1 + \rho(\xi_0, 0, \tau_i) - \rho(\xi_0, 0, 0) - \rho(0, 0, \tau_i)}{2\xi_0\tau_i} \qquad (20)$$

$$M = \frac{1 + P(0,\eta_0,\tau_i) - P(0,\eta_0,0) - P(0,0,\tau_i)}{2\eta_0\tau_i} \qquad (21)$$

$$\text{and } N = \frac{1 - P(\xi_0,\eta_0,0) - P(\xi_0,0,0) - P(0,\eta_0,0)}{2\xi_0\eta_0} \qquad (22)$$

We have thus to evaluate only

$$P(\xi_0, 0, 0),\ P(0, \eta_0, 0),\ P(0, 0, \tau_i)$$
$$P(\xi_0, 0, \tau_i),\ P(0, \eta_0, \tau_i) \text{ and } P(\xi_0, \eta_0, 0)$$

for the determination of all the constants. Yerg, by assuming the general ellipsoid equation, does away with the assumption regarding isotropy and shows that

$$V_x = \frac{H/A + HN/AC}{1 - N^2/AC} \qquad (23)$$

$$V_y = \frac{-H/C + HN/AC}{1 - N^2/AC} \qquad (24)$$

$$\text{and} \qquad V_c' = \frac{B(1 - \tan^2\theta)}{A + C^2\tan^2\theta + 2N\tan\theta} \qquad (25)$$

The value of τ_i is chosen arbitrarily in the above analysis and no criterion exists for the selection of its value. The values of V_x and V_y and Vc in general depend upon the value of τ_i chosen. In order that the results may agree with those obtained by Briggs et al, τ_i should, however, be chosen so that the assumption of anisotropy in their treatment is justified. This is possible only if γ

is such that it is within the linear portion of the curve of τ vs $(\tau'^2 - \tau^2)$.

In the following sections, two records are chosen and analysed by all the above methods as examples. The records chosen for the analysis are also reproduced.

11-5-1958, 0830, 2.6 Mc/s (E layer)

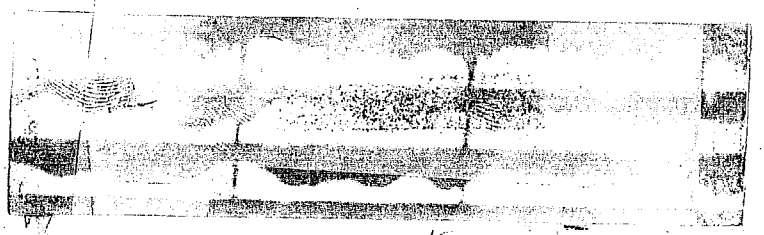

(1) Ratcliffe's method :- The mean values of the time displacements were determined and these were used to calculate the values of the apparent component velocities. The magnitude and direction of the drift were determined by using formulae (4) and (5) with the help of the nomograms given in Sethuraman (1958). The values obtained are 20 m/s and 115°.

(2) Pütter's method :- The velocities corresponding to each set of time shifts are calculated with the help of formulae (4) and (5). These velocities are plotted on polar coordinates. (Fig. 5a) A circle is drawn passing through them and the origin. The diameter to this circle through the origin is drawn and its value gives the magnitude and direction of the drift. The values obtained are V = 17 m/s and θ = 120°.

The individual time shifts are also plotted in

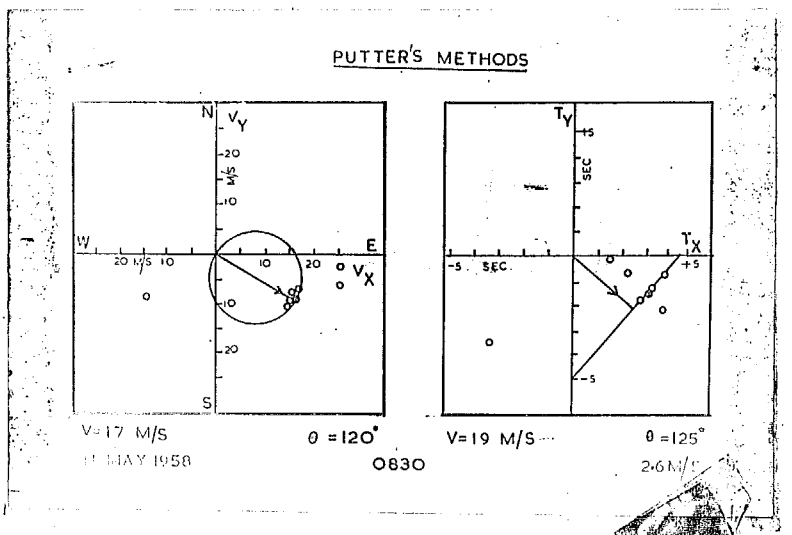

Fig. 5 - Putter's circle and straight line diagrams for determining drift speed and direction.

11th May, 1958, 0830, 2.6 Mo/s.

Fig. 5b. A straight line is drawn through these points and a perpendicular is drawn from the origin to this line. Its direction ($\theta = 125^0$) gives the direction of the drift and the lenght of the hypotenuse gives the value of t. The magnitude of the drift is obtained by dividing the seperation between the aerials by t. The magnitude of the drift obtained by this method is 19 m/s.

The method of Briggs, Phillips and Shinn :- The auto-correlation curves for the three patterns from the central, west and north aerials are plotted in Fig. 6-A. The cross-correlation curves between the central and west and the central and north aerials for various values of time differences, both positive and negative, are given in Fig. 6-B. From these two sets of curves, the value of the time difference on the auto-correlation curve τ' to give a correlation equal to that for a time difference of τ on the cross-correlation curve is determined for both sets of aerials, for various values of τ. Plots of $\tau'^2 - \tau^2$ vs τ are given in Fig. 6-C. Equation (14) viz.

$$\tau'^2 - \tau^2 = \frac{\xi_0^2 - 2 V_x \xi_0 \tau}{V_c'^2} \qquad (14)$$

can be reagranged as

$$\frac{\frac{\xi_0^2}{\tau'^2 - \tau^2}}{V_c'^2} + \frac{\frac{\xi_0}{\tau}}{2 V_x} = 1, \qquad (26)$$

which indicates that the plot would be a straight line. If x' and y' be the intercepts of this line in the X and Y

axes respectively, it can be easily seen that

$$V_x = \xi_o^2/2x' \qquad (27)$$

and $$V_c'^2 = \xi_o^2/y' \qquad (28)$$

The values of V_c' and V_x can thus be calculated. Similarly from the other curve V_y and V_c' can be calculated. The actual value of the drift speed and direction and the mean value of V_c' can be calculated.

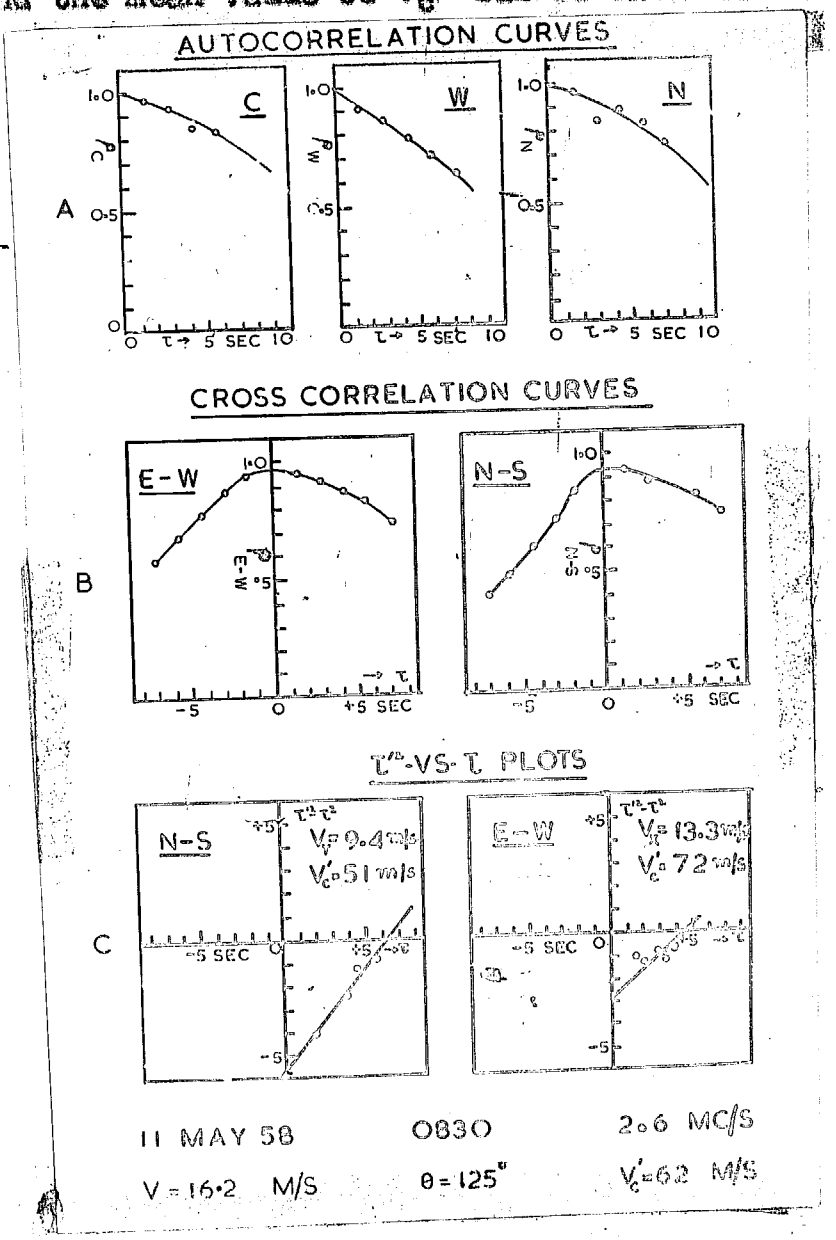

Fig. 6 - Briggs, Phillips and Shinn curves, for

The actual random velocity V_c is given by $V_c^2 = V_c'^2 + V^2$. The values of these quantities obtained by this method are given in Table 1.

Yerg's method :- As mentioned previously, Yerg's method requires the computation of only six correlation coefficients. Three of them are fixed, viz. $\rho(\xi_0,0,0)$, $\rho(0,\eta_0,0)$ and $\rho(\xi_0,\eta_0,0)$ and three involve the choice of an arbitrary time lag τ_i viz. $\rho(0,0,\tau_i)$, $\rho(\xi_0,0,\tau_i)$ and $\rho(0,\eta_0,\tau_i)$. If too large a value of τ_i is chosen, the effects of anisotropy of the pattern would be large and the results would not agree with those obtained by the other methods. In order that such effects may not be large, the time lag chosen should be sufficiently small so that the point corresponding to it on the $\tau'^2 - \tau^2$ vs τ plot lies in the linear portion. In the computation shown below a time lag of three seconds is chosen. The values of the correlation coefficients are

$$\rho(\xi_0,0,0) = 0.97; \quad \rho(0,\eta_0,0) = 0.93$$
$$\rho(\xi_0,\eta_0,0) = 0.94; \quad \rho(0,0,\tau_i) = 0.93$$
$$\rho(\xi_0,0,\tau_i) = 0.88; \quad \rho(0,\eta_0,\tau_i) = 0.91$$

The values of A, B, C, H, M and N are calculated with the help of formulae (17-22) and they are as follows .

$$A = -.03/(120)^2; \quad B = -.07/9; \quad C = -.07/(120)^2$$
$$H = .4/(120)^2; \quad M = +1/120^2 \text{ \& } N = -.02/(120)^2$$

Substituting these values in equations (23-25), we obtain,

V_x = 15.5 m/s, V_y = 8.2 m/s, V = 17.6 m/s, $\theta = 118^0 9'$ and V_0 = 44 m/s. The values of these various parameters obtained by the methods described above are given in table 1.

Table 1

Comparison of the results of drift parameters calculated by different methods (11-5-58, 0830 2.6 Mc/s.)

Method	V or V' m/s	θ Degrees	V_0' m/s	V_0 m/s
Ratcliffe's	20	115	-	-
Putter's circle	17	120	-	-
Putter's St.line	19	125	-	-
B.P.S. method	16	125	62	64
Yerg's method	18	118	40	44

13-9-1959, 2330, 2.6 Mc/s

Ratcliffe's method gives a value of 130 m/s and 25° for the velocity of drift. ~~The~~ Putter's straight line and circle diagrams are drawn in Fig. 7. It will be noticed that the dispersion is greater in this case than in the previous one. This is due to the turbulent nature of the fading pattern. The values of the drift parameters are

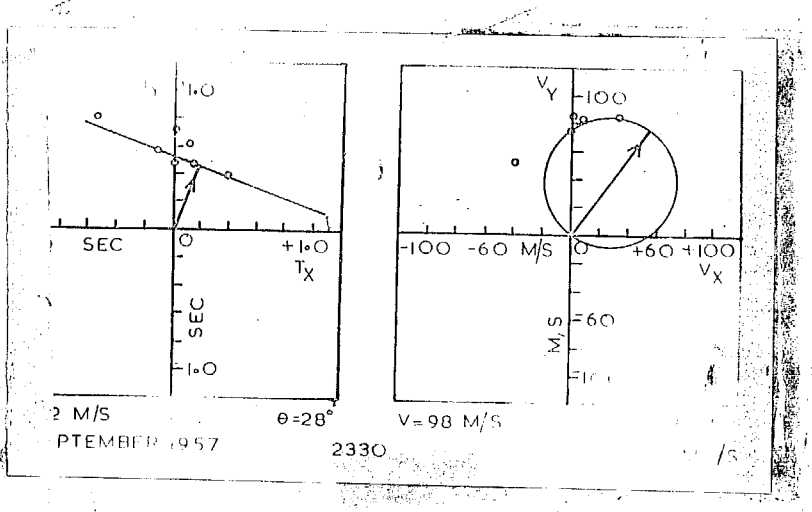

Fig. 7 - Putter's diagrams.

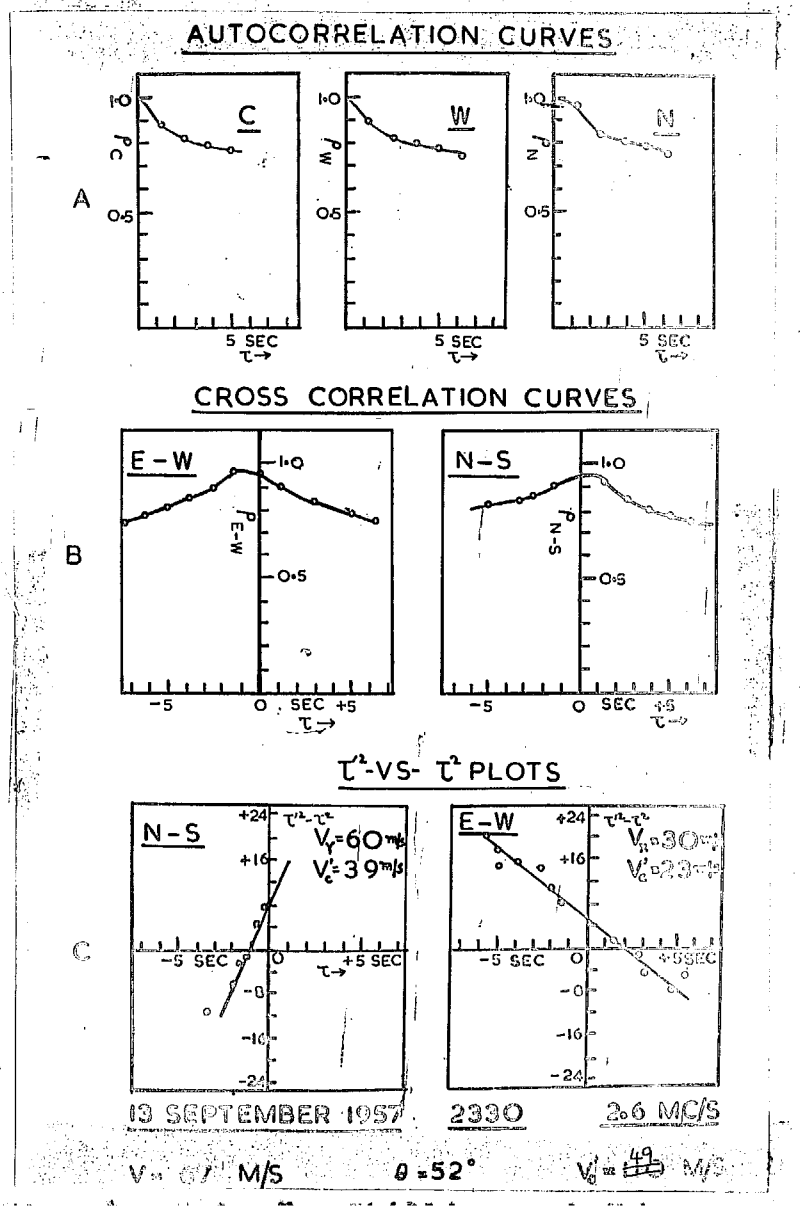

indicated on the diagram itself.

The Briggs, Phillips, Shinn curves are shown in Fig. 8. The values of the drift parameters obtained by this method are given in Table 2.

Yerg's method :- The value of the six correlation coefficients for a time lag of three seconds are as follows.

$$\rho(\xi_o, 0, 0) = 0.96; \quad \rho(0, \eta_o, 0) = 0.97$$
$$\rho(\xi_o, \eta_o, 0) = 0.94; \quad \rho(0, \xi_o, \tau_i) = 0.81$$
$$\rho(\xi_o, 0, \tau_i) = 0.80; \quad \rho(0, \eta_o, \tau_i) = 0.82$$

The values of A, B, C, H, M and N are as given below.

$$A = -0.04/(120)^2; \quad B = -0.19/9 \quad C = -0.03/(120)^2$$
$$H = 0.6/(120)^2; \quad M = 0.8/(120)^2 \text{ \& } N = 0.005/(120)^2$$

The values of V_x and V_y are 19 m/s and 54 m/s giving a value of V of 57.3 m/s and $\theta = 20^\circ$. The value of V_c is 120 m/s. The values are given in Table 2.

Table 2

Comparison of the results of drift parameters calculated by different methods (13-9-1957, 2330, 2.6 Mc/s.)

Method	V or V' m/s	θ degrees	V_c' m/s	V_c m/s
Ratcliffe's	130	25	-	-
Putter's circle	98	35	-	-
Putter's st.line	132	28	-	-
B.P.S. method	67	25 52°	49	83
Yerg's method	57	20	105	120

Thus with records having a large value of the turbulence component, Ratcliffe's method and its variants do not give the true value of the drift. Correlation methods have to be employed in those cases. However, for the analysis of a large number of records obtained at Ahmedabad showing points of clear similarity, the method of similar fades can be used, and this has been done.

References

Banerjee, K.N.	1958	Jour. Atmos. Terr. Phys., 12, 248.
Barber, N.	1957	Jour. Atmos. Terr. Phys. 11, 298.
Briggs, B.H. Phillips, G.J. and Shinn, D.H.	1950	Proc. Phys. Soc., B 63, 106.
Court, C.W.G.	1955	Jour. Atmos. Terr. Phys., 7, 333.
Krautkrämer, J.	1943	Deutsche Luft. S.B.Nr. 1761.
Phillips, G.J. and Spencer, M.	1955	Proc. Phys. Soc., 68B, 481.
Putter, P.C.	1955	Physics of the Ionosphere, Physical Society, London.
Rao, M.S. and Rao, B.R.	1957	Jour. Atmos. Terr. Phys., 10, 307.
Ratcliffe, J.A. and Gawsey,	1933	Proc. Camb. Phil. Soc., 29, 301.
Ratcliffe, J.A.	1954	Jour. Atmos. Terr. Phys., 5, 173.
Ratcliffe, J.A.	1956	Rep. Progr. Phys., 12, 188.
Ramsay, W.J.	1957	Jour. Atmos. Terr. Phys., 11, 255.
Sethuraman, R.	1958	Proc. Ind. Acad. Sc., 48, 84.
Yerg, D.G.	1955	Jour. Geophys. Res., 60, 173.

* * * * * *

CHAPTER II

THE METHOD OF CLOSELY SPACED RECEIVERS

CONTENTS

CHAPTER III

EXPERIMENTAL TECHNIQUE

Contents

CHAPTER III

EXPERIMENTAL TECHNIQUE

The method used ~~in this laboratory~~ at Ahmedabad for drift measurements in the ionosphere is the spaced aerial method originally used by Krauskrämer (1943) and modified by Mitra (1949). The first equipment was designed by Nanda (1955); it could be operated only at a single frequency (5 Mc/s) and its power output was low. The equipment was redesigned by the author for ~~the~~ larger power output and for operation at other desired frequencies. The present chapter gives a brief description of the equipment.

1. General design of the equipment

The whole assembly of the transmitter and receiver is contained in two racks. The aerial system consisting of two dipoles for transmitter and three for receivers were erected in the open space around the laboratory. Separate aerials were used for different frequencies. The transmitter sends out pulses of 100-300 μs duration at the recurrence frequency of the mains supply, which is 50 c/s. Provision is made to go over from one frequency to another by means of switches which connect the appropriate coils in the oscillator and the R.F. amplifier stages of the transmitter. The peak power outputed from the transmitter

is about 1.5 km. The reflected pulses are received at three aerials placed at the corners of an isosceles right angled triangle whose equal sides are 120 meters each. The signals from the three spaced aerials are brought to the receiver unit.

The signals from the three aerials are fed successively into the main receiver by means of an electronic switch. The output from the receiver is applied to one of the Y deflecting plates of the monitor cathode ray tube and to the horizontal plates of the recording cathode ray tube. A gate circuit generates a positive pulse for selecting the set of echoes in the monitor and at the same time it is also applied to the control grid of the recording oscilloscope which is given the cut-off bias. Thus in the recording oscilloscope the spot appears on the screen only when reflections are applied to its deflecting plates. The pulse outputs from the electronic switch are added to give a step wave. This step wave is applied to the other deflecting plate of the recording scope and, in the absence of time base in that scope, appears as three dots one by the side of the other on the screen. The signal from any given aerial and the spot corresponding to that aerial or both synchronised by the common pulse generator which switches the aerial and generates the step. The echoes from the three aerials appear as three bright lines one by the side of the other and are recorded on a movie 35mm film. The detailed description of the component units of the system are given

Transmitting unit

This unit contains the pulse generator, the pulse modulated transmitter and the associated power supply units.

Characteristics of the pulse

The following three characteristics of the pulse are of importance in ionospheric work. (1) Peak power (2) width of the pulse and (3) repetition rate. In addition, the pulse should have short rise and fall times. The design consideration to ensure a satisfactory pulse have been discussed in the literature (Chance et al, 1949) and are summarised below.

The peak power of the transmitter determines the amplitude of the reflected pulse. In the tropics, especially during high sunspot years, the absorption of medium frequency radio waves in the ionosphere is very high and a large power output is therefore required for satisfactory operation. With large powers, however, the design becomes complicated and also the receiver when placed near the transmitter gets paralysed.

The recieved power 'S' of a reflected pulse depends upon the transmitter power, the types of antenna used for transmission and reception, the distribution and nature of the reflecting medium and the absorption in the ionospheric regions. The power density of the transmitted wave is $PG_T/4\pi R^2$, where P is the transmitted power, G_T is the gain of the

antenna and R the distance of the target from the transmitter. When this is radiated without any loss from the target of area σ and reaches the receiver situated close to the transmitter, the received power density is $[P_T/4\pi R^2]\,\sigma/4\pi R^2$ and the power fed into the receiver is obtained by multiplying this quantity by the cross section of the receiving antenna given by $G_R \lambda^2/4\pi$. Thus $S = P.\, G_T G_R \lambda^2 \sigma/(4\pi)^3 R^4$. In ionospheric work, if we define the frequency, we do not have control over any factor except P. It will be seen that the received power is directly proportional to the transmitter power. To be detectable, the reflected signal should have a certain minimum power. This minimum detectable power (S min) is governed principally by the receiver noise and the minimum signal-to-noise ratio which could give a detectable pulse at the recorder.

The transmitter power P depends upon the peak power of the transmitter and the pulse width. The pulse width must be sufficiently small so that at the minimum range at which reflection is to be obtained, usually the E layer in our experiments, the transmitter is quiescent by the time the echo pulse from the layer is returned to the receiver. It is also limited by the resolution required to separate the ordinary and the extraordinary components of the reflected echoes which arrive with a short delay from each other. On the other hand, the minimum pulse width is limited by the band pass restrictions on the R.F. and I.F. amplifiers.

This cannot be very large because of the limitations caused by the interference, the fidelity of reproduction of the pulse, the necessity to restrict the frequency spread of the transmitted side band energy to prevent interference with other services and by the requisite resolution of the critical frequency phenomenon which becomes indistinct when the radiation embraces a very wide band of frequencies. A pulse duration of 100 to 250 μs is used as a compromise. The pulse repetition rate should also be chosen properly. With too high repetition rates, the echo from a given pulse may not return to the receiver until the next pulse is transmitted. This causes an ambiguity since the return echo from any particular pulse cannot be easily identified. At the same time, the repetition rate should be kept high enough to provide an advantageous integrating effect of the received signals from successive pulses.

Although the transmitted peak power is very large (1.5 kW in our case) ordinary tubes can be used in pulse transmitter circuits because of the fact that such large powers are generated only for a short time. Provided the pulse power and the pulse duration are not too large, the average power transmitted can remain well within the rated values for such tubes. In effect, the large period during which the tube is quiescent enables the heat produced to be dissipated safely.

The block diagram of the transmitter unit is given

in Fig. 1.

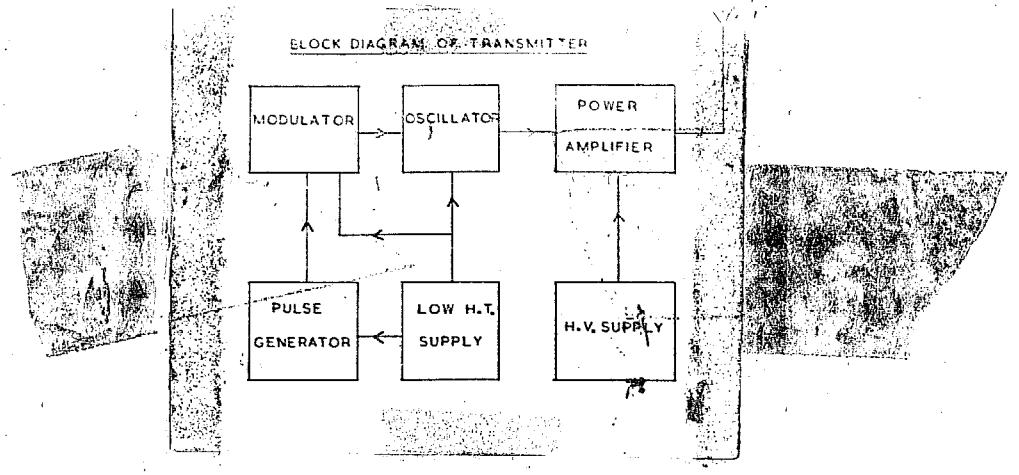

Fig. 1 - Block diagram of transmitter

We shall consider briefly the features of the five sections of the transmitter unit viz. (1) triggered pulse generator (2) modulator (3) power amplifier and (4) power supplies.

Triggered pulse generator :- The circuit diagram of this unit is given in Fig. 2.

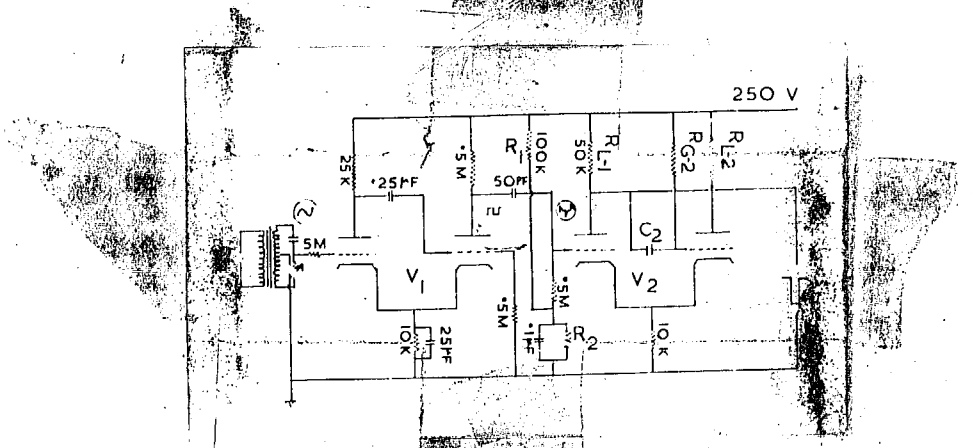

Fig. 2 - Triggered pulse generator

V1 is a square wave generator and is an over-driven amplifier.

An A.C. voltage of about 70V RMS is fed into the grid by the transformer T1. The C-R combination connected across its secondary is used to shift the phase of the input which is fed to the grid of the square wave generator with respect to the mains supply wave. The square wave form obtained at the second anode of the tube is differentiated by the C-R combination at the grid of V2. V2 is operated as a cathode coupled monostable multivibrator, in which the stable state is the one in which the right hand side V1A is nonconducting. During the positive portion of the pipe, indicated at the grid of the first section of V2, the tube starts conducting. This results in the condenser C2 charging upto the value of the D.C. supply voltage. Its charge stops the right hand side of V2 from conducting and leaks through R_{g2} at a rate determined by the $C2R_{g2}$ combination. After a certain interval of time, the tube begins to conduct and the stable state is reached once again. This results in a pulse to be produced which has a negative polarity at the first tube and a positive polarity at the other. This pulse is fed into a differentiating circuit in the transmitter (Fig. 3), in which the resistance part can be adjusted in steps. The output is fed into the pulse-width control tube V3. At the anode of this tube, pulses of variable width are obtained. The modulator tube V5 and V6 are 6L6 tubes. They are amplifiers which invert the polarity of the pulse, thereby making it suitable for modulation and also give it sufficient power to drive the oscillator circuit which they feed. A push-pull oscillator circuit consisting of

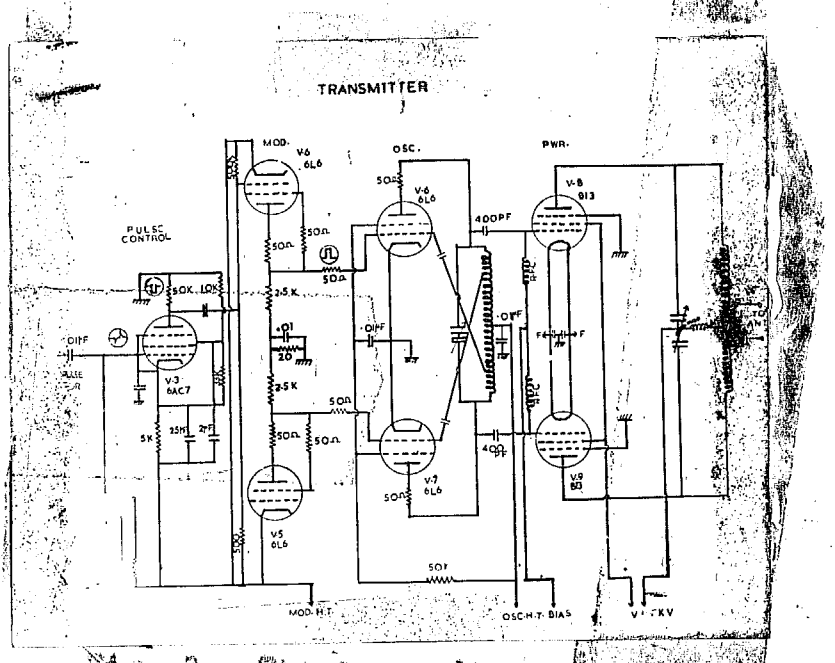

Fig. 3 - The transmitter

V6 and V7 is biassed to cut-off and the pulse from the modulator excites it. The output from the pulsed oscillator is fed into the power tubes V8 and V9 (813's) connected in push-pull and operating under class B conditions. The anode circuit of this stage is tuned and coupled to the antenna. The H.T. applied to the anode of the 813 tubes is 1500 V and it is obtained with the help of a high voltage transformer and a metal rectifier. The bias and the low H.T. supplies are regulated while the H.T. supply for the 813 anode are not.

Dipole antennas are used for both transmission and reception. Two transmitting antennas are used for the transmitter, one for each set of frequencies used in the work. The antennas are brought to the transmitter through an 80 ohm

coaxial cable and coupled to the anode through suitable transformers. The receiving antennas are also dipoles. Only one set of dipole, designed for operation on 2.6 Mc/s, and are used for reception at all frequencies. This arrangement results in a loss of gain at the antenna at all the other frequencies but it was found to be satisfactory. The receiving aerials are connected to an electronic switch through coaxial cables and suitable transformers.

The distance between the receiving aerials is determined by two factors ; with too large separation the correlation between the wave forms at the two aerials decreases while with too small spacing the time shift between corresponding point in the three patterns becomes very small, thereby making it difficult to measure them accurately. Various spacings were tried and it was found that a separation of one wave length at 2.6 Mc/s (120 metere) gave satisfactory results.

Receiving and recording system

The block diagram of this system is given in Fig. 4 . It contains the following elements. (1) An electronic switch to switch-in the three aerials in succession to a common receiver. (2) A receiver suitably modified for pulse reception. (3) A master pulse generator providing a synchronising pulse. (4) Gate generator for selecting the pulse under study and for synchronising the electronic switch. (5) A time base circuit

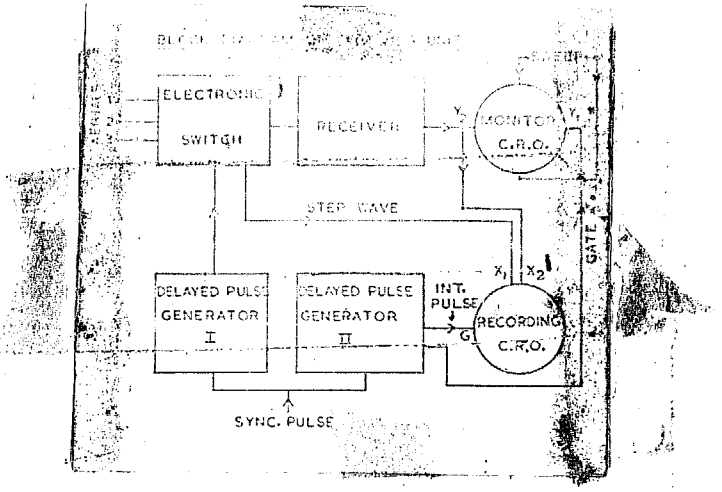

Fig. 4 - Block diagram of receiving unit.

for the monitor cathode ray tube. (6) The monitor and recording cathode ray tubes. (7) Camera unit and time marker for photographing record. (8) Power supply unit for operating all these elements. The various sections are described below.

The electronic switch :- The basic element of the electronic switch used by the author are (1) a three stage ring multivibrator, giving three pulses in succession, (2) three amplifier tubes to which the three aerials are connected and switched in succession by the pulses from the ring multivibrator and (3) an adding circuit which adds up the three pulse wave forms from the ring multivibrator, thereby generating a step-wave form which is applied to the recording oscilloscope. The circuit diagram of the electronic switch is given in Fig. 5 and the various elements are described below.

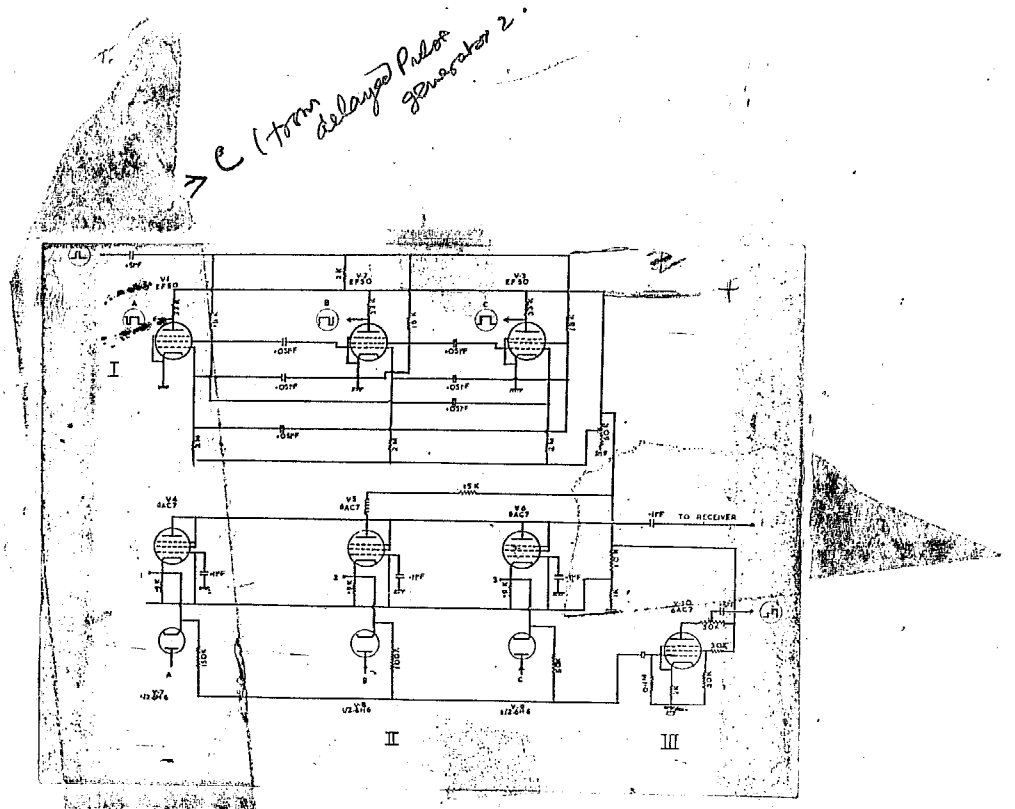

Fig. 5 - The electronic switch.

(1) The ring multivibrator (section I of Fig. 5):- This consists of three tubes V1, V2 and V3 connected as a ring multivibrator. Each of these tubes is triggered by means of synchronising pulse, generated from a delayed pulse generator described later. At any instance, one of the tubes is non-conducting and the other two tubes are conducting. The non-conducting tube charges the C-R combination at its screen to the B+ value and this combination afterwards discharges at a rate determined by its time constant. The next tube then conducts and the cycle is repeated. The whole process is synchronised by the external pulse. The output pulse waveforms are electron-coupled to the anode to prevent interaction of the external circuits on the multivibrator.

(2) The switched R.F. amplifiers (Section II of Fig. 5) :- Three grounded grid amplifiers V4, V5 and V6 are switched by means of the wave-forms A, B and C from the ring multivibrator and these are injected to the cathodes through three diodes. The cathodes of these diodes are returned to a point at a voltage of+27 volts with respect to ground and thus during the positive portions of the pulses it conducts. The cathodes of the 6AC7 tubes (V4, V5 and V6) are kept at a large positive potential with respect to the grid, thereby preventing it from conducting. During the negative portions of the pulses, however, the diodes stop conducting and the grid voltage in the R.F. amplifier tubes is only that due to the 0.9 k ohm the resistance connected in the cathode circuits. The tubes therefore conducts and the R.F. voltage applied to the cathode circuit appears in the output circuit. The anodes of the three tubes are connected to a common load consisting of an R.F. choke and a 15 k ohm resistance. The output from each of the amrials thus appears across the load in succession. This output is taken to the common pulse-receiver through a 0.1 uf condenser.

(3) The step-wave generating circuit (Section III of Fig. 5) :- The switching wave-forms from the ring multivibrator are added through potential divider arrangements having a common resistance of 100 k at the grid of V10 and individual resistor of 50 k, 100 k and 190 k to which the three wave-forms are applied in succession. The resulting step wave-form at the

III

grid of V10 is amplified by the tube and a desired amplitude of the step wave, which determines the spacing between the traces in the recording oscilloscope, is obtained with the help of a potentiometer load at the anode of the amplifier.

The receiver :- Among the desirable characteristics for pulse receiver are (1) a high sensitivity, i.e. the ability to detect weak signals, (2) faithfulness of reproduction, (3) rapid recovery from the effects of large transient input voltages and (4) reasonable linearity between the output and input signal levels.

The useful sensitivity of a pulse receiver for weak signals is influenced by many factors such as the gain of the R.F. stages and the I.F. stages of the receiver, the noise figure of the receiver, the ability to reproduce pulses with as little distortion as possible. The minimum detectable signal by the receiver depends in addition, on the repetition rate of the transmitted pulse. Some of these factors are discussed below.

The noise figure of the receiver :- A signal, no matter how it arrives, has associated with it a certain minimum amount of noise due to the fact that the antenna generates the Johnson noise associated with its radiation resistance at temperature T. It is useful to specify this temperature (noise temperature) of the antenna at which its radiation resistance should be in equilibrium in order to account

for all the noise fed into the receiver. The available noise power is thus equal to kTB, where k is the Boltzman's constant, B the band-width accepted and T the noise temperature. Therefore, at a signal level S, the maximum signal-to-noise ratio at the input terminals is S/kTB. If So and No are the signal and noise outputs from the receivor, the signal-to-noise ratio at the output terminals is So/No. The ratio of these two signal-to-noise ratios is known as the noise figure of the receivor and represents, qualitatively the additional noise introduce by the receiver. In an ideal receivor, this ratio is equal to unity. When the value of S becomes small, as in ionospheric work, where the signal power of the reflected pulse is a few micro-micro-watts, this factor assumes great importance in the design of the receiver. Since the additional noise is confined generally to the first one or two stages and the mixer stage, great care has to be taken in the design of these stages. In radar receivers R.F. stages are omitted for this reason but since a large R.F. gain is essential for ionospheric work, two carefully designed R.F. stages are generally used in the receiver. In fact, the removal or reduction of the noise sources in and around the receiver is one of the major problems of the design of the receiver for ionospheric work.

Band width requirements :- The band width requirements of a receiver for pulse reception are very different from those of a conventional broadcast receivor

and are determined by considering various conflicting factors. Faithful reproduction of the pulse shape requires a large band-width but too large a band-width results in a greater amount of noise to be introduced into the receiver. From the point of view of the best signal-to-noise ratio, the optimum value of the product of the band width B and the duration of the pulse τ is given by $B\tau \simeq 1$. This can be easily seen from the following considerations. Consider an I.F. amplifier whose band-width can be continuously increased from a value zero. At first, the signal level will increase linearly and the noise level will increase as the square root of the band width (since $E_N = \sqrt{4kBTR}$). Thus, there will be an overall increase of the signal-to-noise ratio. When the band-width is sufficiently large to reproduce the flat top of the pulse faithfully, any increase in the band-width will not cause an increase in the signal, but the noise will increase and the S/N ratio will begin to decrease. The optimum value of the band width is obtained when $B\tau = 1$. This value is not critical at all and the band-width twice the value increases the minimum detectable signal by only about 1db. This however, results in a better reproduction of the pulse and therefore in practice this band width is used. Since our minimum pulse width is 100 μs , the band width of the receiver should be 20 kc/s.

There are four methods which have been extensively used to improve the band-width of the receiver. They are,

(1) damping the tuned circuits, thereby reducing the Q and increasing the band-width. Since Q = R/X = fo/B, where the symbols have their usual meanings, knowing X, fo and the B required, the value of R can be calculated.(2) By means of over-coupled circuits. The design of such circuits have been extensively studied (Sturley, 1954). By employing mixed (both capacitive and inductive) couplings of different types double-hump characteristics can be produced in the response curve of the tuned amplifiers giving rise, in effect to flat topped response curves, (3) by means of staggered tuned circuits (Sturley, 1954, Zepler, 1942) and (4) by negative feed back amplifiers where a fraction of the output of a single tuned synchronous amplifier is fed in the inverse phase to the input circuit. More voltage is fed back at resonance than off resonance and hence the response curve becomes flat. Perhaps the simplest of all the methods from the point of view of design is the first method viz. damping of the tuned circuit although this results in a loss of gain of the amplifier. This method is used by the author to get the required band width of 20 kc/s.

A factor of great importance in the design of wide band amplifiers in the figure of merit of the stage. This refers to the ability of the amplifier to give a large gain over a wide band of frequencies. It can be easily shown that in the case of a single tuned amplifier the band width for a 3 db fall in the maximum gain of the amplifier is given by $B = 1/2\pi R_{\parallel} C_{\parallel}$, where $R_{\parallel}$ is the total parallel

impedance across the output circuit and $C_{\parallel}$, the total parallel capacity of the output circuit, including those contributed by the next stage. The gain of the stage is given by $g_m.R_{\parallel}$. The gain band width product is thus $g_m/2\pi C_{\parallel}$. In order to have a large gain over a wide band of frequencies the total parallel capacity across the circuit is kept small by wiring the circuit carefully to reduce the stray capacity and by choosing a tube having a large value of transconductance. Special tubes like 6AC7, 6AK5 with large transconductances have been designed for use in such wide band circuits. In the receiver used in the laboratory, all the amplifiers use 6AC7 tubes.

Rapid recovery from the effects of a strong signal:- A very important further requirement of a pulse receiver situated very near the transmitter, as in the equipment used by the author, is that it should recover rapidly from the effects of the strong ground pulse from the transmitter. The transmitter causes an enormous overloading of the receiver resulting in the paralysis or blocking of the receiver making it insensitive to signals below a certain level for a short while after the ground pulse. This is the result of transient shifts in the electrode voltages of the amplifier tubes produced by charges on the bypass or coupling condensers. The recovery time depends on the time constants of the coupling circuit and may be only a few micro-seconds or several milli-seconds depending on the point

at which the blocking occurs. In extreme cases, as in high power radar, such overloading might burn out the coils and damage the tube. In such cases, a transmit-receive switch is used in conjuction with line transformers to short circuit the receiver terminals while the transmitter is operating (Pink, 1949). Such a procedure is not practicable in ionospheric work because of the low frequency and low power involved. Two methods have been used by the author to eliminate the effect; (1) the use of coupling circuits with short time-constant, consistent with the efficiency of coupling and the fidelity of reproduction and (2) the application of a negative square pulse of suitable width and phase to the supressor grids of the two R.F. stages of the receiver. This cuts out the R.F. stages and thereby the input to the receiver for the duration of the pulse. This pulse is synchronised with the transmitted pulse and thus the receiver is made insensitive when the transmitter is operated.

In addition to the considerations given above, it is also necessary that the receiver has good stability and that no drift occurs in the frequency to which the receiver is tuned. This is achieved by a proper ventilation of the receiver as a whole so that the temperature changes in the oscillator circuits which are mainly responsible for such drifts are minimised and by stabilising the voltages applied to the various circuits

A 52 - 312 receiver, obtained from the Army

surplus disposals equipment, was modified to achieve all the characteristics described above. The following are some of the limitations of the receiver which had to be rectified before it could be used as a pulse receiver. (1) The overall gain of the receiver was small especially when the I.F. stages were damped to get the required band width. This was partly remedied by using 6AC7 tubes which have a large transconductance. (2) The band width of the receiver was 10 kc/s. This band width is sufficient for the purpose for which the receiver was originally intended viz. CW and broadcast reception. As pointed out earlier, the band width expected from the receiver is about 20 kc/s. This is obtained by connecting damping resistors across the I.F. transformers (Fig. 6). This gave an overall band width of

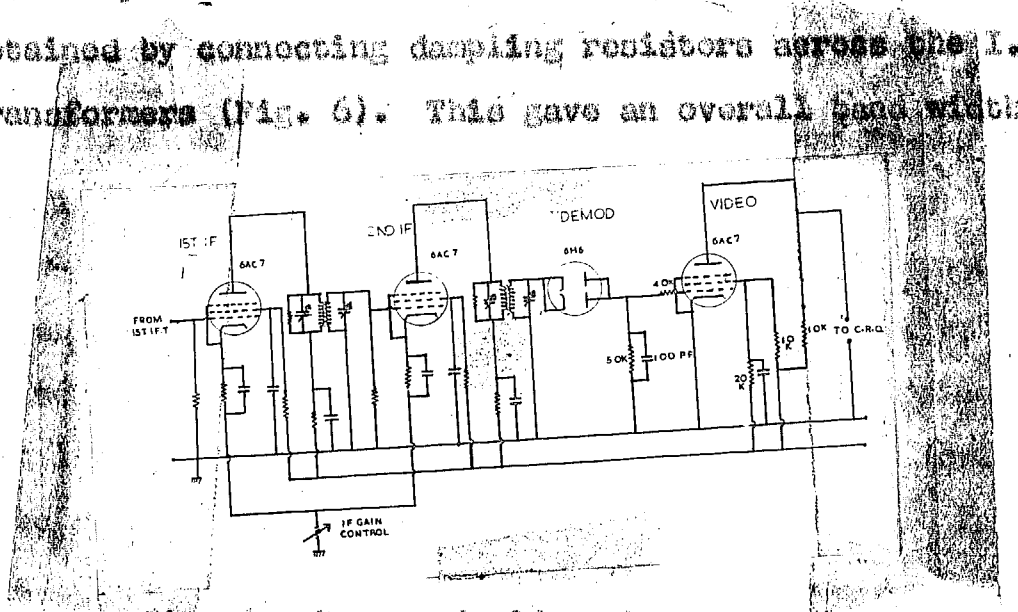

Fig. 6 - I.F. and video stages.

30 kc/s for the I.F. stages for 3 db fall in the signal output from the maximum. The band width of the receiver as a whole however was smaller than this figure because of the tuned circuits in the R.F. stages and was found to be dependent, to some extent, on the frequency to which it

was tuned. A band width of approximately 20 kc/s was obtained at 2.6 Mc/s.

Blocking of the receiver :- When kept near a high power pulse transmitter, the BC-312 receiver suffered from paralysis. This was eliminated by injecting a negative pulse to the supressor grid of the two R.F. stages of the receiver during the period when the transmitter was radiating, thereby rendering the tubes inoperative during those periods.

The A.G.C circuit was removed. The presence of the A.G.C. tends to supress fading which we are interested in studying.

A 6H6 was used as the second detector in the modified receiver. This has the advantage of a low inter-electrode capacitance and a low conducting resistance, the essential requirements of a good detector. It is so connected that a pulse of negative polarity is obtained, so that the limiting action of the cut-off of the following video amplifier could be used to prevent blocking. The time constant of the load circuits in the diode was so chosen as to effect a compromise between obtaining a steep edge for the pulse, which requires a short time constant, and obtaining the largest possible pulse envelope with minimum I.F. component, which requires a large time constant. A load resistance of 50 k ohm and a condenser of 100 pF were used in the circuit.

Video amplifier :- The detected pulse output was too small to be displayed on the cathode ray oscillograph. It had to be amplified by a video amplifier. A 6AC7 tube was used for this purpose without any type of compensation as a resistance-capacity coupled amplifier. The component values were adjusted by trial and error to get a satisfactor response from the stage. The output from the video stage was applied to the display units.

The receiver so modified has an overall gain of 3×10^6 times with a good signal-to-noise ratio and satisfying all the requirements of a pulse receiver.

The trigger pulse generator :- This unit (Fig. 7) supplies a triggering pulse to initiate the time base unit

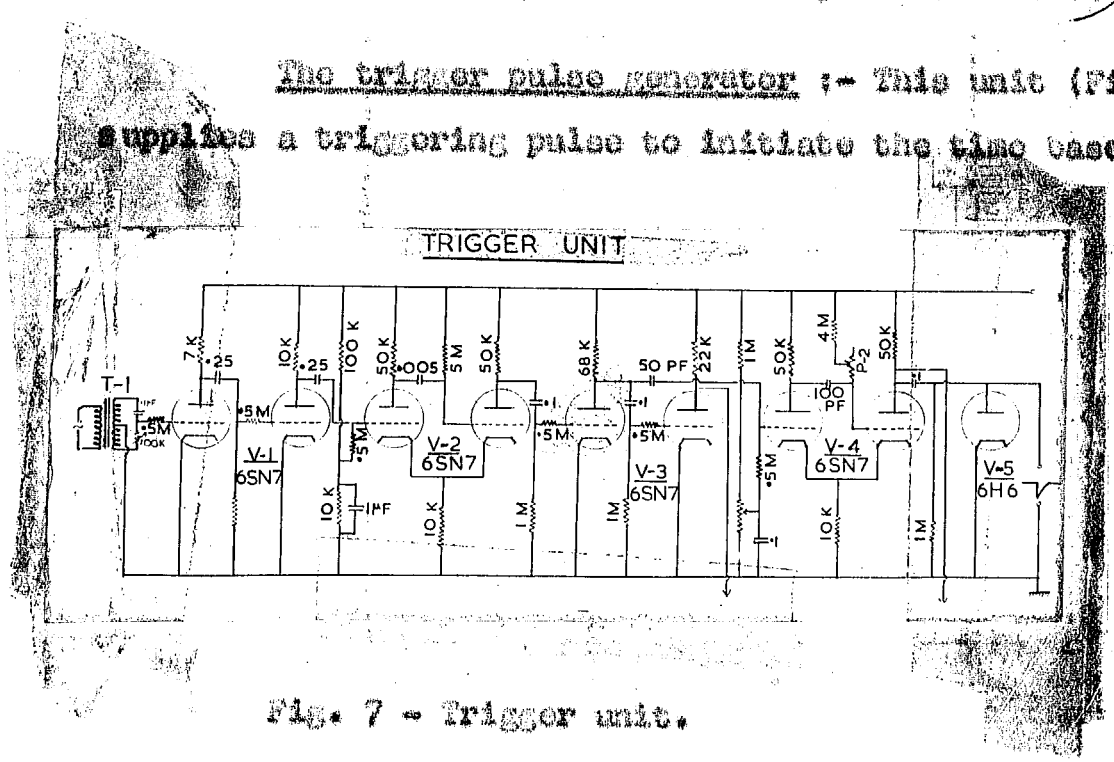

Fig. 7 - Trigger unit.

and the delayed pulse generators described later. The circuit is similar to the one used in the transmitter unit. The pulse output from this unit synchronises the operations of the time base and the gate generator. Originally, a

a common trigger generator supplied the pulse input to the transmitter unit and the receiver unit but it was found that such an arrangement hampered the independent movement of the transmitter and receiver unit racks. Two pulse outputs, isolated from each other by V4 in Fig. 7 were obtained , one for the time base units and the other for the delayed pulse generators.

The delayed pulse generator :- Two delayed pulse generators (Fig. 8) are used to generate pulses of variable width and delay and are used to give the gate wave-form for selection of the echoes in the monitor and to provide the intensifying pulse for exciting recording oscilloscope when the receiver input is applied to its

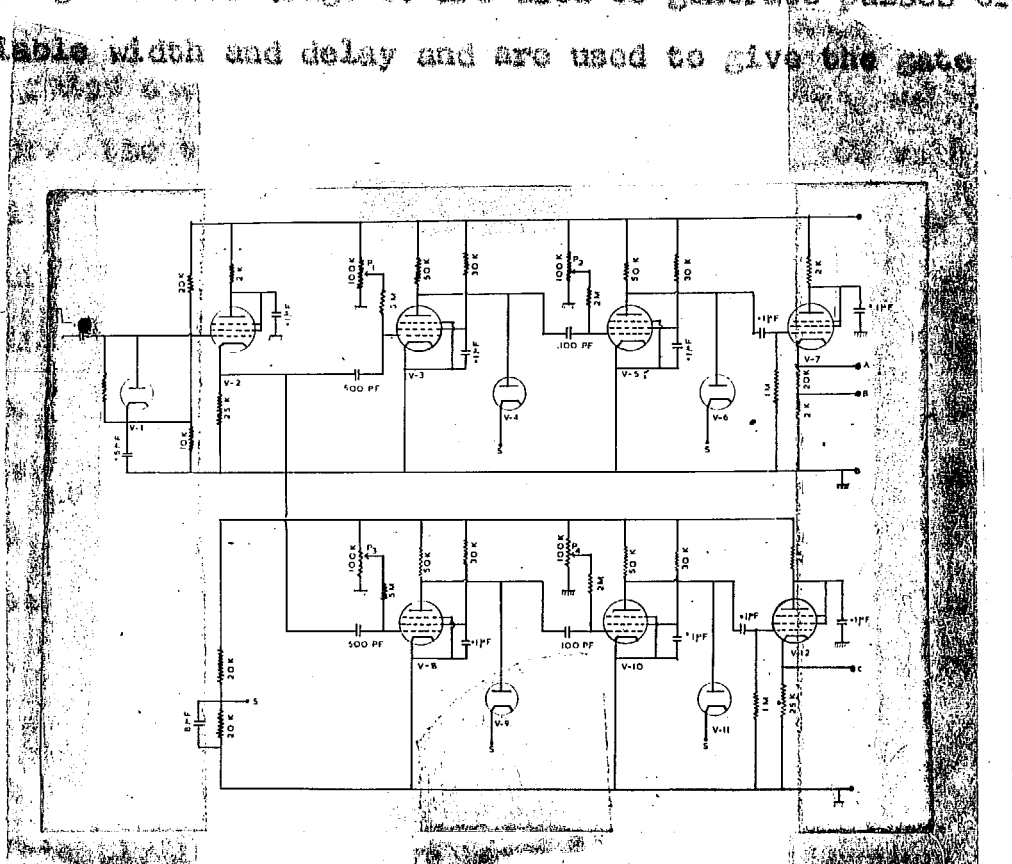

Fig. 8 - Delayed pulse generator.

deflecting plates. It is also used to synchronise the electronic switch circuit described previously. The circuit of these generators are given in Fig.8. There are two sets of such generators, one for providing the synchronising pulse for the switch and the other for providing the gate and the intensifying pulse for the recording scope. These circuits generate pulses of variable width and phase with respect to the transmitted pulse. The input for these two generators are obtained from the triggered pulse generator described above (Fig. 7) This pulse output has an amplitude of 120 volts. Diode V1 restores the upper D.C. level of the pulse to 100 volts and it is then fed into the cathode follower V2. The output of this cathode follower is a positive pulse of amplitude 100 volts. This pulse is coupled to V3 through a C-R combination of 500 pF and 5 M ohm, in series with a potentiometer. Tube V3 is conducting at the commencement of the initiating pulse and stops conducting during the negative portions of the differentiated input pulse at its grid. The condenser at the grid circuit of V3 (500 pF) charges up and discharges at a rate determined by the C-R combination at the grid circuit. When the grid attains a sufficiently large positive potential during the discharge period, the tube again starts conducting. At the anode of V3, we thus get a positive pulse whole duration is controlled by the grid circuit potentiometer. This wave form is further differentiated and applied to the next grid. During the

negative portions of the differentiated wave-form, which occure after a variable time delay with respect to the initiating pulse, depending upon the width of the pulse output from $V3_A$ the tube starts conducting. The width of the pulse output from V5 depends upon the setting of the potentiometer at its grid. Thus at the anode of V3 a pulse of variable width and delay is obtained. This pulse is coupled to the output through a cathode follower V7. The cathode of V7 is stepped to give two outputs, one of amplitude 150 volts for the excitation pulse for the recording oscilloscope and another 15 volts for the echo selecting gate for the monitor tube.

The other pulse genrating circuit consisting of V8, V10 and V12 is identical with the circuit described above and its output from point C in Fig. 6 is used to synchronise the electronic switch.

The display units :- The display arrangement consists of two 5 inch cathode ray tube, one (5 MP 1) for visual monitoring and another (E 4504/B/16) for photographic recording. P1 screen in the monitor tube produces a green trace with medium persistance while the screen of E 4504/B/16 tube produces a blue trace of short persistance suitable for photographic film recording. The screen of the monitor oscilloscope is brought out on the front panel to enable visual observations of the reflected echo and the recording oscilloscope is enclosed in a light-proof box mounted on the

side of the receiving unit rack. The camera unit is mounted in front of its screen. The sweep wave form is applied to X plates of the monitor scope and the gate voltage and the receiver output are applied to the two Y plates. The sweep wave form is not applied to the recording scope. To one of its X plates the step wave from the electronic switch is applied and to the other, the receiver output. The high tension used for the cathode ray display unit is -1500 volts and is obtained with the help of a transformer and a 2X2 high vacuum rectifier.

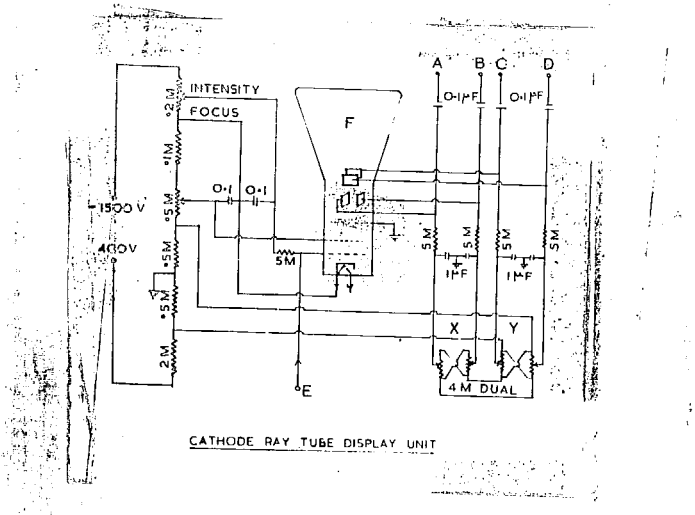

Fig. 9 - Cathode ray display unit.

Terminal	Monitor scope (5UP1)	Recording scope (RA504/B/16)
A	Sweep voltage	Receiver output
B	Sweep voltage	Step wave output
C	Receiver output	Not connected
D	Gate wave form	Not connected
E	Intensifying square wave form from sanatron	Intensifying pulse from delayed pulse generator

Sweep circuits :- The sanatron type Miller integrator circuit is used as the sweep generator (Fig.10) This circuit is capable of generating wave forms as short as one microsecond with a good amount of linearity. In this circuit, V2 with the cathode, supressor and anode of V4 forms a monostable multivibrator generating rectangular wave forms when triggered by an external pulse injected into it through V1 as indicated. The duration of the wave form is controlled by the capacitor C1 and the setting of the potentiometer at the grid circuit of V3. In the circuit used in this laboratory, the variation of the setting of the potentiometer caused a variation in the duration of the wave form from 1.5 to 20 milliseconds. To obtain a push-pull

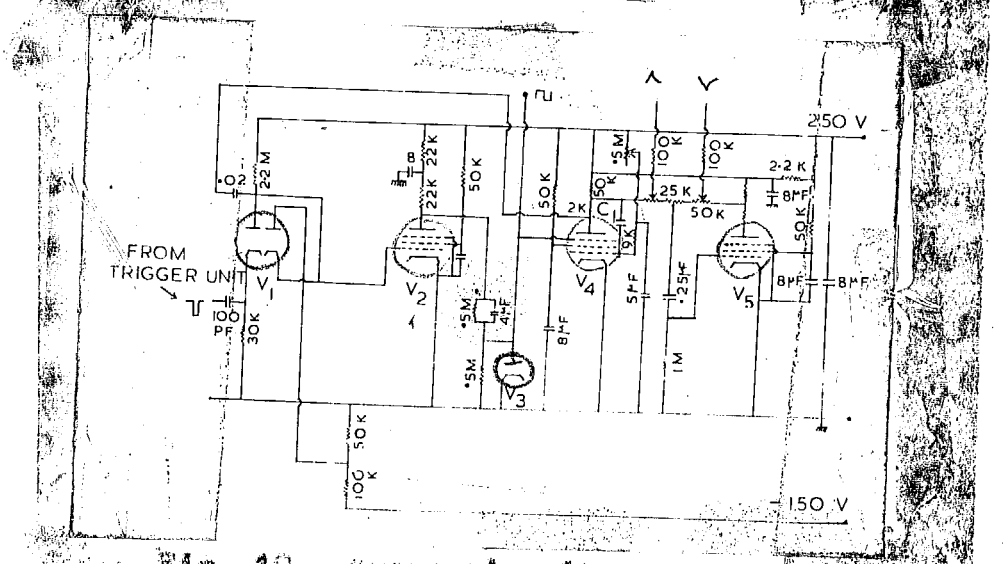

Fig. 10 - Sweep circuit.

output, V4 is coupled to a similar tube V5 in antiphase so that a reverse wave form is obtained at the anode of V5. Ganged potentiometer connected between the anodes of V4 and V5 control the sweep amplitude and the push-pull output is

applied to the X plates of the oscilloscope. Although the push-pull output itself is self balancing, another potentiometer is connected in the input circuit of V5, between the two ganged potentiometers, to compensate for any residual unbalance. Normally, the monitor is given the cut-off bias and no spot appears on its screen. Simultaneous with the sweep output to the X plates, the square wave form at the anode of the sanatron which gives rise to sweep wave form is applied to its grid and it excites the tube. The spot thus appears only when the sweep is applied to the X plates of the oscilloscope. This blanks out the retrace of the pattern.

The diagram of connections of the oscilloscope is given in Fig. 9. There is a common H.T. supply for both the oscilloscope. The low voltage supplies are obtained from conventional circuits. The X and Y shift controls and the focus and intensity controls for the two tubes are kept separate so that each can be adjusted for optimum operation independently.

The camera unit and time marker :- The camera unit is mounted on two rails projecting from the side rack containing the receiving system. The camera is rotated by a motor mounted by its side. It is kept at a distance of about two feet from the oscilloscope screen in light-proof hood, the inside of it is blackened and contains a sliding window for making the necessary adjustments in the oscilloscope.

The camera unit contains a conventional 35mm cine camera obtained from the Army surplus disposals and modified as follows. The lens was changed to one of 2 inches focal length and f/2.8. The drive mechanism was altered to obtain the desired low speed of rotation. The speed is adjusted such that the film moves at the rate of 4 inches per minute. The revolving shutter was removed to obtain continuous exposure and a rotating vane is fixed in front of the lens so as to interrupt the exposure every 12 seconds to provide the time markers.

Power supply units :- To eliminate the instability of the operation of the units, the various power supplies, except the cathode ray H.T. supply and a power supply for the final power amplifier in the transmitter, are regulated. Hunt and Hickman (1939) have discussed the relative merits of the different types of regulating circuits and have come to the conclusion that the degenerative type of regulating circuit, widely used in practice is the most useful. The circuit and its design have been widely discussed in the literature (Koontz and Dilatush, 1947; Hill, 1945) and a design similar to this has been used. There are four supplies giving regulated output of 300 volts, two in a transmitter and two in the receiver and two bias supplies giving -250 volts, one in each unit. Suitable potential dividers are provided in the individual circuits to obtain the necessary voltages. The H.T. for the final stage of the transmitter (+ 2000 volts) is obtained with the help of a stack of CuO-Cu rectifiers. It is found that this arrangement eliminates the interference and is much cooler [illegible]

References

Chance, B.	1949	Waveforms, M.I.T.Radiation Laboratory Series No. 19, McGraw Hill Book Co. Inc.,N.Y.
Fink, D.G.	1949	Radar Engineering, McGraw Hill Book Co. Inc., N.Y.
Hill, A.M.	1945	Proc. I.R.E., 33, 38.
Hunt, F.V. and Hickman, R.W.	1939	Rev. Sc. Instr., 10, 6.
Koontz, P. and Dilatush, E.	1947	Electronics, 20, 119.
Krautkrämer, J.	1943	Deutsche Luftfo. Luft. F.F.Mr.,p-1761.
Nanda, M.C.	1955	M.Sc. thesis (Gujarat University).
Mitra, S.M.	1949	Jour. I. E. E., 96, Pt. III, 441.
Zepler, E.E.	1949	Technique of Radio Design, Chapman & Hall Ltd. London.
Sturley, K.R.	1953	Radio Receiver Design, Vol. 1, Chapman & Hall Ltd. London.

****

Reprinted from the "Proceedings of the Indian Academy of Sciences," Vol. XLII, 1958

MEASUREMENT OF IONOSPHERIC DRIFT AT AHMEDABAD FROM FADING PATTERNS OF REFLECTIONS ON 2·6 AND 4·0 Mc./s. (23° 02′ N; 72° 38′ E)

By

By R. Sethuraman,

PREFACE

Various aspects of the Physics of the Ionosphere are being studied at the Physical Research Laboratory, Ahmedabad under the guidance of Professor K.R.Ramanathan. This thesis presents the results of measurements of drifts in the ionosphere by the closely spaced receiver method. When this work was begun, there were no systematic measurements of ionospheric drift in low latitudes. The data collected by the author will, it is hoped, add to some extent to our knowledge of drifts in these regions.

I am grateful to Professor K.R.Ramanathan for suggesting the problem and for guiding the work in all its stages. The work was carried out under a research scheme supported by the Council of Scientific & Industrial Research, New Delhi. The scheme is now under Dr.U.D.Desai of this laboratory and I am thankful to him for much help and advice. I also wish to place on record my thankfulness to Messrs S.K.Alurkar, Girish D.Desai and U.T.Patel for their help in taking the observations at various stages of the programme. The construction of the apparatus, the work of taking the observations, the reduction and analysis of the data were all done by me with the assistance of my Professor and colleagues as mentioned above. I am also thankful to Mr. M.M.Patel who typed this thesis.

CONTENTS

CHAPTER I

INTRODUCTION

Contents

CHAPTER I

INTRODUCTION

1. Winds and temperatures in the earth's atmosphere upto 100 km.

The existence of winds in the upper atmosphere has been known for a long time. Some idea of the strength and direction of winds in the stratosphere was obtained from the movement of the haze thrown up into it from the Krakatoa eruption of 1883. Observations of noctilucent clouds and of long enduring meteor trails gave us some general knowledge of winds at the levels at which they are usually seen. Today, the efforts of meteorologists have provided us with a systematic body of knowledge regarding winds in the atmosphere upto 30 km from observations of balloons and, indirectly, from a network of stations measuring temperatures. For high levels upto 50 km, we have limited balloon measurements at a few places. Measurements of the velocity of sound from arranged explosions on ground, and in recent years, from explosions of grenades at different levels in the atmosphere released from rockets have added much to our knowledge of winds in the atmosphere upto 80 km. Since 1947, a large number of soundings of high atmosphere have been made with the aid of rockets which have provided us

with valuable information about pressures and densities at different levels in the atmosphere at different latitudes. Systematic measurements of movements above 80 km have been made by the radio methods in recent years.

Drifts in the upper atmosphere above 80 km differ from those in the lower regions in some important respects. Diurnal variations of temperature and tidal movements due to sun and moon are much larger in amplitude in this region and these give rise to daily variations of wind which are very large in magnitude above this level. Large wind shears and turbulent movements are also common.

The effects of solar heating in the upper part of the ozone layer and its variation with latitude gives rise to large seasonal changes of wind at 40-70 km, so also the effect of absorption by oxygen of solar ultra-violet radiation and its dissociation into atoms at levels above 80 km.

The daily variation of the earth's magnetic field is one of the consequences of the tidal movements in the lower ionosphere. But it is not yet possible to define with any exactness the levels whose daily movements give rise to the daily variation in geomagnetic field. At the levels corresponding to the F region, magneto-hydrodynamic forces assume great importance.

General features of circulation in the upper atmosphere.

The results of wind measurements at various

heights by the different methods cannot all be given equal weight. While some of them have been systematic and have been carried over a number of years, others have been made over short periods of time and at a limited number of places. Still, putting them all together, the major features of the circulation upto 100 km can now be pieced into a coherent scheme. This has been done by a few workers (Kellog and Schilling, 1951; Pant, 1956; Murgatroyd, 1957). A simpler version of Murgatroyd's diagrams of average temperatures and zonal winds are reproduced in Figs. 1 & 2. The main features are summarised below.

(a) Temperature distribution.

(i) There is a temperature minimum at the tropopause at a height of about 17 km over the equatorial regions. The temperature there is about 190°K to 200°K. The tropopause level comes down beyond 25° - 30° and is 10 - 11 km in middle latitudes and 8 - 9 km in polar latitudes. The tropopause temperature in middle latitudes is about 220°K.

(ii) A maximum of temperature is found over 50 - 55 km. This maximum is now known to be caused by the absorption of solar ultraviolet radiation by the ozone in the atmosphere, which is itself produced by the photo-chemical action of sun light. The temperatures at 50-55 km are highest over the polar regions in the summer hemisphere

and lowest over the polar night in the winter hemisphere.

(iii) There is another temperature minimum at a height of 80 km. At this level, the temperatures are the lowest over the middle and polar latitudes in the summer hemisphere.

The effect of (ii) and (iii) is to cause large lapse rates between 60 and 80 km in the summer hemisphere and easy vertical mixing.

(iv) Above the upper minimum temperature level or stratopause, temperatures rise with height at all altitudes.

(b) Wind distribution

The main features of the zonal wind distribution are shown in Fig. 2. The directions referred to in the diagram are the directions from which the wind blows. This is in accordance with the meteorological convention, but opposite to that adopted by ionospheric physicists.

(i) Westerly winds are a maximum at the tropopause level in middle latitudes. Strong westerlies are also found over sub-tropical latitudes, particularly in winter at a height of about 12 km. These wind maxima are weaker in ~~winter~~ summer and shift to higher latitudes. Over the equatorial latitudes, easterlies prevail both in summer and in winter in the first 30 km.

I

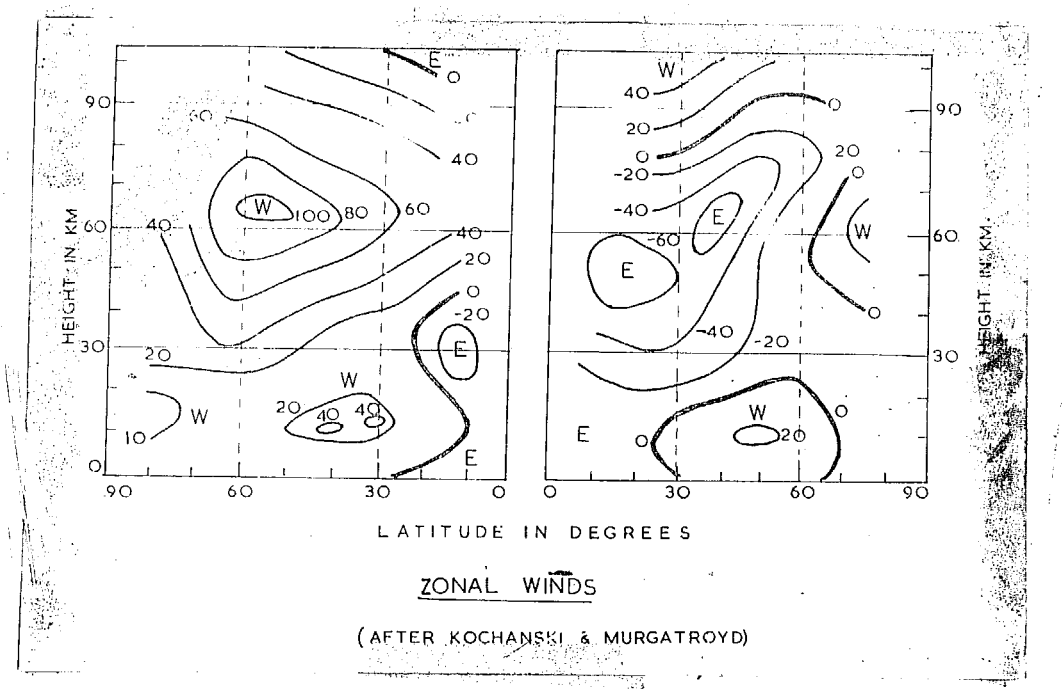

Fig. 1 - Average latitudinal distribution of temperature (after Kochanski and Murgatroyd)

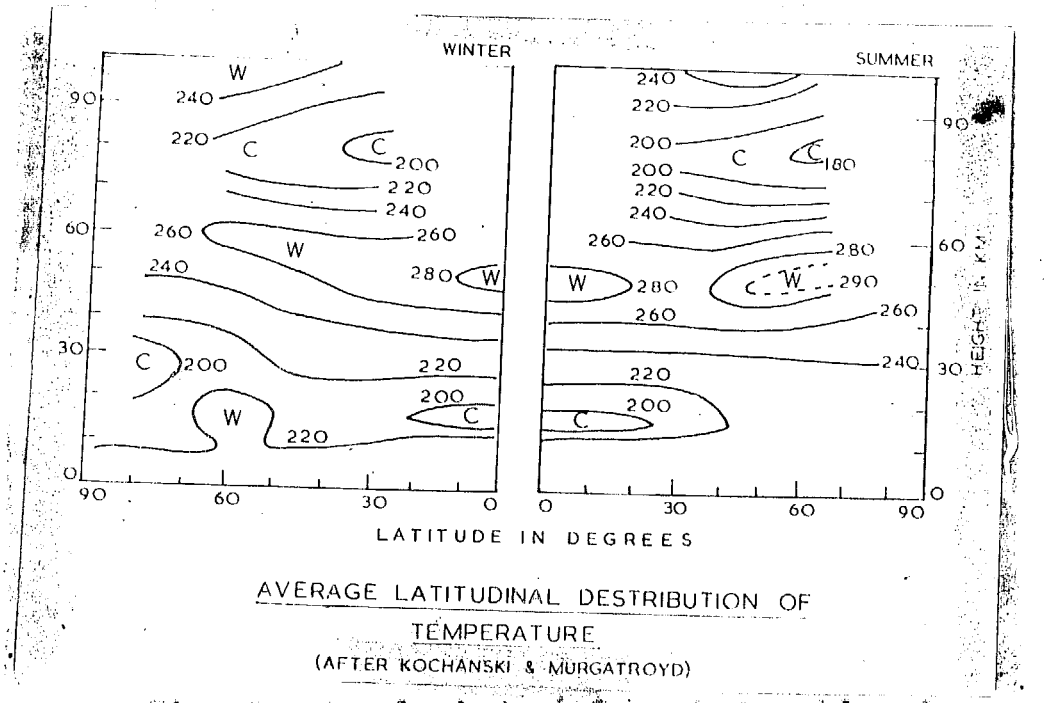

Fig. 2 - Zonal winds (after Kochanski and Murgatroyd)

(ii) In winter, after passing a region of weak winds at 20 - 25 km, a second region of strong westerlies is encountered with maximum at 50-70 km at 40°N - 60°N. The westerlies decrease upward and give place to easterlies above 90 - 100 km.

(iii) The pattern of winds in the middle atmosphere is completely different in summer. The equatorial easterlies extend towards the poles in an upward direction and strong easterlies are met with at 50 - 60 km. over 30° to 40°. These winds give place to westerlies above 70 - 80 km. The westerlies reach a maximum at 90 - 100 km. There is thus in the upper atmosphere whenever there is a fall of temperature towards the poles, an increase of westerly winds with height and whenever there is a rise of temperature towards the pole, a decrease of westerlies or an increase of easterlies with height.

The thermal wind equation, viz.,

$$\frac{dT}{dy} = -\frac{g^2}{f}\left[\frac{2\omega \sin \phi}{}\right] \cdot \frac{d}{dz}\left(\frac{u}{T}\right), \qquad (1)$$

where $\frac{dT}{dy}$ is the horizontal temperature gradient towards the pole, ω the angular velocity of earth's rotation, ϕ, the latitude and u the zonal wind component towards the east, is in general found to satisfy the average features of the circulation. In the following section, some of the methods used for the experimental determinations of these

I

drifts are described.

2. Experimental methods for the study of wind drifts at levels above 75 km.

Among the methods that have been used to investigate drifts in the upper atmosphere above 75 km, three are of particular importance, because they enable systematic measurements to be made over a sufficiently long period of time. They are (1) the radio study of meteor trails both by the pulse and continuous wave methods (2) radio methods including the method of similar fades using closely spaced receivers as originally used by S. N. Mitra and used by the author at Ahmedabad and (3) the method of scintillations using radio stars.

(1) Observations of meteors

Meteors have provided an important means of studying the properties of the upper atmosphere between 60 and 120 km. Meteoric particles fall into earth's atmosphere with velocities exceeding 11 km/sec., the maximum velocity depending upon the circumstances of encounter in the earth's atmosphere. Owing to friction, they get incandescent in the upper atmosphere producing visible trails and columns of ionisation which can scatter radio waves incident upon them. Theories have been put forward to explain the process of disintegration of meteors in the upper atmosphere (Lindemann and Dobson,

1923; Sparrow, 1926; Opik, 1940). Generally, the larger the velocity of the meteors, the higher is the level at which disintegration starts. However, because of the temperature minimum at 80 km, two maxima are observed in the levels of disappearance of meteors (Mitra, 1952).

Extensive visual observations have been made by Olivier (1942, 1947) Fedensky (1944) and others and systematic radio measurements using meteors have been made at Manchester (Greenhow, 1954, 1956) at Adelaide (Elford and Robertson, 1953) and Stanford (Manning et al, 1950). The radio methods for the study of meteors which have been developed since 1945 depend upon the fact that the meteors are vapourised by collision with the molecules of the atmosphere between 120 km and 60 km and leave a trail of electrons and positive ions. This column has initially a radius of a few centimeters and a length of the order of 10 km. It disperses by ambipolar diffusion at a sufficiently slow rate and acts as a convenient scatterer of radio wave. It is found that waves of frequencies 30 to 60 Mc/s can be used. Trails with large electron densities act as regular reflectors while those with densities less than 10^{12} electrons/cm act as scatterers. As the colum diffuses, the amplitude of the reflected wave decreases exponentially (Herlofson, 1948).

Radio observations of meteors have enabled the

determination of meteor heights on a large scale, the velocities of individual meteors and the mean heights of reflection for different velocity groups. The last can be related to the atmospheric pressures at meteoric heights.

Radio techniques have also been developed to determine winds in the upper atmosphere between 80 and 100 km by measurement of the drifts of short duration meteor trails. Two methods are in general use. (1) The pulse method and (2) the CW method. These two methods are described below together with a summary of the results of wind drift observations obtained by them.

(1) The pulse method

This method has advantage of freedom from unwanted echoes by means of receiver suppression and the exact height of reflection could be determined. A typical equipment is capable of giving about 3000 usable echoes daily and a good wind determination could be obtained with an hour's observations. A typical transmitter (Greenhow, 1956) has a power of 50 kW at a repetition rate of 150 pulses per second on a frequency of 36.3 Mc/s. A gating circuit in the receiver part selects out the wanted signals. The received signals are fed into four oscilloscopes from which information regarding the echo range, amplitude and phase variations are recorded. The first of these presents a type A display of the ground

pulse and the received echo and thus facilitates range measurement. The amplitude variations in the received signals are displayed in the second C.R.O. in which the reflected echo is applied to the Y plate and a short period time base (0.3 ms) initiated by the echo, to the X plate. This gives the Fresnal diffraction pattern as the meteor crosses the aerial beam and is used to determine the speed of the meteor. The ground pulse and the received signals are mixed together and the resultant beat signal is applied to the two other scopes, to one with a phase lag of 90^{o}. They record the phase variations as the ionised trail drifts towards or away from the receiving station. A complete cycle in these two represents a phase reversal caused by the drift of the trail by a distance of $\lambda/2$. Knowing the frequency, it is possible to determine the speed of the drift along the line of sight. The sense of the drift is obtained by comparing the patterns obtained in the two oscilloscopes, whether one of them leads the other or lags. Having obtained the radial components of the movement of a few meteors in a particular direction, the aerials are directed in a perpendicular direction or in two other directions for periods of the order of 10 minutes and the radial components are obtained along these directions also. If the heights of the meteors are within a small, defined limits, the actual velocity and direction of drift in the atmospheric layer can be determined.

Measurements of wind drifts by this method have been carried out for a few years and a great deal of information have been collected about the diurnal and seasonal variations by Greenhow (1956) in Manchester. Marked semidiurnal oscillation in the wind components corresponding to a clockwise rotation with a period of halfday have been obtained. In addition, prevailing winds have also been observed. The phase and amplitude of these are found to vary with height in the range 75-105 km and large wind shears have been discovered in these regions. This method assumes that the drift remains steady over the entire period of observations.

Robertson et al (1953), Milford and Robertson (1953), and Hanley (1956), working in Australia, have described a continuous wave method of determining drifts with the help of meteor trails. This equipment operates on a frequency of about 25 Mc/s, with a power output of 250 watts. The receiving station are situated at a distance of about 12 miles from the transmitter and consists of three dipoles placed at the corners of a right angled triangle with a separation of λ. The heights of the aerials are adjusted so that the ground signal is of comparable magnitude with the sky wave signals. There would however be a phase difference between the ground signal and the meteor signal at each aerial and this phase difference would undergo periodic changes as the reflecting colum of ionisation drifts. This results in a periodic

amplitude change showing beats. Knowing the period (t) of the beat, and the wavelength (λ), the ~~vertical~~ radial component of speed V_r can be computed from the relation $V_r = \lambda/2t$. To determine the sense of the radial velocity, whether it moves towards or away from the receiving aerials, a sudden phase shift of 90^0 is introduced into the transmitted signals periodically, followed by a gradual recovery. The sudden change in the phase shift affects the ground wave earlier than the sky wave, producing a resultant signal which is in the form of a spike in the beat signal. From the position of these spikes, it is possible to determine the sense of the drift. The range is measured in the conventional manner and the direction of arrival, by a system of three receiving aerials. The beat signals from all of them are displayed. The actual speed of the drift can then be determined with the help of simple transformations.

The results obtained by this method at Adelaide (39^0S) indicate that the prevailing winds throughout the year are predominently zonal at that place, with eastward winds increasing with height in summer and decreasing with height in winter from 75 - 105 km. Superimposed on these are important diurnal and semidiurnal components. The former varies from month to month and is found to have a regression in phase of 180^0 from summer to winter. The rotation of the diurnal and semidiurnal vectors in the northern hemisphere are clockwise and ~~in~~ in the southern hemisphere,

anticlockwise. The 24 hour components have large amplitudes in spring and summer and smaller amplitudes in autumn and winter. The 12 hour components exhibit irregular amplitude and phase variations. The amplitude of the semidiurnal wave increases withheight and is 25 - 50 m/s at 95 - 105 km. Wind gradients of the order of 2.3 m/s/sec/km in winter and -3.3 m/s/sec/km in summer are obtained at Adelaide.

Drifts in different regions of the ionosphere by radio methods.

The following methods are in general use for the measurement of drifts in the E region. (1) Pulse and C.W. methods using spaced receivers. (2) Pulse and C.W. methods using meteor trails, which have been described above. (3) The study of the variations of certain peculiarities of ionospheric quantities over stations separated from each other. For the F region, the methods in general use are (1) the spaced receiver method, (2) the method of spaced transmitters giving reflections from widely separated points (Munro, 1950; 1953; 1958) and (3) the method utilising the scintillations of radio stars.

In the above methods, the time delay at separated points of some particular feature of the reflected wave is utilised to calculate the drift, assuming that such time delays are produced by drift movements. The feature most extensively used for the study of drifts is the amplitude of the reflected wave. The method, the

equipment used and the analysis of the data are presented in the following chapters of the present thesis.

Certain other features of the ionosphere also show time shifts when studied at stations separated from each other. Munro (1953), for instance noticed that at times, the electron density at a fixed height showed a cyclic change; it first decreases, then increases and later gets back to its normal value. Such disturbances are identified at two points separated by large distances of the order of 900 km and are interpreted as travelling wave disturbances in the ionosphere. The velocity measured by this method however appears to fit in better with the idea of a compressional wave than of bodily movement of neutral air and electrons.

Radio noise from galactic radio sources often exhibits irregular variations in amplitude. Ryle and Hewish (1950) and others, by comparing the records of these variations at separated points have shown that these are due to the effect of irregularities mainly in the F region of the ionosphere. The method (Maxwell and Little, 1952) consists in recording radio noise at a fixed frequency, (between 30 and 100 Mc/s) at separated points and correlating the fluctuations in time. The observations are usually confined to the night time when scintillations largly occur. Extensive observations have been made at Manchester and the results indicate the direction to be towards NW in summer and eastward in winter. It has also been found

that the speeds show a marked dependence on geomagnetic activity, larger speeds being associated with greater activity. During periods of intense magnetic activity, a reversal in the E-W component around midnight has also been noticed.

3. Summary of the thesis

Systematic observations of ionospheric drift has been made by the author at Ahmedabad since 1956 mainly on 2.0 Mc/s and also for certain periods on 4.0 Mc/s and 6.0 Mc/s. This thesis presents the methods and results of observations of these measurements. They refer mostly to the E layer in day time and F layer in the night time.

Chapter II deals with the various methods of analysis that have been used to analyse the data from fading records. There are two principal methods viz. The method of similar fades and correlation method. These two methods are described in this chapter and the relative merits compared with worked examples.

Chapter III gives the description of the equipment used by the author. The design considerations of the various stages are briefly summarised.

Chapter IV discusses the results of drift observations over the period 1956-1958. The first part is a published paper describing the general results obtained upto December 1957 and the second part discusses the later observations

and certain special features observed at Ahmedabad.

Chapter V is a published paper which describes the properties of fading of vertically reflected signals on 2.0 and 4.0 Mc/s at Ahmedabad. The fading records obtained for drift measurements were used for this purpose. An interesting feature that was noticed was the marked dependence of the fading period on the amount of spread F present in the p'-F records at that time.

In chapter VI, a comparison is made of the results at Ahmedabad with those obtained elsewhere. The data obtained by closely spaced receivers and by other methods are used.

CHAPTER I

REFERENCES

Elford, W.G., and Robertson, D.S.	1953	Jour. Atmos. Terr. Phys., 4, 271.
Fedensky, V.V.	1944	Astr. Jour. Sov. Union, 21, 291.
Greenhow, J.S.	1954	Phil. Mag., 45, 364.
Greenhow, J.S.	1956	Phil. Mag., 1, 1157.
Herlofson, N.	1948	Rep. Progr. Phys., 11, 444.
Huxley, L.G.H.	1957	Annals of I.G.Y., 3, 250.
Kellog, W.W. and Schilling, G.F.	1951	Jour. Met., 8, 222.
Kochanski, A.D.	1955	Jour. Met., 12, 95.
Lindemann, F.A. and Dobson, G.M.B.	1923	Proc. Roy. Soc., A102, 411.
Manning, L.A., Villard, O.G. and Peterson, A.M.	1950	Proc. I.R.E., 38, 877.
Maxwell, A. and Little, C.G.	1952	Nature, 169, 746.
Mitra, S.K.	1952	Upper Atmosphere, 1952 Asiatic Society, Calcutta, 569.
Munro, G.H.	1950	Proc. Roy. Soc., A202, 208.
Munro, G.H.	1953	Nature, 171, 693.
Munro, G.H.	1958	Austr. Jour. Phys., 11, 91.
Murgatroyd, R.J.	1957	Quart. Jour. Roy. Met. Soc., 83, 417.
Olivier, C.P.	1942	Proc. Amc.Phil. Soc., 85, 93.
Olivier, C.P.	1947	Proc. Amo. Phil. Soc., 21, 315.
Opik, E.	1940	M.N.Roy. Astr. Soc., 100, 315.
Pant, P.S.	1956	Jour. Geophys. Res., 61, 459.

Robertson, D.S., Liddy, D.T. and Milford, W.G.	1953	Jour. Atmos. Terr. Phys., 6, 459.
Ryle, M. and Newish, A.	1950	M.N.Roy. Astr. Soc., 110, 38.
Sparrow, C.M.	1926	Ap. Jour., 63, 90.

CHAPTER II

THE METHOD OF CLOSELY SPACED RECEIVERS.

When a radio wave, transmitted vertically upward, is reflected from the ionosphere, variations of the reflected signal intensity are observed. This fact has led to the belief that the ionosphere acts as an irregular diffracting screen which produces a diffraction pattern on the ground (Ratcliffe, 1956). If such a diffracting screen remained steady and did not move, the diffraction pattern on the ground would remain fixed, and the amplitude of the reflected wave as recorded by a fixed receiver would remain constant.

Changes in the pattern can occur in two ways; first, the configuration itself might change. The amplitude of the ground signal at any point would then change, and the pattern of change would also be different at different points on the ground. Secondly, the configuration might remain the same but might bodily drift in space with, say, a velocity V. If the pattern remains steady, the diffraction pattern of the reflected wave would move with a velocity 2V in the same direction. Two receivers placed some distance apart would register similar fading patterns, provided the elements of the pattern are larger

than the distance between the receivers but these would be displaced in time by an amount depending upon the direction and speed of the drift. In general, both these types of changes, namely, a bodily drift together with a change in the pattern can occur and the changes in the fading pattern become complicated, although, on many occasions points which are similar can be identified in records obtained at two points which are not too far away from each other. This similarity is found to decrease with the distance between the receivers and vanishes with distances much larger than the wavelength of the signal used. (Ratcliffe and Pawsey, 1933). This indicates that the configurations are finite in size. Some estimates of their sizes have been made.

An estimate of the magnitude and direction of the drift in the horizontal plane, if present, could be obtained if recordings of three receivers suitably placed are obtained. The aerials could have any geometry. By noting the time shifts of corresponding points in the records, the components in two directions of the velocity could be obtained. In addition, it is also possible to obtain an idea of the magnitude of the random velocities which may be superposed on a steady drift. Some idea of the anisotropy and the size of the configuration can also be obtained from records. Typical fading records obtained at Ahmedabad on a frequency of 2.6 Mc/s have been published

in a recent paper by the author (1956a) which is appended to chapter IV. In this chapter, the different methods of analysis that have been suggested are discussed and two records obtained at Ahmedabad are analysed by these different methods and the results are compared.

Methods of analysis of the records :- The methods of analysis can be classified in two groups. (1) The method of similar fades and (2) correlation methods. Among the first are (1) Ratcliffe's method of mean shifts (Ratcliffe, 1954) and Pütters method (Pütter, 1955). Among the correlation methods are (1) the original method proposed by Briggs, Phillips and Shinn (1950), (2) the method proposed by Yerg (1955) and (3) the method of correlation contours (Phillips and Spencer, 1955).

Although the correlation methods yield a much larger amount of information, their use has to be restricted because of the labour involved in the calculation of the correlation coefficients. The author has used the method of similar fades in view of the large number of records that had to be studied. It has been found that it is possible to identify in many of the records obtained at Ahmedabad, a large number of similar points. However, whenever spread-F was present, the records showed little similarity (Sethuraman, 1956a) and had to be rejected for the purpose of drift analysis. Although from a detailed analysis, information regarding the drift movements the turbulent velocities and

the "size" of the pattern could be extracted from the fading record, the method of similar fades yields mainly information about the first of those quantities.

The method of similar fades :- This method depends on the recognition of corresponding points in the record obtained from different aerials. A random velocity, large in comparison with the drift velocity can obliterate this similarity. At Ahmedabad, at the frequency and with the separation (one wave length) used, no difficulty was experienced in identifying such points on most occasions.

Ratcliffe (1954) has given a simple picture of the method of similar fades. A wave, reflected from an irregular ionosphere, produces on the ground an irregular distribution of amplitudes which can be represented, at any instant, by contours of constant amplitude. Fig. 1 gives the diagram of such a system of contours. O, A and B represent three

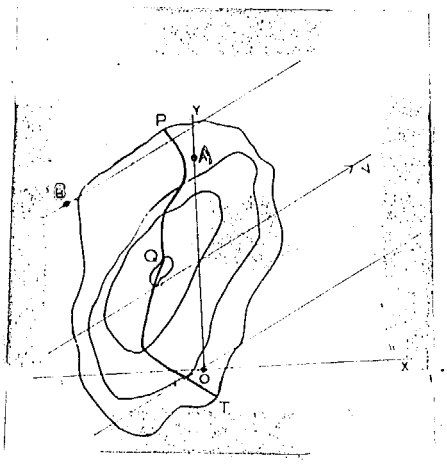

Fig. 1 - Contours of constant amplitude.

spaced receivers on the ground. The closed lines represent

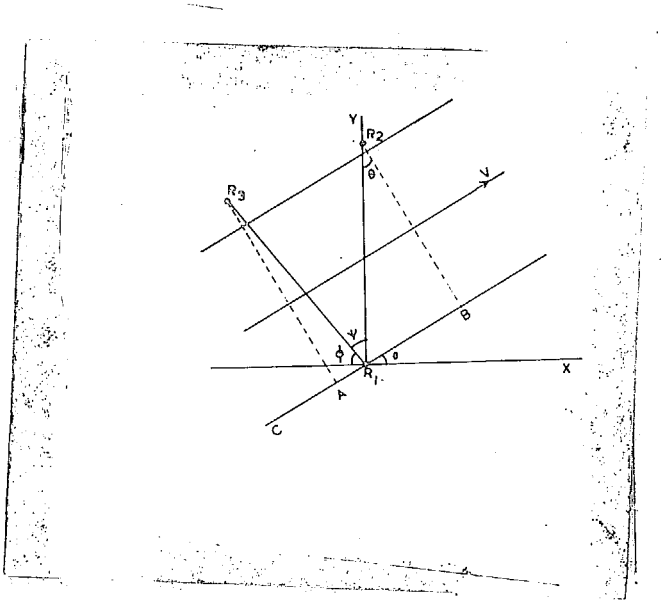

Fig. 2.

contours of equal intensity with maximum intensity near the centre Q. As this pattern moves, O will receive a maximum signal when the contour closest to Q passes over it. This will occur for each of the three receivers and we can draw a line joining those points in the pattern which give maximum intensities at the three aerials. This line is known as the line of maximum intensity. Its orientation depends upon the direction of the drift and the shape of the contours. In general, it need not coincide with the wave front or the plane perpendicular to the direction of movement of the configuration. Neither need it be straight, especially when the area enclosed by the aerials is large and comparable with the size of the configuration. In the first part of the following discussion, the following simplifications are assumed, (1) the line of maximum amplitude is straight. This is justified in view of the close spacing of the aerials in our experiments. (2) The line of maximum amplitude coincides with the wave front. Departures from these assumptions are discussed in the second part.

Making the above assumptions and omitting the contours for clarity, the situation is as shown in Fig. 2. O, A and B are the three aerials and the dashed lines AD and BE are the wave fronts. ψ is the angle between the lines joining the centres of the aerials O and A and O and B and $\phi + \psi = 90^{\circ}$. The wave front moves in the direction CED, inclined to the direction OA by θ. Let 'a' be the distance

between O and A and 'b' that between O and B. Vx and Vy are the component speeds along OX and OY and t_a and t_b, the time shifts observed between the fading patterns at O and A and O and B. We obtain

$$V = \frac{b \sin \theta}{t_b} = \frac{a \cos (\theta+\phi)}{t_a} \qquad (1a)\&(1b)$$

Thus,

$$\frac{b \sin \theta}{a \cos(\theta+\phi)} \cdot \frac{t_a}{t_b} = 1 \quad \text{or}$$

$$\theta = \tan^{-1} \frac{at_b \cos \phi}{bt_a + at_b \sin \phi} \qquad (2)$$

Squaring and adding (1a) and (1b) we obtain, after some manipulation

$$V = \frac{ab}{(a^2t_b^2 + b^2t_a^2)^{\frac{1}{2}}} \left[1 - \frac{1}{2} \cos 2\theta + \frac{1}{2} \cos 2(\theta+\phi)\right]^{\frac{1}{2}} \qquad (3)$$

This is the speed of the pattern as <u>observed</u> on the ground. The real value of the drift is half this quantity.

Two types of geometry are in wide use. In one of them, the aerials A and B of figure 2 are along OX and OY respectively. The calculations with this geometry are simple and the author has used it in his experiments. Thus, $\Psi = 90^0$ and $\theta = 0$ and $a = b$. We obtain,

$$V = \frac{a}{(t_a^2 + t_b^2)^{\frac{1}{2}}} \quad \text{or if, } Vx = \frac{a}{t_a} \text{ and } Vy = \frac{a}{t_b},$$

$$\frac{1}{V^2} = \frac{1}{Vx^2} + \frac{1}{Vy^2} \quad \text{and} \quad \theta = \tan^{-1} \frac{Vx}{Vy} \qquad (4)$$

Krauchrämer (1933) and others have fixed the three aerials at the corners of an equilateral triangle. Ramsay (1958) has shown that this configuration reduces the errors due to curvature, discussed below. Here $\psi = 60^0$ and a = b in expressions (2) and (3).

Ratcliffe (1954) has modified the method to include in it the effects of random orientation of the lines of maximum amplitude with respect to the wave front. He assumed that all values of the angle ψ between the direction of the drift and the direction of maximum amplitude are equally probable. Let O, A and B (Fig. 3) represent the three receivers placed at the corners of a right angled triangle. Let V be the drift vector making an angle θ

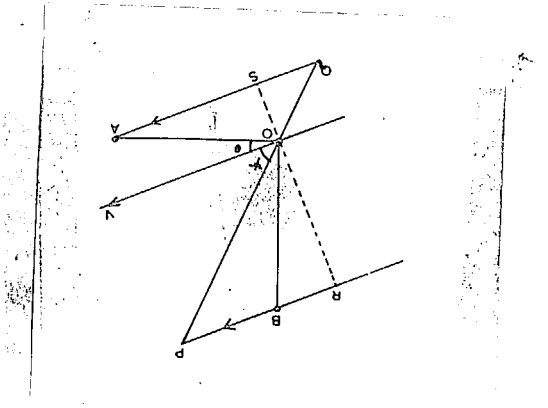

Fig. 3 -

with respect to the direction OA. Let ψ be the angle which the line of maximum amplitude POQ assumed straight makes the direction of the drift. We obtain $t_x = QA/V$ and $t_y = RP/V$.

$$t_x = \frac{QS + SA}{V} = \frac{a}{V}\,(\sin\phi\,\cos\psi + \cos\phi) = \frac{a}{V}\cos\phi\,.$$

and $$t_y = -\frac{(ut-lb)}{V} = \frac{a}{V}\sin\phi\,(1-\cot\phi\cot\psi) \qquad (7)$$

If ψ assumes all values equally randomly the mean value of $t_x = \overline{t_x} = \frac{a}{V}\overline{\cos\phi}$ and $\overline{t_y} = \frac{a}{V}\overline{\sin\phi}$ (8)

giving rise to formulae (4)and (5). Thus if instead of taking the individual values of t_x and t_y we consider their mean values over a length of time, the effect of random orientation of the time of maximum intensity would be taken into account.

We also obtain on differentiating t_x and t_y in (6) and (7),

$$\Delta T_x = \frac{a}{V}\sin\phi\,(1+\cot^2\psi)\,\Delta\psi$$

and $$\Delta T_y = -\frac{a}{V}\cos\phi\,(1+\cot^2\psi)\,\Delta\psi\ .$$

If the directions of the lines of maximum amplitude vary in equal ranges in equal intervals of time, we can find the time for which a unit range of $\Delta\psi$ is occupied. The probability of finding T_x between T_x and $T_x+\Delta T_x$ due to changes in ψ is $P(T_x).\Delta T_x$ and is proportional to

$$\frac{1}{\Delta T_x} \text{ or to } \frac{1}{(1+\cot^2\psi)}\ .$$

Since $$\cot\psi = \frac{T_x - a/V\cos\phi}{a/V\sin\phi} = \frac{T-\overline{T_x}}{T_y}\ ;$$

$$P(T_x) = \frac{1}{1\ \ (T_x-\overline{T_x})^2} \text{ and } P(T_y) = \frac{1}{1\ \ (T_y-\overline{T_y})^2}$$

Thus the probability of finding values of T_x near the mean value is larger than finding it farther away. In other words, a greater accuracy can be obtained if we consider the mean value after excluding all abnormally different values from the set of values obtained in the experiment.

Pütter (1955) proposed another method of analysis of the record which is applicable when the pattern on the ground is elongated. Let O'A represent a line of maximum amplitude (Fig. 4) crossing O at $t = 0$ and A at $t = t_1$.

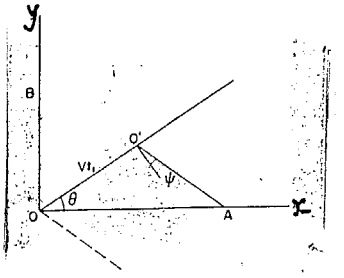

Fig. 4 -

Let V be the velocity of the drift, Θ the direction which it makes with the X axis and ψ the inclination of the line of maximum amplitude to the wave front. We have, putting OA = a

$$\frac{a}{\sin(90+\psi)} = \frac{Vt_1}{\sin(90-\theta-\psi)}$$

$$\text{or} \quad \frac{a}{\cos\psi} = \frac{Vt_1}{\cos(\theta+\psi)}, \text{ giving, } t_1 = \frac{a}{V}\,\frac{(\cos\theta+\psi)}{(\cos\psi)} \qquad (9)$$

Similarly, if 'b' be the separation between the two receivers along the Y direction, we obtain

$$t_2 = \frac{b}{V} \cdot \frac{\sin(\psi + \theta)}{\cos \psi} \qquad (10)$$

Thus $$\frac{t_2}{b} \Big/ \frac{t_1}{a} = \tan(\psi + \theta) = \tan \theta' \qquad (11)$$

and $$\frac{t_2^2}{b^2} + \frac{t_1^2}{a^2} = \frac{1}{V^2 \cos^2 \psi}, \text{ or } \frac{1}{Vx^2} + \frac{1}{Vy^2} = \frac{1}{V^2 \cos^2 \psi} = \frac{1}{V'^2}$$

..(12)

We have the relationships $V' = V \cos \psi$ and $\theta' = (\theta + \psi)$ from (11) and (12)

In Fig. 4(a) V' represents one such vector derived from one set of t_1 and t_2 and θ' the angle it makes with the X axis. We then have for its components

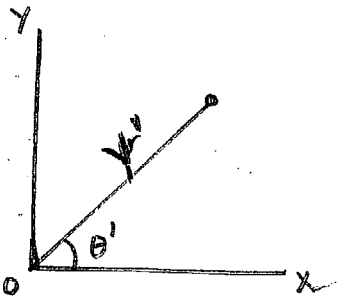

Fig: 4(a)

$$V'_x = V' \cos \theta' = V \cos \psi \cos(\theta + \psi) \quad \text{and} \quad -I$$

$$V'_y = V' \sin \theta' = V \cos \psi \sin(\theta + \psi) \quad \text{or} \quad -II$$

$$V'_x = V/2 \left[\cos(2\psi + \theta) + \cos \theta\right] \quad \text{and}$$

$$V'_y = V/2 \left[\sin(2\psi + \theta) + \sin \theta\right]$$

Thus we have $(V'_x - V/2 \cos \theta)^2 + (V'_y - V/2 \sin \theta)^2 = V^2/4$.

The locus of V' is thus a circle whole centre is at the point V/2 cos θ, V/2 sin θ and whose radius is V/2. Thus the diameter through its centre will represent in magnitude and direction the real velocity of the drift. This property

was utilised by Pütter (1955) in the construction of a circle diagram for the determination of drift speedϕ and direction. The individual speeds were plotted and the diameter of the circle through the origin was drawn. The dispersion of the points in the diagram gives a qualitative idea of the magnitude of the random velocity.

Pütter also described another method of evaluating the drifts parameters in the absence of random velocity. From equation (9) and (10) viz. $t_1 = [a/V\cos\psi] \cos(\psi + \theta)$ and $t_2 = [b/V\cos\psi] \sin(\psi + \theta)$, We obtain on eliminating ψ

$$\frac{t_1}{a} \cos\theta + \frac{t_2}{b} \sin\theta = \frac{1}{V} \qquad (11)$$

Thus the plots of t_1 and t_2 would result in a straight line, the perpendicular to which from the origin gives the direction and $1/V$ of the drift.

In the above two methods, we have assumed that the random velocities are absent. Banerjee (1956) has extended the analysis to the case where random motions are present. He starts with a statistical distribution of the angle between the wave front and the line of maximum amplitude and finds that in the presence of random motion, the Pütter straight line would be changed into an ellipse. The perpendicular to the major axis of the ellipse gives the values of V and θ and the minor axis of the ellipse gives a measure of the random velocity Ve. While Putter's original method requires only two sets of t_x and t_y for drawing the straight line,

Banerjee's method requires a large number of values for drawing the ellipse. Banerjee's method also does not include the effects of anisotropy of the pattern since in evaluating the joint probability distributions of t_x and t_y, the pattern is assumed to be isotropic.

Court (1955) has introduced a modification of the original Pütter's method which reduces the dispersion of points in the straight line or circle. He selects only those portions of the record which show similarity and the shifts obtained from them are used for calculating the velocity. He obtains circle and straight line diagrams with very little dispersion. The dispersion in these diagrams is indicative of the magnitude of the random velocities and by making a choice of the points, Court's modification puts the random element out of the way.

In all this analysis, it is assumed that the lines of maximum amplitude are straight in the region considered. This might not be so, although in practice, over such short distances as are used in practice, this curvature does not amount to much. Rao and Rao (1957), employing four aerials found that the lines of maximum amplitude are indeed curved on certain occasions. Ramsay (1957) has examined the errors introduced into the calculation on account of curvature and conclude that an equilateral array of aerials gives the least amount of error. It has also the advantage of the error being independent of the direction of the drift. Barber

(1957) has shown that the standard deviation of the scatter of points representing the time intervals in any direction is proportional to the radius of gyration of the three receivers about the axis through the centroid of the triangle formed by them. Such a distribution would be circular only in the case of an equilateral array. Since however, calculations with an equilateral array would be more complicated, the right angle array has been used at Ahmedabad for the drift measurements.

The correlation methods of analysis :- The information that can be obtained by the methods described above is limited to the values of the speed and direction of the drift. Nothing is known about the size of the pattern or the magnitude of the random velocities as it drifts. The correlation methods, although laborious, have the advantage of giving these quantities in addition. There are three main methods which employ the correlation technique. (1) The method of Briggs, Phillips and Shinn (1950). (2) The method of Yerg (1955) (3) The method of spatial correlation contour (Phillips and Spencer, 1955).

The method of Briggs, Phillips and Shinn :- This method requires the calculation of auto-correlation and cross-correlation coefficients of amplitudes from the records. These coefficients are defined as follows. If $A(t)$ be the amplitude recorded at a single station at a time t, $A(t+\tau)$, that measure at the same station at a time $t+\tau$ and $\bar{A}$, the mean value of $A(t)$ over the length of the record, $\rho(\tau)$,

the auto-correlation function for interval τ of the record is given by

$$\rho(\tau) = \frac{\sum (R(t) - \bar{R})(R(t+\tau) - \bar{R})}{\sum (R(t) - \bar{R})^2} \qquad (12)$$

It can be seen that when $\tau = 0$, $\rho(\tau) = 1$ i.e. the auto-correlation function has a maximum value of 1 at $\tau = 0$. As the time lag becomes larger, the value of $\rho(\tau)$, in general, becomes smaller.

If ξ_0 be the distance between two aerials and Ra and Rb the amplitudes recorded at the two aerials at a time t, the cross-correlation function $\rho(\xi_0, \tau)$ between the two patterns recorded at the aerials is given by

$$\rho(\xi_0, \tau) = \frac{\sum (Ra(0,t) - \bar{Ra})(Rb(\xi_0, t+\tau) - \bar{Rb})}{\sum (Ra(0,t) - \bar{Ra})^2} \qquad (13)$$

Essentially, it is the product of the amplitude of the signal at the aerial A, at a time t with the signal at the aerial B at a time $(t + \tau)$. Because of the space lag ξ_0, this function never assumes a value 1 and the maximum occurs at a time depending upon the velocity of the drift and the distance between the aerials. Two sets of cross-correlation functions are required for a complete determination of the drift speed and direction. As described later, these coefficients are useful in determining certain other parameters describing changes in the pattern as listed below.